



# TURKISH JOURNAL OF ENGINEERING

## **EDITOR IN CHIEF**

*Prof. Dr. Murat YAKAR*  
Mersin University Engineering Faculty  
Turkey

## **CO-EDITORS**

*Prof. Dr. Erol YAŞAR*  
Mersin University Faculty of Art and Science  
Turkey

*Prof. Dr. Cahit BİLİM*  
Mersin University Engineering Faculty  
Turkey

*Assist. Prof. Dr. Hüdaverdi ARSLAN*  
Mersin University Engineering Faculty  
Turkey

## **ADVISORY BOARD**

*Prof. Dr. Orhan ALTAN*  
Honorary Member of ISPRS, ICSU EB Member  
Turkey

*Prof. Dr. Armin GRUEN*  
ETH Zurich University  
Switzerland

*Prof. Dr. Hacı Murat YILMAZ*  
Aksaray University Engineering Faculty  
Turkey

*Prof. Dr. Artu ELLMANN*  
Tallinn University of Technology Faculty of Civil Engineering  
Estonia

*Assoc. Prof. Dr. E. Çağlan KUMBUR*  
Drexel University  
USA

## **TECHNICAL EDITORS**

*Prof. Dr. Roman KOCH*  
Erlangen-Nurnberg Institute Palaontologie  
Germany

*Prof. Dr. Hamdalla WANAS*  
Menoufyia University, Science Faculty  
Egypt

*Prof. Dr. Turgay CELİK*  
Witwatersrand University  
South Africa

*Prof. Dr. Muhsin EREN*  
Mersin University Engineering Faculty  
Turkey

*Prof. Dr. Johannes Van LEEUWEN*  
Iowa State University  
USA

*Prof. Dr. Elias STATHATOS*  
TEI of Western Greece  
Greece

*Prof. Dr. Vedamanickam SAMPATH*  
Institute of Technology Madras  
India

*Prof. Dr. Khandaker M. Anwar HOSSAIN*  
Ryerson University  
Canada

*Prof. Dr. Hamza EROL*  
Mersin University Engineering Faculty  
Turkey

*Prof. Dr. Ali Cemal BENİM*  
Duesseldorf University of Applied Sciences  
Germany

*Prof. Dr. Mohammad Mehdi RASHIDI*  
University of Birmingham  
England

*Prof. Dr. Muthana SHANSAL*  
Baghdad University  
Iraq

*Prof. Dr. Ibrahim S. YAHIA*  
Ain Shams University  
Egypt

*Assoc. Prof. Dr. Kurt A. ROSENTRATER*  
Iowa State University  
USA

*Assoc. Prof. Dr. Christo ANANTH*  
Francis Xavier Engineering College  
India

*Prof. Dr. Bahadır K. KÖRBAHTI*  
Mersin University Engineering Faculty  
Turkey

*Assist. Prof. Dr. Akın TATOGLU*  
Hartford University College of Engineering  
USA

*Assist. Prof. Dr. Şevket DEMİRCİ*  
Mersin University Engineering Faculty  
Turkey

*Assist. Prof. Dr. Yelda TURKAN*  
Oregon State University  
USA

*Assist. Prof. Dr. Gökhan ARSLAN*  
Mersin University Engineering Faculty  
Turkey

*Assist. Prof. Dr. Seval Hale GÜLER*  
Mersin University Engineering Faculty  
Turkey

*Assist. Prof. Dr. Mehmet ACI*  
Mersin University Engineering Faculty  
Turkey

*Dr. Ghazi DROUBI*  
Robert Gordon University Engineering Faculty  
Scotland, UK

#### **JOURNAL SECRETARY**

*Nida DEMİRTAŞ*  
nidademirtas@mersin.edu.tr

#### **TURKISH JOURNAL OF ENGINEERING (TUJE)**

Turkish Journal of Engineering (TUJE) is a multi-disciplinary journal. The Turkish Journal of Engineering (TUJE) publishes the articles in English and is being published 4 times (January, April, July and October) a year. The Journal is a multidisciplinary journal and covers all fields of basic science and engineering. It is the main purpose of the Journal that to convey the latest development on the science and technology towards the related scientists and to the readers. The Journal is also involved in both experimental and theoretical studies on the subject area of basic science and engineering. Submission of an article implies that the work described has not been published previously and it is not under consideration for publication elsewhere. The copyright release form must be signed by the corresponding author on behalf of all authors. All the responsibilities for the article belongs to the authors. The publications of papers are selected through double peer reviewed to ensure originality, relevance and readability.

#### **AIM AND SCOPE**

The Journal publishes both experimental and theoretical studies which are reviewed by at least two scientists and researchers for the subject area of basic science and engineering in the fields listed below:

- Aerospace Engineering
- Environmental Engineering
- Civil Engineering
- Geomatic Engineering
- Mechanical Engineering
- Geology Science and Engineering
- Mining Engineering
- Chemical Engineering
- Metallurgical and Materials Engineering
- Electrical and Electronics Engineering
- Mathematical Applications in Engineering
- Computer Engineering
- Food Engineering

#### **PEER REVIEW PROCESS**

All submissions will be scanned by iThenticate® to prevent plagiarism. Author(s) of the present study and the article about the ethical responsibilities that fit PUBLICATION ETHICS agree. Each author is responsible for the content of the article. Articles submitted for publication are priorly controlled via iThenticate® (Professional Plagiarism Prevention) program. If articles that are controlled by iThenticate® program identified as plagiarism or self-plagiarism with more than 25% manuscript will return to the author for appropriate citation and correction. All submitted manuscripts are read by the editorial staff. To save time for authors and peer-reviewers, only those papers that seem most likely to meet our editorial criteria are sent for formal review. Reviewer selection is critical to the publication process, and we base our choice on many factors, including expertise, reputation, specific recommendations and our own previous experience of a reviewer's characteristics. For instance, we avoid using people who are slow, careless or do not provide reasoning for their views, whether harsh or lenient. All submissions will be double blind peer reviewed. All papers are expected to have original content. They should not have been previously published and it should not be under review. Prior to the sending out to referees, editors check that the paper aim and scope of the journal. The journal seeks minimum three independent referees. All submissions are subject to a double blind peer review; if two of referees gives a negative feedback on a paper, the paper is being rejected. If two of referees gives a positive feedback on a paper and one referee negative, the editor can decide whether accept or reject. All submitted papers and referee reports are archived by journal Submissions whether they are published or not are not returned. Authors who want to give up publishing their paper in TUJE after the submission have to apply to the editorial board in written. Authors are responsible from the writing quality of their papers. TUJE journal will not pay any copyright fee to authors. A signed Copyright Assignment Form has to be submitted together with the paper.

### **PUBLICATION ETHICS**

Our publication ethics and publication malpractice statement is mainly based on the Code of Conduct and Best-Practice Guidelines for Journal Editors. Committee on Publication Ethics (COPE). (2011, March 7). Code of Conduct and Best-Practice Guidelines for Journal Editors. Retrieved from [http://publicationethics.org/files/Code%20of%20Conduct\\_2.pdf](http://publicationethics.org/files/Code%20of%20Conduct_2.pdf)

### **PUBLICATION FREQUENCY**

The TUJE accepts the articles in English and is being published 4 times (January, April, July and October) a year.

### **CORRESPONDENCE ADDRESS**

Journal Contact: [tuje@mersin.edu.tr](mailto:tuje@mersin.edu.tr)

# CONTENTS

*Volume 3 – Issue 4*

## ARTICLES

<b>CLOSED LOOP SUPPLY CHAIN MANAGEMENT PERFORMANCE EVALUATION CRITERIA</b> <i>Emel Yontar and Süleyman Ersöz</i> .....	157
<b>AUTOMATIC DETECTION OF CYBERBULLYING IN FORMSPRING.ME, MYSPACE AND YOUTUBE SOCIAL NETWORKS</b> <i>Çiğdem İnan Acı, Eren Çürük and Esra Saraç Eşsiz</i> .....	168
<b>BEHAVIOR OF R/C FRAMES WITH CONCRETE PLATE BONDED INFILLS</b> <i>Mehmet Baran</i> .....	179
<b>LOGIC THRESHOLD FOR MICRORING RESONATOR-BASED BDD CIRCUITS: PHYSICAL AND OPERATIONAL ANALYSES</b> <i>Ozan Yakar and İlke Ercan</i> .....	189
<b>EXPERIMENTAL INVESTIGATION OF A NOVEL FRICTION MODIFIER IN COMPOSITE MATERIALS</b> <i>İlker Sugözü and Mücahit Güdük</i> .....	197
<b>REMOVAL OF COLOUR POLLUTIONS IN DYE BATHS WITH MORDANTS</b> <i>Aslıhan Koruyucu</i> .....	201
<b>FLEXURAL BEHAVIOR OF HYBRID FRP-CONCRETE BRIDGE DECKS</b> <i>İlker Fatih Kara, Ashraf F. Ashour and Cahit Bilim</i> .....	206

# Turkish Journal of Engineering



*Turkish Journal of Engineering (TUJE)*  
*Vol. 3, Issue 4, pp. 157-167, October 2019*  
*ISSN 2587-1366, Turkey*  
*DOI: 10.31127/tuje.503959*  
*Research Article*

## **CLOSED LOOP SUPPLY CHAIN MANAGEMENT PERFORMANCE EVALUATION CRITERIA**

Emel Yontar \*<sup>1</sup> and Süleyman Ersöz <sup>2</sup>

<sup>1</sup>Tarsus University, Vocational High School, 33400 Mersin, Turkey  
ORCID ID: 0000-0001-7800-2960  
eyontar@tarsus.edu.tr

<sup>2</sup>Kırıkkale University, Faculty of Engineering, Department of Industrial Engineering, 71450 Kırıkkale, Turkey  
ORCID ID: 0000-0002-7534-6837  
serso40@hotmail.com

---

\* Corresponding Author

Received: 27/12/2018 Accepted: 11/02/2019

---

### **ABSTRACT**

Evaluating chain performance to develop an effective supply chain has become a necessity because it plays a critical role in the success of businesses. The most important decision to evaluate the chain performance is the correct selection of indicators. The closed-loop supply chain method consists of a whole of forward and reverse logistics activities. For this reason, advanced supply chain management and reverse supply chain management performances are handled separately in this study. The performance evaluation criteria which are discussed by the authors who work on the supply chain management performance evaluation issues are analyzed and it is stated that the authors make a study by taking into consideration the evaluation criteria. At the same time, the articles examined in reverse supply chain management performance evaluation studies are examined and all criteria are summarized as a table. In the light of these studies, the planned criteria for the use of closed loop supply chain management performance evaluation of the enterprises have emerged. With the main criteria being divided into Economic, Social and Environmental headings, which are supposed to bring innovation to the literature, the sub-criteria are detailed. These titles were brought together both for the first time in closed loop supply chain management performance evaluation and as a main topic in advanced supply chain management. The performance criteria reduced to subheadings will help the experts to continue their studies, and it is thought that they will guide the future studies.

**Keywords:** *Closed Loop, Supply Chain Management, Performance Evaluation*

## 1. INTRODUCTION

The closed loop supply chain concept was first described by Thierry *et al.* made in 1995 by "strategic issues related to product recovery" is at study "integrated systems" has been defined as. Closed loop supply chain management is a concept that emerges when product recovery is both economically and environmentally valuable and growing in importance. Research on the subject has a history of about 20 years and the origin of this concept stems from the reverse logistics literature.

Closed loop supply chain is expressed as the implementation and re-introduction of the end-of-life products (End-Of-Life) from the end-use point and to recycle them to make them re-valued. (Thierry *et al.* 1995, Guide *et al.* 2003).

Another general recognition by the forward and reverse supply chain system operates as an integrated structure (Fig. 1) is expressed as (Fleischmann *et al.*, 1997; Paksoy, 2012; Talbot, 2006);

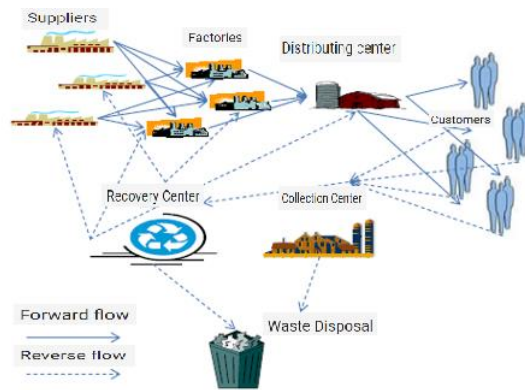


Fig. 1. Closed loop supply chain

The closed loop supply chains collect products from the raw material suppliers through the collection channels of the products used by the customers and produced in the production facilities of the products and delivered to the customers with various distribution channels. Then, by providing recycling, it considers the entirety of a forward and reverse logistics operations.

The closed loop supply chain is an important structure that integrates reproduction and reverse logistics. The closed loop enables the establishment of a triple network between the community, the enterprise and the environment.

According to Van Nunen and Zuidwijk (2004), Prahinski and Kocabaşoğlu (2006), the main reasons for supply chain and closed loop supply chain to be more important (Mondragon *et al.* 2011):

- the amount of product returns which can be very high;
- sales opportunities in secondary of products considered previously discarded;
- the adoption of recycling and environmentally friendly recycling and disposal policies;
- the adoption of laws making manufacturers responsible for handling their products once their life ends;
- the emergence of alternatives including repackaging, remanufacturing and recycling; and

- consumers have more rights to return products that do not meet their expectations.

The most important of these basic reasons are the high return on product quantities. Because the technological rapid changes in the electronic sector cause the users to change their products frequently.

As a result, businesses that integrate product recycling systems into existing supply chain structures can lead to the following opportunities (Pochampally *et al.* 2009):

- Saving natural resources
- Energy saving
- Clean air and water saving
- Save waste
- Economic savings

With this information, it can be said that the reverse supply chain and closed loop supply chain network structures increase the competitiveness and customer satisfaction levels of the enterprises and lower the production costs (Demirel and Gökçen, 2008a). It is a fact that these benefits have been provided by various companies such as Dell, HP, Kodak, GM and Xerox for years (Akçalı and Çetinkaya, 2011). Kodak and Xerox reproduce the used products and take them to secondary markets for resale. For example, Xerox has saved approximately \$ 200 million over the last five years from the reproduction of single-use cameras (Vishwa *et al.* 2010). According to another example, Kodak uses an average of 76% of a used camera in the production of a new camera (Savaşkan *et al.* 2004). In the US, 20% of glass, 30% of paper products and 61% of aluminum cans are recycled; 10 million cars and 95% of the trucks are recycled every year and 75% of these vehicles can be recycled for reuse (Demirel and Gökçen, 2008a). Dell has implemented the 'Recycling your Dell' program to recover useful components from used computers. According to a study, 58% re-use and re-fabrication can be made in products such as washing machines, computers, telephones and refrigerators. Recycling activities performed at these rates have been found to reduce the production costs significantly (Akçalı and Çetinkaya, 2011).

## 2. LITERATURE REVIEW

Extensive preliminary studies on reverse supply chain and closed loop supply chain networks were conducted by Fleischmann *et al.* 1997. In these studies, quantitative models of recycling in logistics activities were examined and a general framework was provided to the researchers. Within the framework of the presented framework, it was emphasized that 3 main topics should be included in distribution design (forward and reverse direction), stock control (zero and used product) and production planning (assembly and disassembly) in the network designs containing recycling.

In this study, closed loop supply chain management in many subjects such as network design, solution-oriented modeling studies, production planning, capacity planning, vehicle routing and facility selection has been discussed in the literature.

Bloemhof-Ruwaard *et al.* (2005), Amaro and Barbosa-Povoa (2009), in the closed-loop supply chain, have studied in mixed integer programming model. Amin and Zhang (2013), studied stochastic mixed integer linear

programming model, Paydar *et al.* (2017), studied a mixed integer linear programming model.

In addition to these modeling studies, other studies that have been published in the literature that Hu *et al.* (2002), a model of discrete / continuous analytical structure, Krikke *et al.* (2003), a model development in which both product design and logistics network design are discussed, Sheu *et al.* (2005) have developed a multi-purpose inventory model with a multi-purpose optimization model, Özceylan *et al.* (2014) developed an integrated model that optimizes both strategic and tactical decisions of a closed loop supply chain, Shakourloo *et al.* (2016) developed with a general network model for closed loop procurement management.

Another area of work in closed loop supply chain management is network design. Qiang *et al.* (2013), Aldemir (2016), have studied the issue of network design. At the same time Paksoy *et al.* (2011) examined the network design for multiple product closed loop supply chain. Özceylan *et al.* (2017) ELV realized a network design for the recycling system.

The literature gains increased with different studies. Schultmann *et al.* (2006) worked on vehicle routing problem in closed loop supply chain management. Kenne *et al.* (2012), Otay (2015) studied production planning. Chen *et al.* (2017), also performed inventory control studies.

Lu and Bostel (2007) addressed the problem of plant layout in closed loop supply chain management. Tsao *et al.* (2016) covered the literature by examining the effects of RFID in closed loop supply chain management. Finally, Olugu and Wang (2011) conducted a performance evaluation study on closed-loop supply chain management for the automotive sector.

After a detailed literature review of the closed loop supply chain management, it was observed that many subjects were studied. However, due to the low number of studies conducted with performance evaluation, it is thought that our study will have an important place in the literature.

### **3. PERFORMANCE EVALUATION CRITERIA AT CLOSED LOOP SUPPLY CHAIN MANAGEMENT**

Performance is a qualitative or quantitative expression of what an individual, a group, or an organization doing a job can achieve and what they can achieve in order to achieve that goal (Karakaş *et al.*, 2003).

Evaluation of operational performance; is a sequence of operations that determines the extent to which businesses have reached their predetermined objectives, olup, determining performance objectives, performance measurement, feedback and motivation stages of the performance management process (Zerenler, 2005). It is difficult to analyze the target and the current situation for a process that cannot be evaluated, and identify the points that are open to improvement and direct the resources to these points. An effective management depends on an effective evaluation of performance results.

In this respect, it is a necessity to evaluate the chain performance in order to develop an effective and effective supply chain, as enterprises play a critical role in their success.

Closed-loop supply chain method, because it is a totality of forward and reverse of the logistics activities, it is necessary to combine performance criteria with forward supply chain management and reverse supply chain management performances, taking into account the studies conducted in the literature.

Supply chain performance has many elements in it. These elements are composed of many variables that can be measured by quantitative and qualitative methods. There are a number of studies on supply chain performance in the literature, and a significant part of them has been focused on the evaluation of supply chain performance and the criteria used in performance evaluation. However, there are few studies conducted for closed loop supply chain management performance evaluation.

Developing a system to measure the performance of the supply chain requires the right selection of criterias. In the Table 1, by evaluating the performance evaluation criteria of 53 authors, it is stated that the authors make a study by considering the evaluation criteria.

The authors of the criteria they use in their work are given in Table 1 as the main title, these main criteria were reduced to independent sub-headings. Criteria were used; Cost-18, Flexibility-18, Financial/Economic-13, Customer Satisfaction/Return-13, Innovation-12, Quality-10, Time-9, Internal Process-8, Responsiveness-8, Assets-7, Reliability-7 times in these studies. 19 criteria are used (Competitiveness, Lead Time, Lead-Time Variability, Dependent Variables, Independent Variables, Non-Financial, Society, Diagnostic Measures, Integration, Marketing, System Dynamics, Operations Research, Profitability, Order Book Analysis, Pricing, Facility, Human, Capacity, Including Trading Partners Measures) in performance evaluation by taking part in 1 study.



supply chain management performance evaluation studies are discussed.

As in the supply chain performance evaluation analysis, in the case of reverse supply chain management performance evaluation studies, the evaluation criteria of the authors were studied. (Table 2).

The criterias used Customer/Customer Service/Stakeholder-13, Innovation and Growth-10, Financial-9, Process/ Internal and External-9, Environmental-7, Recovery (Asset/Value/Product/Facility)-5, Suppliers/Supplier

Commitment-4 times in these studies. The 22 criterions used in the evaluation (Legal Programs, Manufacturers, Distributors, Intermediate Measures, Management Commitment, Material Features, Recycling Efficiency, Recycling Cost, Dependability, Cost Efficiency, Returns Flow and Time Related, Collection, Degree of Disassembly, Manufacturing Plant, Distribution Center/Warehouse, Lead Time, Products Reused, Products Remanufactured, Products Recycled, Products Parts Harvested, Input Quantity Level, Output Quantity Level) were included in the literature by the authors once.

Table 2. Reverse Supply Chain Performance evaluation metrics according to the authors

Author	Metrics	1	2	3	4	5	6	7	8	9	10	11	12	13	14	15	16	17	18	19	20	21	22	23	24	25	26	27	28	29	30	31	32	33	34	35	36	37	38			
Yellepeddi et. al. (2005)		o	o	o	o																																					
Wang (2006)		o	o	o	o																																					
Yellepeddi (2006)								o	o	o	o																															
Yang et. al. (2009)		o	o	o	o	o																																				
Hernandez et. al. (2009)													o	o	o																											
Tonanont (2009)		o					o				o																				o	o										
Yang (2010)		o	o	o	o	o																																				
Nizaroyani (2010)						o	o									o	o											o	o													
Arun et. al. (2011)							o	o	o	o																																
Olugu and Wong (2011)		o									o												o	o	o	o																
Shaik and Abdul-Kader (2012)		o	o	o	o	o						o																														
Momeni et. al. (2014)		o									o								o	o	o																					
Bansia et. al. (2014)		o	o	o	o																																					
Pandian (2014)																																			o	o	o	o	o	o	o	o
Shaik (2014)		o	o	o	o	o						o																														
Guimaraes and Salomon (2015)		o											o	o	o			o																								
Moshtaghfard et. al. (2016)		o	o	o	o	o																																				
Butar et. al. (2016)						o											o	o									o															
Fernandes et. al. (2016)		o	o	o	o	o					o	o																														
Sangwan (2017)							o	o																															o			

(1-Customer/Customer Service/Stakeholder 2-Financial 3-Process/ Internal and External 4-Innovation and Growth 5-Environmental 6- Recovery (Asset/Value/Product/Facility) 7- Sorting and Storing/Inspection and Sorting 8-Gate Keeping 9-Transportation 10-Suppliers/Supplier Commitment 11-Social 12-Economic Programs 13-Image Programs 14-Citizenship Programs 15-Flexibility 16-Quality 17-Legal Programs 18-Manufacturers 19-Distributors 20-Intermediate Measures 21-Management Commitment 22-Material Features 23-Recycling Efficiency 24-Recycling Cost 25-Dependability 26-Cost Efficiency 27>Returns Flow and Time Related 28-Collection 29-Degree of Disassembly 30-Manufacturing Plant 31-Distribution Center/Warehouse 32-Lead Time 33-Products Reused 34-Products Remanufactured 35-Products Recycled 36-Products Parts Harvested 37-Input Quantity Level 38-Output Quantity Level)

As a result of these studies, the performance criteria in forward supply chain and reverse supply chain management were analyzed in detail and the criteria that are planned to be used in performance evaluation in closed loop supply chain management are determined in our study. As shown in Fig. 2, the criteria of the study are exemplary of many studies.

The main headings and sub-headings that will bring innovation to the supply chain performance evaluation

criteria are; It has been called Economic, Social and Environmental. These headings, which are used in different studies in reverse supply chain management, have been brought together both for the first time in closed loop supply chain management performance evaluation and as a main topic in forward supply chain management.

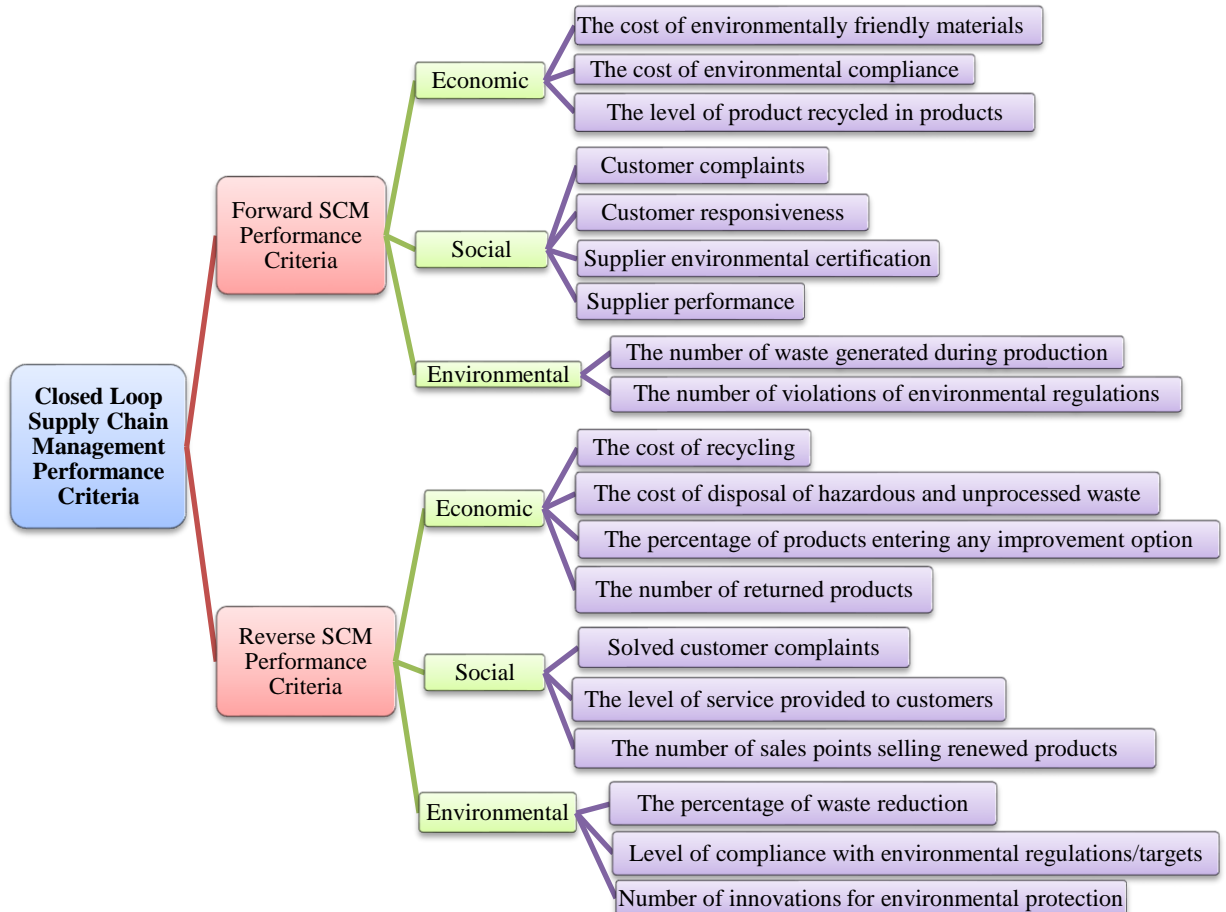


Fig. 2. Closed loop supply chain management performance criteria

Sub-headings of economic criteria in forward supply chain management performance criteria; the cost of environmentally friendly materials, the cost of environmental compliance, the level of product recycled in products. Sub-headings of social criterion; customer complaints, customer responsiveness, supplier environmental certification, supplier performance and Finally, the sub-headings of environmental criteria are the number of waste generated during production and the number of violations of environmental regulations.

The sub-headings of the economic criterion in the reverse supply chain performance evaluation criteria, which is another area of evaluation; the cost of recycling, the cost of disposal of hazardous and unprocessed waste, the percentage of products entering any improvement option, and the number of returned products. The sub-headings of the social criterion are selected as follows; solved customer complaints, the level of service provided to customers, the number of sales points selling renewed products. The sub-headings of the environmental

criterion, which is another main topic; percentage of waste reduction, level of compliance with environmental regulations/targets and number of innovations for environmental protection.

As can be seen, businesses that want to examine their chain performances with their environmentally compatible, economic and social indicators can perform performance evaluation and analyze their deficiencies by using these criteria. Starting with the improvement studies, it allows businesses to increase their competition rate by keeping pace with our age with less waste and more efficient working methods.

#### 4. CONCLUSION

In the literature on closed loop supply chain management, closed loop supply chain management has been the subject of many topics such as network design, solution-oriented modeling studies, production planning, capacity planning, vehicle routing, facility location

selection. However, performance evaluation in closed loop supply chain management is quite low. As a result of this, forward and reverse supply chain management performance evaluation studies were investigated. In our study; supply chain management issues 53 articles evaluating employee performance, employee performance evaluation reverse supply chain management issues 20 articles were discussed. The performance evaluation criteria discussed by these studies were analyzed. It is stated that the authors are working by taking into account the evaluation criteria. In 73 articles analyzed, performance criteria are summarized by converting them into tables. As a result of these studies, the criteria that are planned to be used in closed loop supply chain management performance evaluation of the enterprises are determined in our study.

The study's criteria are sufficient to be an example to many studies. The main topics that will bring innovation to the supply chain performance evaluation criteria, which are composed of main headings and sub-headings, have economic, social and environmental headings. These main criteria are handled separately by different authors in the literature. In the studies Yellepeddi *et al.* (2005), Wang (2006) Yang (2010), Shaik and Abdul-Kader (2012), Bansia *et al.* (2014), Shaik (2014), Moshtaghfar *et al.* (2016), Fernandes *et al.* (2016) studied this heading in reverse supply chain management. Likewise, in the forward supply chain management Fitzgerald *et al.* (1991), Kaplan and Norton (1997), Brewer and Speh (2000), Bullinger *et al.* (2002), Tao (2009), Xu *et al.* (2009), Rodriguez-Rodriguez *et al.* (2010), Özbakır (2010), Zhu (2010) Shafiee and Shams-e-alam (2011), Carvalho and Azevedo (2012) Golrizgashti (2014), Shi and Gao (2016) studied as the main criteria of the economic title. The environmental main criteria has not been studied as a head of forward supply chain management, as it involves more recycling issues. As a result, Yang *et al.* (2009), Yang (2010), Nizaroyani (2010) Shaik and Abdul-Kader (2012), Shaik (2014), Moshtaghfar *et al.* (2016), Fernandes *et al.* (2016) considered environmental criteria in their studies. Although the social criteria is less preferred, Shaik and Abdul-Kader (2012), Shaik (2014), Fernandes *et al.* (2016), Chimhamhiwa *et al.* (2009) were used by.

In our study, economic, environmental and social criteria are compiled together. The main topics that will bring innovation to the supply chain performance evaluation criteria consisting of main headings and subheadings have been economic, social and environmental headings. These headings are put together for the first time in closed loop supply chain management performance evaluation. Innovations were made to the literature by using it as the main topic in forward supply chain management. The performance criteria, which are then reduced to subheadings, have been detailed to help the experts to continue their study. For this purpose, businesses that want to examine chain performances can perform performance evaluation using these criteria and they can analyze our deficiencies and implement improvement studies.

## REFERENCES

Ağar F., Tedarik zinciri yönetiminde scor modeli, tedarik süreci performans değerlendirmesi ve scorcard

uygulaması, İstanbul Teknik Üniversitesi, Fen Bilimleri Enstitüsü Yüksek Lisans Tezi, İstanbul, 2010.

Akçali, E. and Çetinkaya, S., Quantitative models for inventory and production planning in closed-loop supply chains, *International Journal Of Production Research*, 49 (8), 2373–2407, 2011.

Aldemir G., A Closed loop sustainable supply chain network design for waste electrical & electronic equipment, Yüksek Lisans Tezi, İstanbul Teknik Üniversitesi, İstanbul, 2016.

Alomar, Madani, and Zbigniew J. Pasek. "Linking supply chain strategy and processes to performance improvement." *Procedia CIRP* 17 (2014): 628-634.

Amaro, A. C. S., and Barbosa-Povoa, A. P. F. D.. The effect of uncertainty on the optimal closed-loop supply chain planning under different partnerships structure. *Computers & Chemical Engineering*, 33(12), 2144–2158, 2009.

Amin, S. H., Zhang, G., A Multi-Objective facility location model for closed-loop supply chain network under uncertain demand and return, *Applied Mathematical Modelling*, 37 (2013) 4165–4176, 2013.

Anand, Neeraj, and Neha Grover. "Measuring retail supply chain performance: Theoretical model using key performance indicators (KPIs)." *Benchmarking: An international journal* 22.1 (2015): 135-166.

Angerhofer, Bernhard J., and Marios C. Angelides. "A model and a performance measurement system for collaborative supply chains." *Decision support systems* 42.1 (2006): 283-301.

Aramyan, Lusine H., *et al.* "Performance measurement in agri-food supply chains: a case study." *Supply Chain Management: An International Journal* 12.4 (2007): 304-315.

Arif-Uz-Zaman, Kazi, and A. M. M. Nazmul Ahsan. "Lean supply chain performance measurement." *International Journal of Productivity and Performance Management* 63.5 (2014): 588-612.

Arun Vasantha Geethan, K., S. Jose, and C. Sunil Chandar. "Methodology for performance evaluation of reverse supply chain." *International Journal of Engineering and Technology* 3.3 (2011): 213-224

Ayçın E., Özveri O., Bulanık modelleme ile tedarik zinciri performansının değerlendirilmesi ve imalat sektöründe bir uygulama, *Journal of Economics and Administrative Sciences*-Volume: XVII Issue:1, 51-60, 2015.

Aydoğdu F., Tedarik Zinciri Yönetiminde SCOR Modeli ve veri zarflama analizi entegrasyonu, Yüksek Lisans Tezi, Endüstri Mühendisliği, Gazi Üniversitesi, Fen Bilimleri Enstitüsü, Ankara, 2011.

Bagchi, Prabir K. "Role of benchmarking as a competitive strategy: the logistics

- experience." *International Journal of Physical Distribution & Logistics Management* 26.2 (1996): 4-22.
- Bansia, Milind, Jayson K. Varkey, and Saurabh Agrawal. "Development of a Reverse Logistics Performance Measurement System for a battery manufacturer." *Procedia Materials Science* 6 (2014): 1419-1427.
- Beamon, Benita M. "Measuring supply chain performance." *International journal of operations & production management* 19.3 (1999): 275-292.
- Beamon, Benita M. "Supply chain design and analysis: Models and methods." *International journal of production economics* 55.3 (1998): 281-294.
- Beierlein, James G., and Christopher A. Miller. "Performance Measures, and Measurement in Supply Chains in the Food System." *Food Industry Report* (2000).
- Bloemhof-Ruwaard, J.M., Van Wassenhove, L.N., Gabel, H.L. And Weaver, P.M., An environmental life cycle optimization model for the European pulp and paper industry, *Omega*, 24 (6), 615–629, 2005.
- Brewer, Peter C., and Thomas W. Speh. "Using the balanced scorecard to measure supply chain performance." *Journal of Business logistics* 21.1 (2000): 75.
- Bullinger, Hans-Jörg, Michael Kühner, and Antonius Van Hoof. "Analysing supply chain performance using a balanced measurement method." *International Journal of Production Research* 40.15 (2002): 3533-3543.
- Butar, Maulida Butar, David Sanders, and Regina Frei. "Measuring performance of reverse supply chains in a carpet manufacturer." *Journal of Advanced Management Science* 4.2 (2016): 152-158.
- Cai, Jian, *et al.* "Improving supply chain performance management: A systematic approach to analyzing iterative KPI accomplishment." *Decision support systems* 46.2 (2009): 512-521.
- Carvalho, Helena, Susana Garrido Azevedo, and Virgilio Cruz-Machado. "Agile and resilient approaches to supply chain management: influence on performance and competitiveness." *Logistics research* 4.1-2 (2012): 49-62.
- Chae, Bongsug. "Developing key performance indicators for supply chain: an industry perspective." *Supply Chain Management: An International Journal* 14.6 (2009): 422-428.
- Chan, Felix TS, *et al.* "A conceptual model of performance measurement for supply chains." *Management decision* 41.7 (2003): 635-642.
- Chen Vd., Inventory management in a closed-loop supply chain with advance demand information, *Operations Research Letters* 45, 175–180, 2017.
- Chimhamhiwa, Dorman, *et al.* "Towards a framework for measuring end to end performance of land administration business processes—A case study." *Computers, environment and urban systems* 33.4 (2009): 293-301.
- Cho, Dong Won, *et al.* "A framework for measuring the performance of service supply chain management." *Computers & Industrial Engineering* 62.3 (2012): 801-818.
- De Toni, Alberto, and Stefano Tonchia. "Performance measurement systems-models, characteristics and measures." *International Journal of Operations & Production Management* 21.1/2 (2001): 46-71.
- Demirel, N. and Gökçen, H., A Mixed integer programming model for remanufacturing in reverse logistics environment, *International Journal of Advanced Manufacturing Technology*, 39 (11–12), 1197–1206, 2008a.
- Easwaran, G. and Üster, H., A Closed-Loop supply chain network design problem with integrated forward and reverse channel decisions, *IIE Transactions*, 42 (11), 779–792, 2010.
- Elrod, Cassandra, Susan Murray, and Sundeep Bande. "A review of performance metrics for supply chain management." *Engineering Management Journal* 25.3 (2013): 39-50.
- Fernandes, Sheila Mendes, *et al.* "Systematic literature review on the ways of measuring the of reverse logistics performance." *Gestão & Produção AHEAD* (2017): 0-0.
- Fitzgerald, L., Johnston, R., Brignall, S., Silvestro, R. and Voss, C., "Performance measurement in service businesses." *Management Accounting* 69.10 (1991): 34-36.
- Fleisch, Elgar, and Christian Tellkamp. "Inventory inaccuracy and supply chain performance: a simulation study of a retail supply chain." *International journal of production economics* 95.3 (2005): 373-385.
- Fleischmann, M., Bloemhof-Ruwaard, J.M., Dekker, R., Van Der Laan, E., Van Nunen, J.A.E.E. And Van Wassenhove, L.N., Quantitative models for reverse logistics: a review, *European Journal Of Operational Research*, 103 (1), 1–17, 1997.
- Gamme N., Johansson M., Measuring Supply Chain Performance Through KPI Identification and Evaluation, *Department of Technology Management and Economics, Master's thesis in "Supply Chain Management" and "Quality and Operations Management", Chalmers University of Technology, Gothenburg, Sweden* 2015.
- Ganga, Gilberto Miller Devós, Luiz Cesar Ribeiro Carpinetti, and Paulo Rogério Politano. "A fuzzy logic approach to supply chain performance management." *Gestão & Produção* 18.4 (2011): 755-774.

- Golrizgashti, Seyedehfatemeh. "Supply chain value creation methodology under BSC approach." *Journal of Industrial Engineering International* 10.3 (2014): 67.
- Guide, V. D. R., Jayaraman V., Linton J. D., Building Contingency Planning For Closed-Loop Supply Chains With Product Recovery, *Journal Of Operations Management*, 21 (2003) 259–279, 2003.
- Guimarães da Silveira, José Leonardo, and Valério Antonio Pamplona Salomon. "ANP applied to the evaluation of performance indicators of reverse logistics in footwear industry." *Procedia Computer Science* 55 (2015): 139-148.
- Gunasekaran, Angappa, Chaitali Patel, and Ercan Tirtiroglu. "Performance measures and metrics in a supply chain environment." *International journal of operations & production Management* 21.1/2 (2001): 71-87.
- Gunasekaran, Angappa, Christopher Patel, and Ronald E. McGaughey. "A framework for supply chain performance measurement." *International journal of production economics* 87.3 (2004): 333-347.
- Hernández, Cecilia Toledo, *et al.*. "Using AHP and ANP to evaluate the relation between reverse logistics and corporate performance in Brazilian automotive industry." *Proceeding of Proceedings of the 10th International Symposium on the Analytic Hierarchy/Network Process Multi-criteria Decision Making held at Pennsylvania, USA*. 2009.
- Hu, T., Sheu, J. And Huan, K., A Reverse logistics cost minimization model for the treatment of hazardous wastes, *Transportation Research Part E*, 38 (6), 457–473, 2002.
- Kaplan, R.S., Norton, D.P., *Balanced scorecard: translating strategy into action*. 4 th Edition. Harvard Business School Press, Boston, 1997.
- Karakaş, B. and Ak R., "Kamu yönetiminde performans yönetimi önemli midir?", *Kamu Yönetiminde Kalite* 3. Ulusal Kongresi Bildirileri, TODAİE Yayınları No: 319, Ankara, 2003, ss. 337-351.
- Kenne, J.-P., Dejax, P. and Gharbi, A., Production planning of a hybrid manufacturing-remanufacturing system under uncertainty within a closed-loop supply chain, *International Journal Of Production Economics*, 135 (1), 81–93, 2012.
- Kocaoğlu B., Tedarik zinciri performansı ölçümü için stratejik ve operasyonel hedefleri bütünleştiren SCOR modeli temelli bir yapı, *Doktora Tezi, Yıldız Teknik Üniversitesi, Fen Bilimleri Enstitüsü, İstanbul*, 2009.
- Krikke, H., Bloemhof-Ruwaard, J. and Van Wassenhove, L.N., 2003, Concurrent product and closed-loop supply chain design with an application to refrigerators, *International Journal of Production Research*, 41 (16), 3689–3719, 2003.
- Li, Zhengping, Xiaoxia Xu, and Arun Kumar. "Supply chain performance evaluation from structural and operational levels." *Emerging Technologies and Factory Automation, 2007. ETFA. IEEE Conference on. IEEE*, 2007.
- Lu, Z., and Bostel, N., A Facility location model for logistics systems including reverse flows: the case of remanufacturing activities. *Computers & Operations Research*, 34(2), 299–323, 2007.
- Momeni, Ehsan, *et al.*. "A new fuzzy network slacks-based DEA model for evaluating performance of supply chains with reverse logistics." *Journal of Intelligent & Fuzzy Systems* 27.2 (2014): 793-804.
- Mondragon, A.E.C., Lalwani, C. And Mondragon, C.E.C., Measures for auditing, performance and integration in closed-loop supply chains, *Supply Chain Management: An International Journal*, 16 (1), 43–56, 2011.
- Moshtaghfar R., Arbabshirani B., Alinaghian M., Reverse Logistics Performance Measurement by Integrated Balanced Scorecard and Data Envelopment Analysis (Case Study in Pak Dairy Co.), *International Journal of Advances in Management Science (IJ-AMS)*, Volume 5, 2016.
- Narasimhan, Ram, Jayaram Jayanth, Causal linkages in supply chain management: an exploratory study of north American manufacturing firms", *Decision Sciences*, Volume 29, Number 3, Summer, 1998.
- Neely, Andy, Mike Gregory, and Ken Platts. "Performance measurement system design: a literature review and research agenda." *International journal of operations & production management* 15.4 (1995): 80-116.
- Nizaroyani, Saibani, *Performance measurement for reverse and closed-loop supply chains*. Diss. University of Nottingham, 2010.
- Olugu E. U. and Wong K. Y., Fuzzy logic evaluation of reverse logistics performance in the automotive industry, *Scientific Research and Essays* Vol. 6(7), pp. 1639-1649, 4 April, 2011.
- Otay İ., Geri kazanımlı kapalı çevrim tedarik zinciri için dağıtım planlama, *Doktora Tezi, İstanbul Teknik Üniversitesi, Fen Bilimleri Enstitüsü, İstanbul*, 2015.
- Otto, Andreas, and Herbert Kotzab. "Does supply chain management really pay? Six perspectives to measure the performance of managing a supply chain." *European Journal of Operational Research* 144.2 (2003): 306-320.
- Özalp Ö., Tedarik zinciri performansının ölçümü: ekonomik katma değer yönteminin analizi, *Dokuz Eylül Üniversitesi, Sosyal Bilimler Enstitüsü, Yüksek Lisans Tezi, İzmir*, 2016.
- Özbakır S., Tedarik zincirinde dengeli performans kartı yaklaşımı, *İstanbul Üniversitesi, Sosyal Bilimler*

Enstitüsü, İşletme Anabilim Dalı, Yüksek Lisans Tezi, İstanbul, 2010.

Özceylan E. *et al.*, A Closed-Loop supply chain network design for automotive industry in Turkey, *Computers & Industrial Engineering* Xxx, Xxx–Xxx, 2017.

Özceylan, E., Paksoy, T., Ve Bektaş, T., Modeling and optimizing the integrated problem of closed-loop supply chain network design and disassembly line balancing, *Transportation Research Part E: Logistics and Transportation Review*, 61, 142-164, 2014.

Paksoy, T. and Özceylan, E., Supply chain optimization with u-type assembly line balancing, *International Journal of Production Research*, 50 (18), 5085– 5105, 2012.

Paksoy, T., Bektaş, T. and Özceylan, E., Operational and environmental performance measures in a multi-product closed-loop supply chain, *Transportation Research Part E*, 47 (4), 532–546, 2011.

Pandian G., Performance Evaluation of a Reverse Logistics Enterprise-An Agent-Based Modelling Approach, *A Thesis the Degree of Master of Applied Science University of Windsor, Department of Industrial and Manufacturing Systems Engineering, Windsor, Ontario, Canada*, 2014.

Paydar vd., An engine oil closed-loop supply chain design considering collection risk, *Computers And Chemical Engineering* 104, 38–55, 2017.

Persson, Fredrik, and Jan Olhager. "Performance simulation of supply chain designs." *International journal of production economics* 77.3 (2002): 231-245.

Pires, Sílvia RI, and Carlos HM Aravechia. "Measuring supply chain performance." *Anais da XII annual conference of POMS*. 2001.

Pochampally, K.K., Nukala, S. And Gupta, S.M., Strategic planning models for reverse and closed-loop supply chains, CRC Press, U.S.A, 2009.

Prahinski, C. and Kocabaşoğlu, C., Empirical research opportunities in reverse supply chains, *Omega*, 34 (6), 519–32, 2006.

Qiang, Q., Ke, K., Anderson, T. and Dong, J., The Closed-Loop supply chain network with competition, Distribution Channel Investment, And Uncertainties, *Omega*, 41 (2), 186–194, 2013,

Rodriguez-Rodriguez, Raul, *et al.*. "Building internal business scenarios based on real data from a performance measurement system." *Technological Forecasting and Social Change* 77.1 (2010): 50-62.

Sangwan, Kuldip Singh. "Key activities, decision variables and performance indicators of reverse logistics." *Procedia CIRP* 61 (2017): 257-262.

Savaşkan, R.C., Bhattacharya, S. And Van Wassenhove, L.N.V., Closed-Loop supply chain models with product

remanufacturing, *Management Science*, 50 (2), 239–252, 2004.

Schultmann, F., Zumkeller, M. Ve Rentz, O., Modeling Reverse logistic tasks within closed-loop supply chains: an example from the automotive industry, *European Journal of Operational Research*, 171, 1033–1050, 2006.

Sellitto, Miguel Afonso, *et al.*. "A SCOR-based model for supply chain performance measurement: application in the footwear industry." *International Journal of Production Research* 53.16 (2015): 4917-4926.

Shafiee, Morteza, and N. Shams-e-Alam. "Supply chain performance evaluation with rough data envelopment analysis." *2010 International Conference on Business and Economics Research*. Vol. 1. 2011.

Shaik, Mohammed Najeeb, and Walid Abdul-Kader. "Comprehensive performance measurement and causal-effect decision making model for reverse logistics enterprise." *Computers & Industrial Engineering* 68 (2014): 87-103.

Shakourloo A. Vd., A New Model For More Effective Supplier Selection And Remanufacturing Process In A Closed-Loop Supply Chain, *Applied Mathematical Modelling* 40, 9914–9931, 2016.

Shepherd, Craig, and Hannes Günter. "Measuring supply chain performance: current research and future directions." *Behavioral Operations in Planning and Scheduling*. Springer, Berlin, Heidelberg, 2010. 105-121.

Sheu, J.B., Chou, Y.H. and Hu, C.C., An Integrated logistics operational model for green supply chain management, *Transportation Research Part E*, 41 (4), 287–313, 2005.

Shi, Wenli, and Tianbao Gao. "Supply Chain Performance Evaluation Model Based on Unascertained Clustering." *Rev. Téc. Ing. Univ. Zulia*. Vol. 39, N° 6, 195- 201, 2016.

Sillanpää, Ilkka. "Empirical study of measuring supply chain performance." *Benchmarking: An International Journal* 22.2 (2015): 290-308.

Stock, James R., and Jay P. Mulki. "Product returns processing: an examination of practices of manufacturers, wholesalers/distributors, and retailers." *Journal of business logistics* 30.1 (2009): 33-62.

Şen, E., Kobilerin Uluslararası Rekabet Güçlerini Artırmada Tedarik Zinciri Yönetiminin Önemi", *İGEME Yayınları*, Ankara, 1-56, 2006.

Talbot, S., Lefebvre, E., & Lefebvre, L. A. Closed-Loop supply chain activities and derived benefits in manufacturing SMES. *Journal Of Manufacturing Technology Management*, 18(6), 627–658, 2007.

Tao, Xiaoyan. "Performance evaluation of supply chain based on fuzzy matter-element theory." *Information Management, Innovation Management and Industrial*

*Engineering, 2009 International Conference on.* Vol. 1. IEEE, 2009.

Thierry, M., Salomon, M. And Van Wassenhove L., Strategic Issues in Product Recovery Management, *California Management Review*, 37 (2), 114–135, 1995.

Tonanont, Ake. *Performance evaluation in reverse logistics with data envelopment analysis*. Diss. Thesis for Degree of PhD, Faculty of the Graduate School, University of Texas at Arlington, 2009.

Tsao Vd., Closed-Loop Supply Chain Network Designs Considering RFID Adoption, *Computers & Industrial Engineering* Xxx, Xxx–Xxx, 2016.

Van Hoek, Remko I. "“Measuring the unmeasurable”-measuring and improving performance in the supply chain." *Supply Chain Management: An International Journal* 3.4 (1998): 187-192.

Van Nunen, J.A.E.E. And Zuidwijk, R.A., E-Enabled Closed-Loop Supply Chains, *California Management Review*, 46 (2), 40–53, 2004.

Vishwa, V.K. Chan, F.T.S., Mishra, N. And Kumar, V., Environmental Integrated Closed Loop Logistics Model: An Artificial Bee Colony Approach, 8th International Conference On Supply Chain Management And Information Systems, 1–7, 2010.

Wang, Jui-Chi, and H. Wu. "Corporate performance efficiency investigated by data envelopment analysis and balanced scorecard." *The Journal of American Academy of Business* 9.2 (2006): 312-318.

Xu, Jiuping, Bin Li, and Desheng Wu. "Rough data envelopment analysis and its application to supply chain performance evaluation." *International Journal of Production Economics* 122.2 (2009): 628-638.

Yang, Jianhua, Lidong Zang, and Zhangang Hao. "Study on the performance evaluation system of reverse supply chain based on BSC and triangular fuzzy number AHP." *Information Engineering and Computer Science, 2009. ICIECS 2009. International Conference on.* IEEE, 2009.

Yang, Jianhua. "On the construction and implementation methods for performance measurement of reverse supply chain." *Fuzzy Systems and Knowledge Discovery (FSKD), 2010 Seventh International Conference on.* Vol. 2. IEEE, 2010.

Yavuz O., Ersoy A., Tedarik zinciri performansının değerlendirilmesinde kullanılan değişkenlerin yapay sinir ağı yöntemiyle değerlendirilmesi, *Gazi Üniversitesi İktisadi ve İdari Bilimler Fakültesi Dergisi* 15 /2, 209-256, 2013.

Yellepeddi, S. S., S. Rajagopalan, and D. H. Liles. "A balanced scorecard approach for an effective reverse supply chain in electronics industry." *Proceedings of the Annual Conference of International Journal of Industrial Engineering, Clearwater, Florida, USA, December.* 2005.

Yellepeddi, Srikanth. "An Analytical Network Process (ANP) approach for the development of a reverse supply chain performance index in consumer electronics industry." Faculty of the Graduate School of the University of Texas at Arlington in Partial Fulfillment of the Requirements for the Degree of Doctor of Philosophy, The University of Texas at Arlington (2006).

Yeong-Dong Hwang, Yi-Ching Lin, and Jung Lyu Jr. "The performance evaluation of SCOR sourcing process—The case study of Taiwan's TFT-LCD industry." *International Journal of Production Economics* 115.2 (2008): 411-423.

Zerenler, M. Performans ölçüm sistemleri tasarımı ve üretim sistemlerinin performansının ölçümüne yönelik bir araştırma. *Ekonomi ve Sosyal Araştırmalar Dergisi*, 1: 1-36, 2005.

Zhu, Jiulong. "Notice of Retraction Evaluation of supply chain performance based on BP neural network." *Computer Engineering and Technology (ICCT), 2010 2nd International Conference on.* Vol. 1. IEEE, 2010.

# Turkish Journal of Engineering



*Turkish Journal of Engineering (TUJE)*  
*Vol. 3, Issue 4, pp. 168-178, October 2019*  
*ISSN 2587-1366, Turkey*  
*DOI: 10.31127/tuje.554417*  
*Research Article*

## **AUTOMATIC DETECTION OF CYBERBULLYING IN FORMSPRING.ME, MYSFACE AND YOUTUBE SOCIAL NETWORKS**

Çiğdem İnan Acı <sup>\*1</sup>, Eren Çürük <sup>2</sup> and Esra Saraç Eşsiz <sup>3</sup>

<sup>1</sup> Department of Computer Engineering, Mersin University, 33340, Mersin, Turkey  
ORCID ID 0000-0002-0028-9890  
caci@mersin.edu.tr

<sup>2</sup> Department of Electrical-Electronics Engineering, Mersin University, 33340, Mersin, Turkey  
ORCID ID 0000-0002-4631-7834  
erencuruk@gmail.com

<sup>3</sup> Department of Computer Engineering, Adana Alparslan Türkeş Science and Technology University, 01250, Adana, Turkey  
ORCID ID 0000-0002-2503-0084  
esarac@adanabtu.edu.tr

---

\* Corresponding Author

Received: 16/04/2019 Accepted: 03/05/2019

---

### **ABSTRACT**

Cyberbullying has become a major problem along with the increase of communication technologies and social media become part of daily life. Cyberbullying is the use of communication tools to harass or harm a person or group. Especially for the adolescent age group, cyberbullying causes damage that is thought to be suicidal and poses a great risk. In this study, a model is developed to identify the cyberbullying actions that took place in social networks. The model investigates the effects of some text mining methods such as pre-processing, feature extraction, feature selection and classification on automatic detection of cyberbullying using datasets obtained from Formspring.me, Myspace and YouTube social network platforms. Different classifiers (i.e. multilayer perceptron (MLP), stochastic gradient descent (SGD), logistic regression and radial basis function) have been developed and the effects of feature selection algorithms (i.e. Chi2, support vector machine-recursive feature elimination (SVM-RFE), minimum redundancy maximum relevance and ReliefF) for cyberbullying detection have also been investigated. The experimental results of the study proved that SGD and MLP classifiers with 500 selected features using SVM-RFE algorithm showed the best results (F<sub>measure</sub> value is more than 0.930) by means of classification time and accuracy.

**Keywords:** Cyberbullying, Automatic Detection, Social Networks, Feature Selection, Classification.

## 1. INTRODUCTION

Traditional bullying is defined as aggressive acts that repeatedly occur between individuals with power imbalances that cause harm or distress. Cyberbullying is defined as deliberate and continuous actions that are aggressive towards vulnerable people by using many electronic methods such as internet, e-mail, blog, text and social media message (Snakenborg *et al.*, 2011). Traditional bullying and cyberbullying have similarities, such as power imbalance among individuals, aggressiveness, and the introduction of negative actions. In a study conducted in 2012, the researcher has identified two different types of cyberbullying, as indirect and direct (Langos, 2012). While direct cyberbullying is the only act between the victim and attacker who performs the action, in the indirect cyberbullying, the attacker uses many electronic media to carry action into platforms that can be accessed by more and more people. In addition to these types of actions, cyberbullying actions that may be of different types are still being investigated by researchers (Kowalski *et al.*, 2019). Cyberbullying actions are different in content and contain many features. However, in general, the most common cyberbullying activities include sexuality, gender differences, disability, racism, terrorism, personal character, belief, behavior, external appearance, and weight. The realization of cyberbullying acts, to be able to hide the identity in cyberspace, can be expressed as the key to cyberbullying. Thus, the individuals who cannot make any bullying in real life can turn into cyberbullies (Poland, 2010).

Cyberbullying is carried out in different species depending on the aggressors of attackers and the gender and age of the victim. It has been found that the social-emotional consequences of cyber victimization are comparable to the victimization of traditional bullying (Diamanduros *et al.*, 2008). Initial research has shown that exposure to cyberbullying can negatively affect physical and social development. It can also lead to psychological, emotional and academic problems (Hinduja *et al.*, 2008; Li, 2005; Wolak *et al.*, 2007; Ybarra *et al.*, 2007). In addition, it has been observed that victims of cyberbullying were adversely affected by violence, loneliness, suicidal tendencies (Andreou, 2004). The work done so far, they show that cyberbullying is increasingly occurring and that it causes many negative effects. Therefore, it is necessary to take some precautions to detect and prevent cyberbullying. So the first and most important part of the fight against cyberbullying is the reporting of cyber action. Informing should be done after reporting and detection. In this process, the information of both the victim and the attacker should be shared by informing the official units and internet service providers first. However, reporting gives us information about only bullying acts, and we cannot prevent action. This means that the situation requires online software to automatically detect and prevent cyberbullying.

In this study, automatic detection of cyberbullying was performed on datasets obtained from YouTube, Formspring.me and Myspace social network platforms. A method consisting of four main steps has been identified and implemented on the datasets. First, upper/lower-case conversion, stemming and stopwords removal were used for pre-processing. In the second step, feature extraction was performed and the performances of Multilayer

Perceptron (MLP), Stochastic Gradient Descent (SGD), Logistic Regression (LR) and Radial Basis Function (RBF) classifiers were measured using the obtained features. Then, the performances of classifiers are tested using Chi2, Support Vector Machine-Recursive Feature Elimination (SVM-RFE), Minimum Redundancy Maximum Relevance (MRMR) and ReliefF feature selection algorithms to reduce classification time. The best results are achieved by an SVM-RFE algorithm using the selected 500 features. The performance criteria (i.e. F\_measure) for test data classification is 0.953, 0.911 and 0.988 for YouTube, Formspring.me and Myspace datasets respectively. In addition, classification durations after applying feature selection algorithms were reduced by 20 times for YouTube, 2.5 times for Formspring.me and 10 times for Myspace datasets.

The remainder of this article follows as Section 2 presents related work on cyberbullying detection. Section 3 gives the details of materials and methods used to detect cyberbullying. Section 4 describes the comparison of the results obtained from experimental studies. Section 5 concludes the study.

## 2. RELATED WORK

In recent years, a number of studies have been performed for the analysis of cyberbullying detection. When some of these studies are examined, it is seen that classifiers like SVM, k Nearest Neighbours (kNN), Naïve Bayes (NB), J48 decision tree were used frequently (Dadvar and Jong, 2012a; Dinakar *et al.*, 2011; Eşsiz, 2016; Kontostathis, 2009; Ozel *et al.*, 2017).

Noviantho and Ashianti (2017) compared the performances of SVM and NB classifiers as a classification method for cyberbullying detection. Average accuracy of 92.81% was measured for the NB classifier while the SVM had 97.11% accuracy on average in the study conducted. In other steps of the study, the performances of the kNN and J48 decision tree methods were also measured and the best values were obtained as a result of the classification with SVM classifier.

Different labeling and weighting methods are used in addition to cyberbullying detection and text mining classification methods. N-gram method was used for labeling and term frequency \* inverse document frequency (tf \* idf) method was used for weighting by Yin *et al.* (2009). A supervised machine learning approach was applied, YouTube comments were collected, manually tagged, and binaries and multi-class classifications were applied on three different topics: sexuality, physical appearance, intelligence, and perception by Dinakar *et al.* (2011). In the test results, 80.2% accuracy was achieved in binary classifications and 66.7% accuracy in multi-class tests. In a study conducted at the Massachusetts Institute of Technology, a system has been developed that performs cyberbullying detection in textual contexts from YouTube video comments. The system defines the interpretation as a sequence of classes in sensitive subjects such as sexuality, culture, intelligence, and physical characteristics, and identifies which interpretation belongs to which class (Dadvar *et al.*, 2012b). In a study of the basic text mining system using the bad-of-word approach, an accuracy of 61.9% was achieved in a model that was developed by developing emotional and contextual features (Yin *et al.*,

2009). Bullying traces were defined using a variety of natural language processing techniques by Dadvar and Jong (2012a). Online and offline cyberbullying patterns were examined and emotion analysis system and secret Dirichlet discrimination methods were used to determine the type of bullying. In this method, bullying patterns were not correctly detected.

Cyberbullying has recently been recognized as a serious health problem among online social network users and has an enormous influence in developing an effective perception model. In order to increase the accuracy of the cyberbullying detection studies and to obtain faster methods, feature selection methods are used in the detection of cyberbullying. By Algaradi *et al.* (2016), a set of attributes based on the content of the network, activity, user, and tweet produced from Twitter data is proposed for feature selection. A supervised machine learning method has been developed to detect cybercrime on Twitter and three different feature selection algorithms, Chi2 test, information gain, and Pearson correlation, have been used. As a result of the experiments, a F<sub>measure</sub> value of 0.936 was reached in the model developed based

on the proposed features. These results show that the proposed model provides a suitable solution for detecting cyberbullying in online communication environments. An effective approach to identify cyberbullying messages from social media by weighting the feature selection was proposed by Nahar *et al.* (2012). Datasets contain data collected from three different social networks: Kongregate, Slashdot, and MySpace. The weighted tf \* idf scheme is used on bullying contained attributes. The number of bad words is scaled by two factors. LibSVM has been applied to the classification problem of two classes. For the MySpace dataset, 0.31 and 0.92 F<sub>measure</sub> values were obtained for the basic and weighted tf \* idf approximations. In another study conducted in this area, the Ant Colony Optimization algorithm was used in selecting subsets of attributes. Formspring.me, YouTube, MySpace and Twitter datasets by combining a novel method is proposed by Eşsiz (2016). In the experimental results, it is observed that the proposed method gives better results than the classical feature selection methods such as information gain and Chi2.

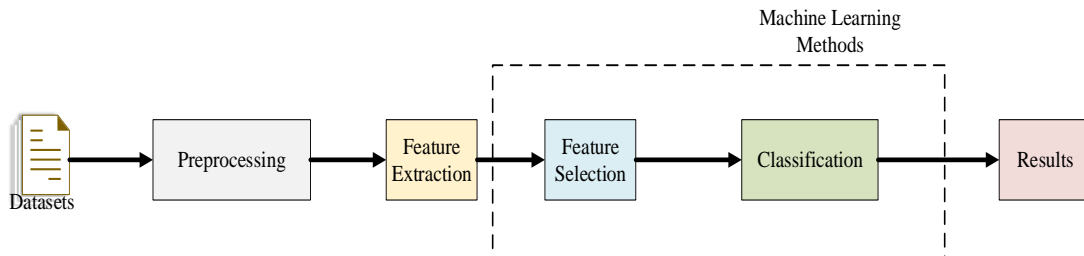


Fig. 1. The architecture of the proposed model

### 3. MATERIALS AND METHODS

Three different datasets obtained from YouTube, Formspring.me and Myspace social networks were used in the study. Experimental results were obtained by applying four main steps; pre-processing, feature extraction, feature selection, and classification. The architecture of the proposed model consisting of these steps is shown in Fig. 1. Different methods have been tested and applied to determine the optimal method for each step. Classification performances were compared by using SVM, RBF, MLP, SGD and LR classifiers. In addition, MRMR, ReliefF, Chi2, and SVM-RFE feature selection algorithms have been used to demonstrate the effect of selection algorithms on classification time and performance.

#### 3.1. Datasets

The Formspring.me dataset is an XML file consisting of 13158 messages from the Formspring.me website published by 50 different users. This dataset was prepared for a study conducted in 2009 (Yin *et al.*, 2009). The dataset is divided into two classes as "Cyberbullying Positive" and "Cyberbullying Negative". While negative messages represent messages that do not contain cyberbullying, Positive messages represent messages that contain cyberbullying. The Cyberbullying Positive class has 892 messages and the Cyberbullying Negative class has 12266 messages. To separate the dataset into training

and test sets, the "holdout" method used in datasets with similar dimensions was applied (Bing, 2011). Some well-known data clusters, such as Reuters and 20NewGoups (20NG), have similar size and number of samples as specified in (Chakrabarti, 2003). So that have been used the same methods as in these examples.

Myspace dataset consists of messages collected from Myspace group chats. Group chats contained in the dataset are labeled and grouped into 10 message groups. For example, if a group conversation contains 100 messages, the first group includes 1-10 messages, the second group includes 2-11 messages, and the last message group includes 91-100 messages. Labeling is done once for every group of 10 and it is labeled whether there are messages containing bullying in those 10 messages. There are a total of 1753 message groups in this dataset, divided into 10 groups with 357 positive and 1396 negative labels.

The last dataset is made up of comments collected from YouTube, the world's most popular video site. YouTube has a large audience, it is becoming a platform where some bad behaviors such as cyberbullying are frequently seen. YouTube dataset used in this study is labeled as positive (hosting cyberbullying) or negative (not hosting cyberbullying) in a study conducted in 2013 (Dadvar *et al.*, 2013). This corpus is a collection of 3464 messages written by different users. Approximately 75% of the samples in all dataset were randomly selected as the training set and the rest were taken as the test set. For all datasets, the number of comments in the training and test clusters for both positive and negative classes is

presented in Table 1.

Table 1. The number of training and test messages of datasets

Dataset	Label	Training	Test
Formspring.me	Positive	669	223
	Negative	9199	3067
Myspace	Positive	267	90
	Negative	1047	349
YouTube	Positive	312	105
	Negative	2285	762

### 3.2. Pre-processing

In the pre-processing step, combinations of three different pre-processing steps: conversion to lower/uppercase, stemming and with or without stop words were used. It is desirable to observe the effects on the classification performance of these pre-processing combinations in the processes carried out in this stage. The first pre-processing criterion is the lowercase/uppercase conversion. Normally, writing a word with a lowercase or uppercase does not cause any change in the meaning of that word, so all the words used are usually converted to lower case letters.

Sometimes, in blogs, forums, and other electronic communication platforms, a word can be written in capital letters to emphasize its significance or to mean loud. In this case, two different cases were examined in the pre-processing step of the case conversion of this study:

1. For the first case, all words are converted to lower case.
2. In the second case, all the words except the words with all the letters written in upper case are converted to lower case, and all the words written in upper case are left with uppercase letters. For example, if a word is written in ABCD format, the word is preserved in upper case format, but if it is written as Abcd or aBCd, that word is converted to abcd format.

The second pre-processing criterion is stemming. In this step, looking at the roots of words, words with the same root are removed from the feature subset. Porter's stemmer method was used to obtain the roots of the words in this study.

As the third and final pre-processing criterion, the meaningless words, called stopwords, have been examined. Meaningless words (prepositions, conjunctions, etc.) are defined as word groups that do not make sense when used alone. Generally, stopwords are not used as the feature in studies like subject classification, because they do not affect classification performance. However, the cyberbullying detection is slightly different from the subject classification, it was used as a pre-processing criterion in this study to investigate the effect of the stopwords on the classification performance.

All possible combinations of the three pre-processing methods mentioned above are considered. For a clearer understanding of these pre-processing steps, the eight different situations shown in Table 2 with code in the binary system.

### 3.3. Feature Extraction

In this study, only the comments in the dataset are used in the feature extraction step. Features such as username, age, gender are not included. The n-gram method is used for the feature extraction and  $n = 1$  is taken. In addition, a document frequency (df) of 0.001 was used to discard misspelled words and very rarely used words from the subset of features.

Table 2. Binary representation of pre-processing methods

Pre-processing Methods	Lowercase(0) / Uppercase(1)	Stemming off(0) / on(1)	With Stopwords(0) / Without Stopwords(1)
000	0	0	0
001	0	0	1
111	1	1	1

The main problem in classification is the unbalanced distribution of the classes in the datasets used. In such problems, the main class to be used for analysis is represented by very few examples, relative to the other classes in the dataset. As shown in Section 3.1, the datasets used in this study are unbalanced. The number of positive messages in terms of cyberbullying in the datasets is very small compared to negative messages. When working on such datasets, it is ensured that the class distributions are equalized using methods such as oversampling or undersampling to remove the unbalanced distribution between classes. In oversampling, positive samples are replicated until the class distributions in the dataset are equalized. Since the number of positive samples in the dataset used in this study is not high enough, the undersampling method is not suitable for our datasets. Thus, in order to remove the imbalance of the class distribution, positive samples were replicated for each dataset and oversampling method is applied until a balanced dataset was formed. Table 3 shows the number of features obtained by oversampling and applying 0.001 df.

### 3.4. Feature Selection

After the feature extraction step, the feature selection methods were applied in order to select the best feature subsets. Chi2, ReliefF, MRMR, and SVM-RFE feature selection algorithms were used separately in this step. The results were compared with each other in order to determine the most suitable method of feature selection for cyberbullying detection by different methods used. The number of features is reduced to 10, 50, 100 and 500 using the feature selection algorithms to shorten the classification duration. Reducing the number of features can sometimes lead to lose some features that have low weight but has a positive effect on classification. This leads to a decrease in classification performance. It is very important to maintain the classification performance while reducing the classification duration.

Table 3. Number of extracted features

Pre-processing Methods	Datasets		
	Formspring.me	Myspace	YouTube
000	1865	9824	14496
001	1653	9547	14215
010	1802	8224	13128
011	1640	8017	12920
100	1980	10212	15961
101	1769	9936	15680
110	1931	8619	14481
111	1767	8413	14273

### 3.4.1. Chi2

The Chi2 test is (McHugh, 2013) a method used to statistically determine the independence between two variables. Chi2 is a statistical test that is often used to make a comparison between the expected data and the observed data according to a given hypothesis. When the Chi2 test is used as part of the feature selection, it is used to determine whether a particular term is associated with a particular class.

To illustrate the application of the Chi2 test in the selection of features with an example; we assume that our dataset has two classes (positive/negative) with N samples. When given a feature X, it can use the Chi2 test to assess the importance of distinguishing the class. By calculating Chi2 scores for all features, features can be sorted by Chi2 scores, then top-ranked features for model training are selected.

Table 4. Chi2 feature selection

	Positive Class	Negative Class	Total
Containing feature X	A	B	A+B=M
Not containing feature X	C	D	C+D=N-M
Total	A+C=P	B+D=N-P	N

A, B, C, D represent the observed value and  $E_A, E_B, E_C, E_D$  indicate the expected value. Based on the Null Hypothesis that the two events are independent, we can calculate the expected  $E_A$  value using Eq. (1)

$$E_A = (A + C) \frac{A + B}{N} \quad (1)$$

$E_B, E_C, E_D$  values can be calculated with a similar formula. The basic idea is that if the two events are independent, the probability of X occurring in Positive class instances must equal the likelihood that X occurs in all instances of the two classes. Using the formula of the Chi2 test in Eq. (2). After a few simple steps of the process, a formula is obtained that shows the Chi2 score of the X quality shown in Eq. (3).

$$Chi2 = \sum_{k=1}^n \frac{(O_k - E_k)^2}{E_k} \quad (2)$$

$$Chi2 = \frac{N(AN - MP)^2}{PM(N - P)(N - M)} \quad (3)$$

### 3.4.2. Minimum Redundancy Maximum Relevance (MRMR)

The MRMR algorithm is a filter-based feature selection method that operates on two conditions, that is, combines the minimum redundancy and the maximum relevance with class labels (Hanchuan *et al.*, 2005). These conditions are combined by calculating mutual information to obtain the value of relevance and redundancy. MRMR is a discriminant analysis method that selects a subset of features that best represent the entire feature space. Calculation of mutual information between two features is shown in Eq. (4).

$$I(X, Y) = \sum_{y \in Y} \sum_{x \in X} p(x, y) \log \frac{p(x, y)}{p(x)p(y)} \quad (4)$$

The MRMR algorithm uses the values in the feature vector generated in the dataset.  $f_i$  represents the value of  $i$  in the feature vector,  $F_i$  is an example of a discrete random variable of  $i$ . Thus, the mutual information between the  $i$  and  $j$  attributes is expressed as  $I(F_i, F_j)$ . Mutual information is used not only between two features, but also for calculating the similarity between a feature and a class. In this case, if the class label vector is expressed as  $h$ , the discrete randomness corresponding to the class label is denoted as variant  $H$  and the mutual information value between  $i$  and class is  $I(F_i, H)$  (Gülgezen, 2009). MRMR algorithm consists of combining two algorithms. These algorithms are maximum relevance and minimum redundancy. For a dataset consisting of S features, these algorithms are shown in Eq. (5) and Eq. (6).

The maximum relevance:

$$\max W, W = \frac{1}{|S|} \sum_{F_i \in S} I(F_i, H) \quad (5)$$

The minimum redundancy:

$$\min V, V = \frac{1}{|S|^2} \sum_{F_i \in S} I(F_i, H) \quad (6)$$

The MRMR algorithm combines these two algorithms into two different methods: Mutual Information Difference ( $\max(V - W)$ ) and Mutual Information Quotient ( $\max(V / W)$ ). The formulas for these methods are shown in Eq. (7) and Eq. (8).

Mutual Information Difference:

$$\max \left[ I(F_i, H) - \frac{1}{|S|} \sum_{F_i \in S} I(F_i, F_j) \right] \quad (7)$$

Mutual Information Quotient:

$$\max \left[ I(F_i, H) / \left( \frac{1}{|S|} \sum_{F_j \in S} I(F_i, F_j) \right) \right] \quad (8)$$

### 3.4.3. ReliefF

The Relief feature selection algorithm is a method of a filter feature selection. Relief algorithm is firstly defined as a simple, fast and effective feature weighting approach. The output of the Relief algorithm is a weight between -1 (worst) and 1 (best) for each feature, features with a higher positive value indicate features indicating a better predictor result. (Rosario and Thangadurai, 2015). The original Relief algorithm is now rarely used in practice. The ReliefF algorithm is used as the most known and most used Relief-based algorithm (Urbanowicz *et al.*, 2017). "F" in ReliefF refers to the proposed sixth (A to F) algorithm variant. ReliefF algorithm has high efficiency and does not limit the properties of data types. Relief ensures discrete or continuous interest in data clusters. While dealing with multi-class problems, the ReliefF algorithm selects the nearest neighbors from each of the samples in different categories. First, after selecting a random sample X from the training set, it finds the nearest neighbors of sample X and subtracts random nearest neighbor samples from the neighbors in the different classes. The formula in Eq. (9) is used in the ReliefF algorithm to update the weight value of the property.

$$W_f^{i+1} = W_f^i + \sum_{c \neq \text{simf}(x)} \frac{\frac{p(x)}{1 - p(\text{simf}(x))} \sum_{j=1}^k \text{diff}_f(x, M_j(x))}{m * k} - \frac{\sum_{j=1}^k \text{diff}_f(x, H_j(x))}{m * k} \quad (9)$$

### 3.4.4. Support Vector Machines-Recursive Feature Elimination (SVM-RFE)

The RFE algorithm is an efficient algorithm for feature selection depending on the specific learning model. SVM is used in the learning method of the RFE attribute selection algorithm. So the method used is called the SVM-RFE. The SVM-RFE algorithm is a wrapper feature selection method. The SVM-RFE algorithm is actually a recursive elimination process. In this iteration, the irrelevant, no-comprehension or noisy qualities are removed in order and the important qualities are kept. The SVM-RFE algorithm is basically composed of the following three steps:

1. The SVM classifier is trained with the current samples and information about SVM capability is obtained. For example, when the linear cadence is used in SVM, weight information of each characteristic is obtained.
2. According to some evaluation criteria, the score of each qualification is calculated.
3. The feature corresponding to the smallest score from the current feature set is removed.

The output of the SVM-RFE algorithm is a feature

list that lists the features according to their importance. In the case of using Linear Kernel SVM as the learning method in the algorithm, the weight value ( $\omega$ ) is used to calculate the evaluation criterion ( $c_i$ ) (Wang *et al.*, 2011).

$$c_i = (\omega_i)^2 \quad (10)$$

In Eq. (10),  $\omega_i$  is  $i^{\text{th}}$  element of the weight vector (W). If the value of  $c_i$  is the smallest value  $i^{\text{th}}$  feature is removed from the feature set.

## 4. RESULTS AND DISCUSSIONS

In this study, well-known machine learning based classification algorithms such as SGD, RBF, LR, SVM, and MLP are used separately for cyberbullying detection and the results were compared with each other to determine the most ideal classification algorithm. Python programming language is used for feature extraction and feature selection, MATLAB and Weka software packages are used to develop classification algorithms.

Eight different pre-processing combinations have been applied and the results have been tested with the SGD classifier. Because it is known that the SGD classifier gives faster results than the other classifiers, the comparisons are made with the SGD classifier at this step. The effect of the pre-processing methods described in Section 3.2 on the classification performance for each dataset has been investigated. The F\_measure (Eq. (11)) values of each pre-processing method were compared using the SGD classifier and the results are presented in Fig. 2. Eq. (12) and Eq. (13) are used for F\_measure calculation.

$$F_{\text{measure}} = \frac{2 * \text{recall} * \text{precision}}{\text{recall} + \text{precision}} \quad (11)$$

$$\text{recall} = \frac{\text{TruePositive}}{\text{TruePositive} + \text{FalseNegative}} \quad (12)$$

$$\text{precision} = \frac{\text{TruePositive}}{\text{TruePositive} + \text{FalsePositive}} \quad (13)$$

The best pre-processing combination for Myspace, Formspring.me and YouTube datasets are 111, 011 and 100 respectively. F\_measure values for these combinations are calculated as 0.970, 0.934 and 0.842. As is seen from Fig. 2, the 001 combination of the pre-processing methods achieved the best F\_measure score for all datasets. The 001 combination is chosen as the default pre-processor for the rest of the paper. Since the datasets used in this study are unbalanced, the number of positive samples is increased by using the oversampling method. The micro (i.e. the harmonic mean of micro-averaged recall and precision) and macro-averaged F\_measure (i.e. the harmonic mean of macro-averaged recall and precision) values obtained using the SGD classifier with 001 pre-processing combination are shown in Table 5. It is seen that when the oversampling method is used, the micro and macro average F\_measure values increase and reach the same values. This indicates that our dataset has become a balanced dataset.

Table 5. Effect of oversampling on F\_measure classification performance

Datasets	With Oversampling		Without Oversampling	
	Macro Average F_measure	Micro Average F_measure	Macro Average F_measure	Micro Average F_measure
YouTube	0.982	0.982	0.569	0.839
Formspring.me	0.951	0.951	0.707	0.930
Myspace	0.983	0.983	0.953	0.968

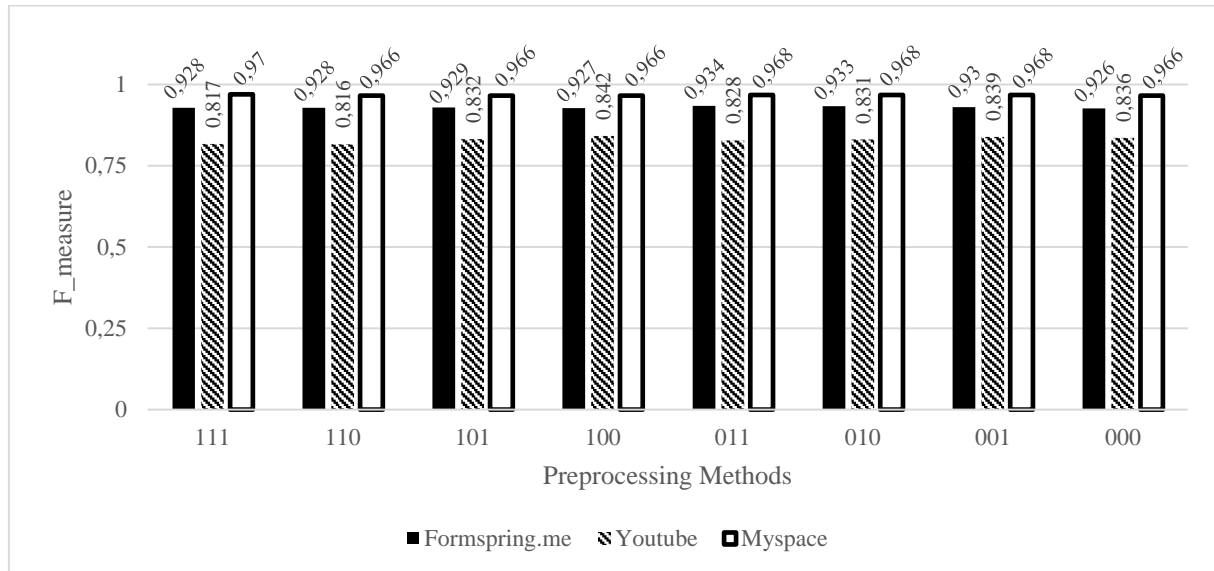


Fig. 2. F\_measure comparison of the pre-processing methods

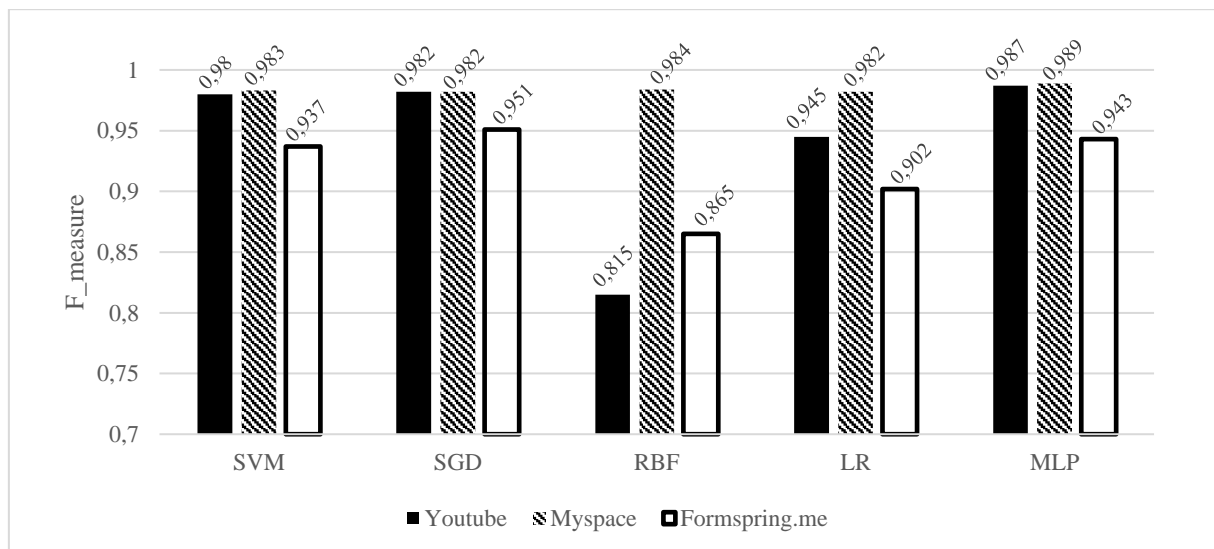


Fig. 3. Performance comparison of SVM, SGD, RBF, LR and MLP classifiers

#### 4.1. Performance Analysis of Classifiers

RBF, SVM, LR, MLP, and SGD classifiers have been tested to have a correct classification method for cyberbullying detection problem. 0.001 df and 001 pre-processing combinations were used in the experiments. A single intermediate layer consisting of 10 neurons was used in the MLP algorithm and the scaled conjugate gradient (*trainscg*) back propagation method was used as the learning method. The classification results are shown in Fig. 3 for all datasets.

MLP and RBF classifiers give the best results for the Myspace dataset. The  $F_{\text{measure}}$  values for these classifiers are 0.989 and 0.984 respectively. The best results were obtained in the MLP and SGD classifiers with  $F_{\text{measure}}$  values of 0.987 and 0.982 for YouTube dataset; 0.951 and 0.943 for Formspring.me dataset as is presented in Fig. 3. As a result of these experiments, it has been found out that the most suitable classifications for the detection of cyberbullying are SGD and MLP classifiers.

It may be erroneous to evaluate only the classifier's accuracy when comparing classifier performances. The classification speed is also an important parameter as well as the accuracy of classification. Classification times (sec.) of classifiers are shown in Table 6. It can be seen that the LR and SVM algorithms are very slow and the RBF classifier is the fastest algorithm. The SGD and MLP classifiers generally appear to have both a high degree of accuracy and a classification duration at an acceptable level. Given the speed and accuracy of classification at the same time, SGD and MLP algorithms can be considered as the best classifiers.

#### 4.2. The Effects of Feature Selection Algorithms

When you are working on problems where the feature set is too large such as cyberbullying detection problems, the classification time is quite high. In order to decrease the time of classification in such problems, the best sub-features in the feature set are selected. When this method is applied, some important features are lost and the classification performance decreases. Therefore, we have identified the most appropriate feature selection algorithm that preserves the classification performance. The number of features was selected as 50, 100, 250 and

500 using Chi2, ReliefF, SVM-RFE and MRMR algorithms in the experiments and their performances were compared.

Since the comparison results are generally similar, the results obtained from only the YouTube dataset are presented in Fig. 4. The results of all datasets are also summarized in Table 7. In Fig. 4, it can be seen that the best classification accuracy is achieved from the MLP classifier for all feature selection algorithms. The highest  $F_{\text{measure}}$  value (i.e. 0.953) is obtained from the SVM-RFE algorithm with 500 attributes.

As is seen from Table 7, the ReliefF algorithm gives lower results than the other feature selection algorithms by means of  $F_{\text{measure}}$ . While the MRMR and Chi2 algorithms show accuracy performance with close results, the highest results for all datasets are obtained from the SVM-RFE algorithm. It can be seen that the feature selection paradigm leads to a decrease in classification accuracy. This is because some unselected features have an important role in the training of classification algorithms. However, when the classification time analysis shown in Fig. 5 is examined, it is seen that the feature selection algorithms significantly reduce the classification time. Choosing of 500 as the number of features has the least effect on classification performance and the best results have achieved in terms of time and classification accuracy.

#### 5. CONCLUSION

In this study, a feature-based model is developed on the datasets obtained from YouTube, Formspring.me and Myspace social network platforms. The developed model performs a classification according to whether the comments in the datasets contain cyberbullying. SVM, RBF, MLP, LR, and SGD algorithms are used as classifiers. SGD and MLP classifiers showed better results than other classifiers by giving a  $F_{\text{measure}}$  value above 0.930. In order to overcome high classification time problem, MRMR, ReliefF, SVM-RFE and Chi2 algorithms are used as feature selection methods. The SVM-RFE method with 500 selected features reduced the classification time by 20 times for Youtube, 2.5 times for Formspring.me, and 10 times for Myspace datasets while preserving the classification performance.

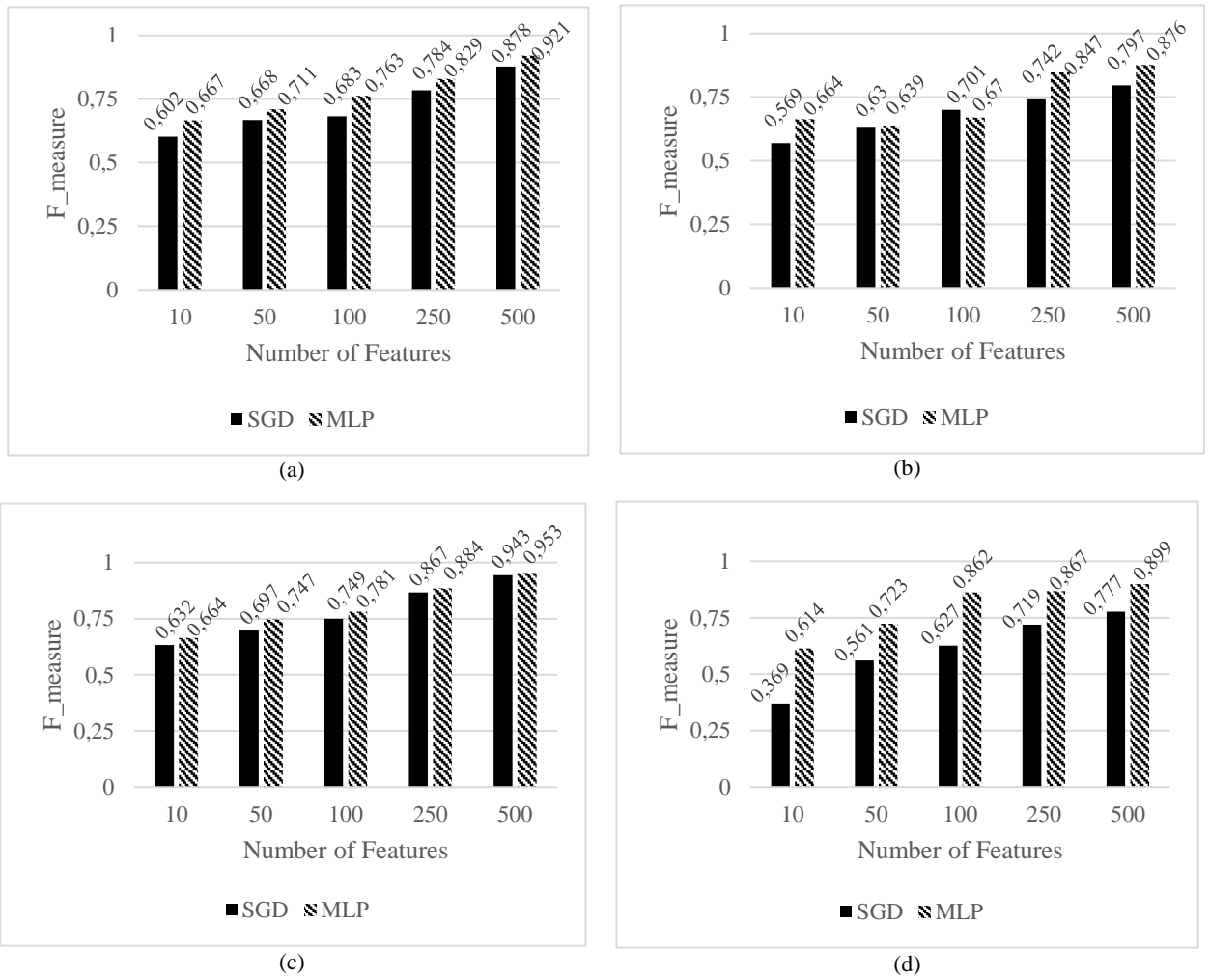


Fig. 4. Performance on SGD and MLP classifiers of the feature selection algorithms for YouTube dataset (a) Chi2; (b) MRM; (c) SVM-RFE; (d) ReliefF

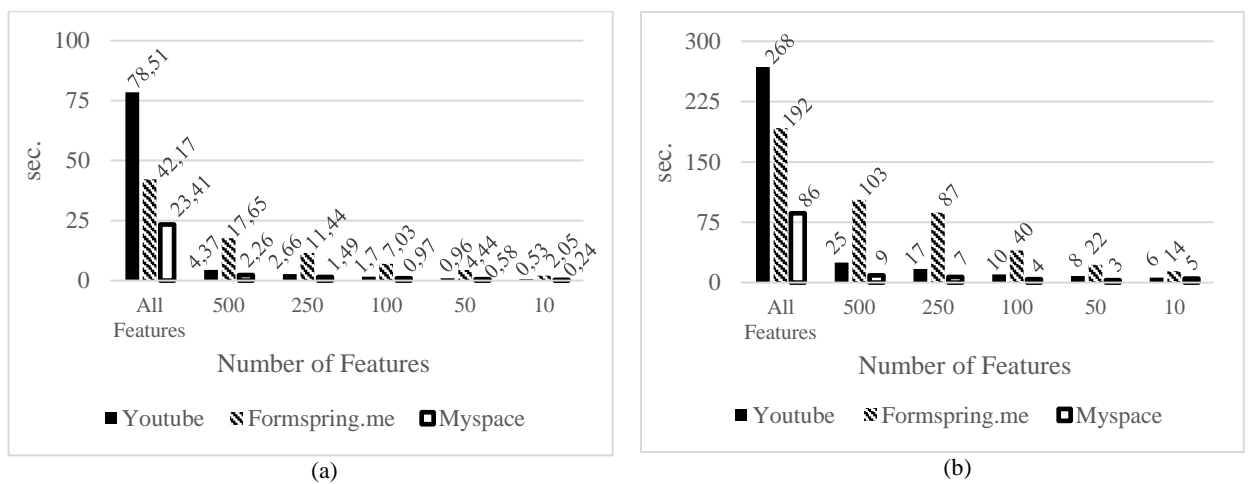


Fig. 5. Comparison of runtime performance of the SVM-RFE algorithm with and without feature selection for all datasets (a) SGD; (b) MLP

Table 7. F\_measure results of all experiments

		YouTube		Formspring.me		Myspace	
		SGD	MLP	SGD	MLP	SGD	MLP
MRMR	10	0.566	0.664	0.689	0.779	0.752	0.798
	50	0.630	0.639	0.771	0.802	0.871	0.945
	100	0.701	0.670	0.792	0.821	0.923	0.941
	250	0.742	0.847	0.829	0.837	0.967	0.986
	500	0.797	<b>0.876</b>	<b>0.871</b>	<b>0.871</b>	0.980	<b>0.988</b>
ReliefF	10	0.369	0.614	0.362	0.663	0.434	0.653
	50	0.561	0.723	0.419	0.647	0.559	0.755
	100	0.627	0.862	0.464	0.670	0.686	0.771
	250	0.719	0.867	0.561	0.662	0.805	0.832
	500	0.777	<b>0.899</b>	0.658	<b>0.708</b>	0.853	<b>0.895</b>
Chi2	10	0.602	0.667	0.699	0.786	0.640	0.793
	50	0.668	0.711	0.774	0.811	0.870	0.911
	100	0.683	0.763	0.803	0.842	0.908	0.967
	250	0.784	0.829	0.847	0.860	0.969	0.970
	500	0.878	<b>0.921</b>	0.878	<b>0.909</b>	<b>0.986</b>	0.982
SVM-RFE	10	0.632	0.664	0.489	0.760	0.653	0.782
	50	0.724	0.747	0.656	0.776	0.892	0.920
	100	0.749	0.781	0.768	0.824	0.932	0.976
	250	0.867	0.884	0.871	0.837	0.978	0.972
	500	0.943	<b>0.953</b>	<b>0.911</b>	0.908	<b>0.988</b>	0.986
Without any selection		0.982	<b>0.987</b>	<b>0.951</b>	0.943	0.983	<b>0.989</b>

\*The best values are emphasized in bold font.

## REFERENCES

- Al-garadi, M.A., Varathan, K.D. and Ravana, S.D. (2016). "Cybercrime detection in online communications: The experimental case of cyberbullying detection in the Twitter network" *Computers in Human Behavior*, Vol. 63, pp. 433–443.
- Andreou, E. (2004). "Bully/victim problems and their association with Machiavellianism and self-efficacy in Greek primary school children" *British Journal of Educational Psychology*, Vol. 74, No. 2, pp. 297–309.
- Bing Liu (2011). *Web Data Mining: Exploring Hyperlinks, Contents, and Usage Data*, 2nd Ed., Springer Publishing Company, Chicago, USA.
- Chakrabarti, S. (2003). *Mining the Web : discovering knowledge from hypertext data*, Morgan Kaufmann, San Francisco, USA.
- Dadvar, M. and Jong, F.M.G. de (2012). "Improved cyberbullying detection through personal profiles." *International Conference on Cyberbullying*, Paris, France.
- Dadvar, M., Jong, F.M.G. de, Ordelman, R.J.F. and Trieschnigg, R.B. (2012). "Improved cyberbullying detection using gender information" *12th Dutch-Belgian Information Retrieval Workshop*, Ghent, Belgium, pp 1-6.
- Dadvar, M., Trieschnigg, R.B. and Jong, F.M.G. de (2013). "Expert knowledge for automatic detection of bullies in social networks." *25th Benelux Conference on Artificial Intelligence*, Delft, Netherlands, pp. 1-7.
- Diamanduros, T., Downs, E. and Jenkins, S.J. (2008). "The role of school psychologists in the assessment, prevention, and intervention of cyberbullying" *Psychology in the Schools*, Vol. 45, No. 8, pp. 693–704.
- Dinakar, K., Reichart, R. and Lieberman, H. (2011). "Modeling the Detection of Textual Cyberbullying. The Social Mobile Web", *5th International AAAI Conference on Weblogs and Social Media*, Barcelona, Catalonia, Spain.
- Eşsiz, E.S. (2016). *Selecting Optimum Feature Subsets With Nature Inspired Algorithms for Cyberbullying Detection*, Çukurova University, Adana, Turkey.
- Gülgezen, G. (2009). *Stable and Accurate Feature Selection*, Istanbul Technical University, İstanbul, Turkey.
- Hanchuan Peng, H., Fuhui Long, F. and Ding, C. (2005). "Feature selection based on mutual information criteria of max-dependency, max-relevance, and min-redundancy" *IEEE Transactions on Pattern Analysis and Machine Intelligence*, Vol. 27, No. 8, pp. 1226–1238.
- Hinduja, S. and Patchin, J.W. (2008). "Cyberbullying: An Exploratory Analysis of Factors Related to Offending and Victimization" *Deviant Behavior*, Taylor & Francis Group, Vol. 29, No. 2, pp. 129–156.
- Kononenko, I. (1994). *Estimating attributes: Analysis and extensions of RELIEF*. *European Conference on Machine Learning*, Springer, Berlin, Heidelberg, pp. 171–182.
- Kontostathis, A. and Kontostathis, A. (2009). "ChatCoder: Toward the Tracking and Categorization of Internet Predators". *9th Siam International Conference*

on Data Mining, Nevada, USA.

Kowalski, R.M., Limber, S.P. and McCord, A. (2018). "A developmental approach to cyberbullying: Prevalence and protective factors" *Aggression and Violent Behavior*, Vol. 45, pp. 20-32.

Langos, C. (2012). "Cyberbullying: The Challenge to Define" *Cyberpsychology, Behavior, and Social Networking*, Vol. 15, No. 6, pp. 285–289.

Li, T.B.Q. (2005). "Cyber-Harassment: A Study of a New Method for an Old Behavior" *Journal of Educational Computing Research*, Vol. 32, No. 3, pp. 265–277.

McHugh, M.L. (2013). "The Chi-square test of independence" *Biochemia Medica, Medicinska naklada*, Vol. 23, No. 2, pp. 143–149.

Nahar, V., Unankard, S., Li, X. and Pang, C. (2012). "Sentiment Analysis for Effective Detection of Cyber Bullying." *14th Asia-Pacific international conference on Web Technologies and Applications*, Springer-Verlag, Beijing, China, pp. 767–774.

Noviantho, Isa, S.M. and Ashianti, L. (2017). "Cyberbullying classification using text mining." *1st International Conference on Informatics and Computational Sciences*, IEEE, Semarang, Indonesia, pp. 241–246.

Ozel, S.A., Sarac, E., Akdemir, S. and Aksu, H. (2017). "Detection of cyberbullying on social media messages in Turkish." *International Conference on Computer Science and Engineering*, IEEE, Antalya, Turkey, pp. 366–370.

Poland, S. (2010). "Cyberbullying Continues to Challenge Educators" *District Administration*, Vol. 46, No. 5, p. 55.

Rosario, S.F. and Thangadurai, K. (2015). "RELIEF: Feature Selection Approach" *International Journal of Innovative Research and Development*, Vol. 4, No. 11.

Snakenborg, J., Van Acker, R. and Gable, R.A. (2011). "Cyberbullying: Prevention and Intervention to Protect Our Children and Youth" *Preventing School Failure*, Vol. 55, No. 2, pp. 88–95.

Urbanowicz, R.J., Meeker, M., LaCava, W., Olson, R.S. and Moore, J.H. (2017). "Relief-Based Feature Selection: Introduction and Review" *Journal of Biomedical Informatics*, Vol. 85, pp. 189-203.

Wang, J., Shan, G., Duan, X. and Wen, B. (2011). "Improved SVM-RFE feature selection method for multi-SVM classifier." *International Conference on Electrical and Control Engineering*, IEEE, Yichang, China, pp. 1592–1595.

Wolak, J., Mitchell, K.J. and Finkelhor, D. (2007). "Does Online Harassment Constitute Bullying? An Exploration of Online Harassment by Known Peers and Online-Only Contacts" *Journal of Adolescent Health*, Vol. 41, No. 6, pp. S51–S58.

Ybarra, M.L., Diener-West, M. and Leaf, P.J. (2007). "Examining the Overlap in Internet Harassment and School Bullying: Implications for School Intervention" *Journal of Adolescent Health*, Vol. 41, No. 6, pp. S42–S50.

Yin, D., Xue, Z., Hong, L., Davison, B.D., Kontostathis, A. and Edwar, L. (2009). "Detection of Harassment on Web 2.0." *Content Analysis in the WEB 2.0*, Madrid, Spain, pp. 1–7.

# Turkish Journal of Engineering



*Turkish Journal of Engineering (TUJE)*  
*Vol. 3, Issue 4, pp. 179-188, October 2019*  
*ISSN 2587-1366, Turkey*  
*DOI: 10.31127/tuje.555268*  
*Research Article*

## BEHAVIOR OF R/C FRAMES WITH CONCRETE PLATE BONDED INFILLS

Mehmet Baran \*<sup>1</sup>

<sup>1</sup> Ankara Yıldırım Beyazıt University, Engineering and Natural Sciences Faculty, Civil Engineering Department, Ankara, Turkey  
ORCID ID 0000-0001-6674-7308  
mehmet.baran@ybu.edu.tr

---

\* Corresponding Author

Received: 17/04/2019

Accepted: 09/05/2019

---

### ABSTRACT

A practical, economic and effective as well as occupant friendly seismic strengthening technique had been developed for reinforced concrete (RC) framed buildings lacking sufficient lateral stiffness. In this technique, high strength concrete plates are bonded onto the existing plastered hollow brick infill walls using a thin layer of epoxy mortar in order that infill walls are converted into lateral load resisting shear walls resulting from the composite action of infill wall with the plates bonded onto it. By this way, the building gains sufficient lateral stiffness. To analyze the behavior of RC frames strengthened by the aforementioned technique, results of eight one-third scale, one-bay, one or two storey deficient RC frames tested under reverse-cyclic lateral loading until failure are given in detail. Three different types of plates were used to strengthen the frames. Test results showed that the proposed strengthening technique considerably increased the lateral load capacities as well as the initial stiffness and energy dissipation capacities of the strengthened specimens, for both types of frames. Additionally, present study focuses on the comparison results of one-storey specimens with those of equivalent two-storey specimens to well-understand the behavior of such strengthened frames under lateral load, and infill walls under compressive and shear forces as well as tensile forces.

**Keywords:** *Epoxy Mortar, High Strength Concrete Plate, Reverse-cyclic Lateral Loading, Seismic Strengthening, Shear Force*

## 1. INTRODUCTION

Although Turkey is a seismically active country, most of the existing RC residential buildings are non-engineered, lacking sufficient lateral stiffness. They endanger public safety as well as country's economical well-being in a possible future earthquake. So, they should immediately be strengthened after a vulnerability assessment process. Up to past few years, researches concentrated on studies in which new shear walls were added into the building's RC frame. Although this method has been proved to be very effective structurally, it has a disadvantage which cannot be undervalued. This method requires evacuation of the building since huge volumes of construction material have to be carried into the building as well as a long construction period. The technique presented in this study promise a non-evacuation strengthening, even without causing more disturbance to the occupants than a painting job where the idea is to convert the existing hollow brick infill wall into a load carrying system acting as a cast-in-place concrete shear wall by reinforcing it with relatively thinner high strength PC plates to be bonded to the plastered infill wall and connected to the frame members by epoxy mortar.

In the experimental researches conducted by various researchers (Yuzugullu, 1979; Kahn and Hanson, 1979; Hanson, 1980; Kaldjian and Yuzugullu, 1983; Phan *et al.*, 1995; Nakashima, 1995; Roberts, 1995; Frosch, 1996, 1999; Frosch *et al.*, 1996; Li, 1997; Matsumoto, 1998; Han *et al.*, 2003; Isao *et al.*, 1999; Kanda *et al.*, 1998; Kesner, 2003; Kesner *et al.*; 2001, 2003, 2005) plates had been used as strengthening elements. These studies showed that the use of plates is an effective and convenient method which increases strength and stiffness of RC frames considerably, whereas it saves cost and time.

In the content of the present project, nearly fifty tests had been conducted on RC frames strengthened by PC plates. Current study presents the comparison of behaviors of eight RC frames strengthened by bonding RC plates on to infills.

## 2. EXPERIMENTAL INVESTIGATION

### 2.1. Test Frames

One-third scale, one-bay, one-storey and two-storey RC frames with common structural deficiencies observed in real practice in Turkey were used as test frames. Such deficiencies are insufficient lateral stiffness, non-ductile members, bad detailing and low concrete quality. Dimensions and reinforcement of the test frames are illustrated in Fig. 1.

### 2.2. Materials

Low strength concrete was intentionally used in the test frames to represent the concrete commonly used in existing building structures whereas relatively strong concrete is preferred for the PC plates to provide the required load carrying capacity by using relatively thin layer of concrete, minimizing the plate weight. For the same reason, mild steel plain bars were used as longitudinal reinforcement in beams and columns. Typical properties of reinforcing bars used in this study

are listed in Table 1.

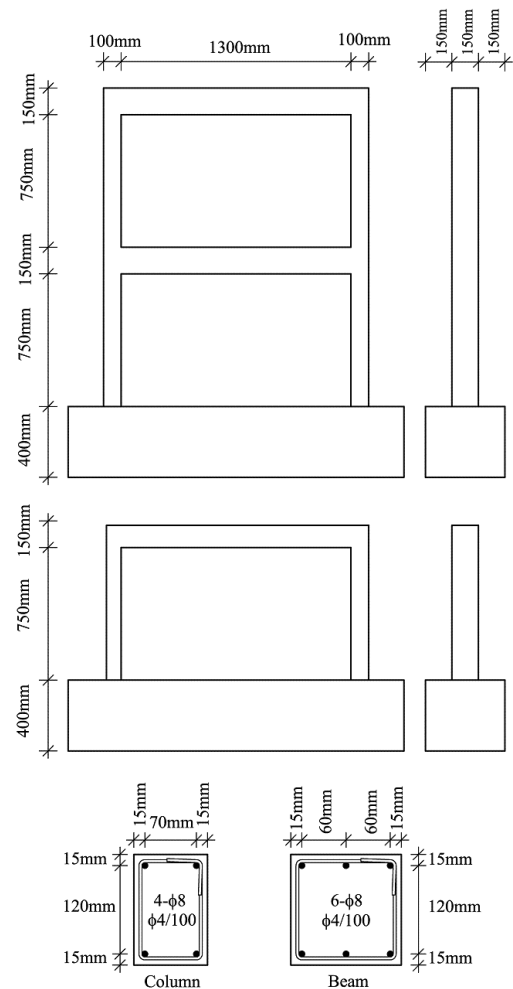


Fig. 1. Dimension and reinforcement of frames

Table 1. Properties of Reinforcing Bars

Bar	Property	Location	$f_y$ (MPa)	$f_u$ (MPa)
φ3	Plain	Mesh steel for plate reinforcement	670	750
φ4	Plain	Stirrup for beam and column Plate reinforcement	220	355
φ6	Deformed	Dowel for frame-to-plate connection	580	670
φ8	Plain	Beam and column longitudinal bars	330	445
φ8	Deformed	Anchorage bar between adjacent plates	350	470
φ16	Deformed	Foundation beam longitudinal bar	420	580

Both the first storey and second storey bays were infilled with scaled (one-third scale) hollow brick infill

covered with scaled layer of plaster at both faces. Ordinary cement-lime mortar with ordinary workmanship was used during the plaster application and wall construction, reflecting the usual practice. The hollow bricks used in this study is illustrated in Fig. 2.

Because of the superior compressive and tensile strength, Sikadur-31 was preferred to be used as epoxy mortar having a compressive strength of 65 MPa used in plate joints and between the plates and the plaster on the wall. According to the manufacturer's manual, its tensile strength is nearly 20 MPa, its adhesion strength to steel and concrete is 30 MPa and 3.5 MPa, respectively. For the embedment of the dowels to the frame members, Spitecon was used as epoxy in the present study.

### 2.3. Infill Wall Strengthening Plates

Within the study reported, three different types of PC plates having two basic shapes were designed and tested to observe their performances as infill wall strengthening elements. One approach was to have rectangular shaped plates by arranging them in three rows and four columns, and another was to have full height strip shaped plates by using the full height of the infill in several lines. Plate thickness for all types was chosen as 20 mm. Therefore, the plates came out to be about 3 kg in weight. This weight is for one-third scale plates, so the corresponding weight for the actual sized plates would be about 80 kg, which is not too heavy to be carried manually by two workers. The plates "I" and "III" have nearly square geometry whereas the plate "II" has full height strip geometry. The method of bonding plates on to infill is illustrated in Fig. 3.

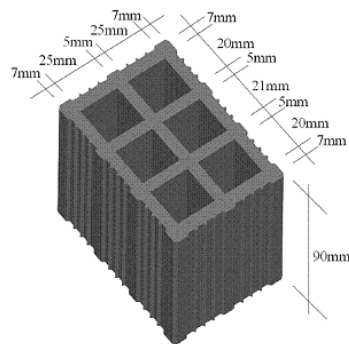


Fig. 2. Hollow Brick Dimensions

## 3. TEST SET-UP AND INSTRUMENTATION

### 3.1. Loading and Supporting System

As it can be seen in Fig. 4, the setup consists of a universal base, test specimen, loading system and a reaction wall. The main foundation was fixed to the strong floor and the specimens were fixed on top of the main foundation by steel bolts.

Specimens were placed inside a steel frame which was fixed to the main frame. The steel frame was also supported by the laboratory wall by L-section steel bars forming a steel frame which was intended to prevent out-

of-plane deformations, i.e., torsion of the specimen by providing lateral support to the beam(s) with rollers.

During the tests, a constant axial load was applied on to the columns of the specimens. The load was applied by two hydraulic jacks on both sides of the specimens and the load was transferred to the cross beam by cables. The axial load applied on both columns, equal to 60 kN (~20% of column's axial load capacity), were continuously and carefully monitored and adjusted manually.

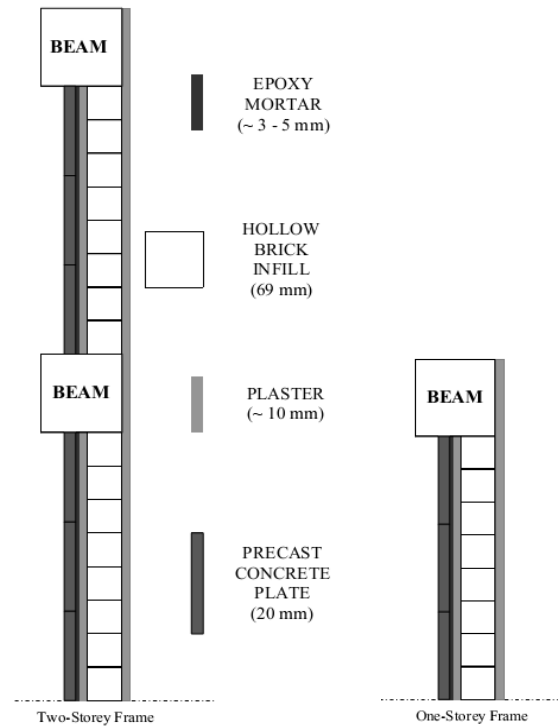


Fig. 3. Plate Bonding Method

The specimens were tested with hysteretic lateral loading for modelling ground motion effect. The system consisted mainly of an adjustable steel frame attached to the reaction wall, a load cell, a hydraulic pump and pin connections at either end of the loading column consisting of the jack and load cell. Loading was applied by the assemblage of a hydraulic jack and a load cell with pin connections at the ends. The pin connections at the ends provide the system to create axial stress only. The lateral load was planned to act in two directions; pushing and pulling. To achieve this aim by a loading system at one side, steel plates were attached to both ends of the beam with four steel bars. For one-storey specimens, lateral load was applied at first storey beam level. For two-storey specimens, lateral load was applied at one third span of the spreader beam to ensure that it was divided in 1:2 ratio between the first and second story beam levels. In the tests, the loading was applied in cycles. Each load level was repeated in reverse direction before proceeding to the next load level.

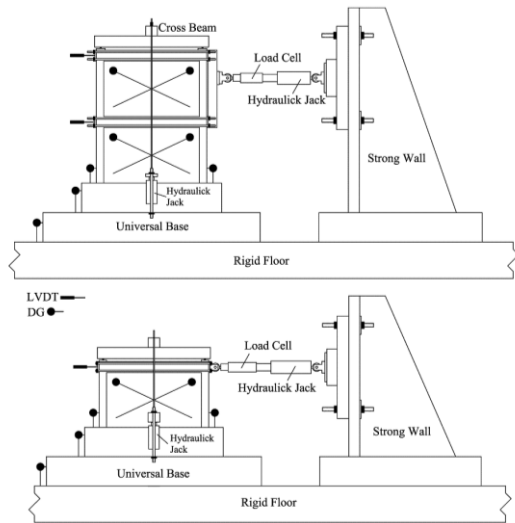


Fig. 4. Test Set-ups and Instrumentation

### 3.2. Deformation Measurement System

In order to record deformations, linear variable displacement transducers (LVDT) and dial gauge type measurement devices were used. The positions of the gauges are shown in Fig. 4. The lateral load was being recorded by a load cell throughout the tests.

Lateral displacement of stories was measured with respect to the universal base. The readings from the LVDTs were used to construct load-displacement, load-story drift and load-infill shear displacement curves.

Shear deformations were measured on infill walls by means of two diagonally placed dial gauges. Transducers were located 130 mm away from the corner of the infill walls. The reason for choosing this location was to avoid localized effects like crushing of concrete during experiment.

## 4. EXPERIMENTAL RESULTS

### 4.1. Behavior of Test Frames

In this section, test results of one-storey specimens are compared with the test results of equivalent two-storey specimens. Behavior of equivalent pairs are compared with respect to ultimate strength and interstorey drift ratio characteristics to analyze the similarities and differences between the pairs.

#### 4.1.1. Reference Frames, CR

CR denotes unstrengthened specimens which had continuous reinforcement and only plastered hollow brick infill. The two test frames had similar concrete strength. From Table 2, it can be seen that the one-storey frame had a lateral load capacity of 86.6 kN which was greater than that of equivalent two-storey frame with a value of 76.8 kN. Corresponding first story drift ratio values at the maximum forward load were 0.0037 and 0.0042 for one-storey and two-storey CR frames respectively. But when loading in the negative direction is considered, one-storey

and two-storey frames had lateral load capacities of 79.1 kN and 78.8 kN, respectively. Corresponding first story drift ratio values at the maximum backward load were 0.0033 and 0.0030 for one-storey and two-storey CR frames respectively. Both frames exhibited typical masonry infilled frame behavior. The plastered hollow brick infill considerably contributed to the lateral load capacity at the initial stage, however, this contribution decreased rapidly as crushing started in the infill leading to a behavior similar to that of the bare frame where significant deformations took place under rather small lateral loads. The closeness of the capacity and corresponding first storey drift ratio values can be observed in the comparison of load-displacement curves and comparison of response envelopes, as shown in Fig. 5.

In the tests, diagonal cracking started earlier on the first storey infill of the two-storey frame than that of the one-storey frame. First hairline cracks on columns were observed together with the cracks on the infill at a lateral load capacity of 50 kN. This situation was observed in the test of one-storey frame at a lateral load capacity of 80 kN. For both frame types, infill started crushing from the corners and the lateral load started to be carried by the frame members. Transformation of behavior into bare frame action occurred about the eighth cycle for both frames, at a lateral load capacity of nearly 60 kN, where half cycle loadings were controlled by the top storey level displacement. The behavior was very similar considering the first stories and the failure of the frames occurred by crushing at column bases. Photographs of both first storey infills of both reference frames are given in Fig. 6., where the upper one is of two-storey frame and the lower is one-storey.

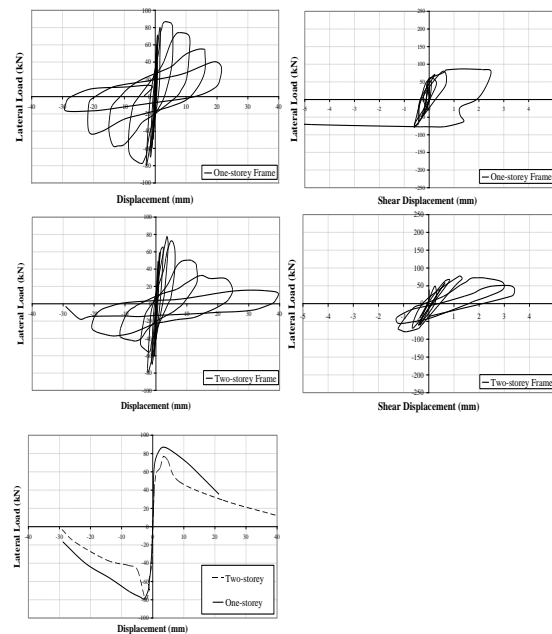


Fig. 5. Comparison of Lateral Load vs. First Storey Displacements of both CR Specimens

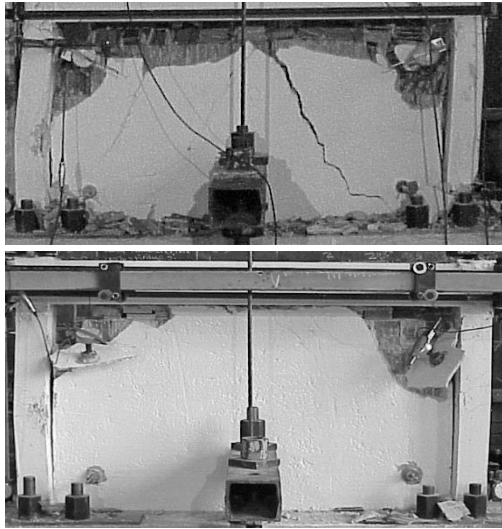


Fig. 6. Photographs of first storey infills (CR Specimens)

#### 4.1.2. Frames Strengthened by Using Type I Plates, CI

Both CI Specimens were strengthened by using Type I PC plates. The plate arrangement for both CI specimens is shown in Fig. 7. The lateral load capacities cannot be considered as close values since they were 209.6 kN and 186.2 kN for one-storey and two-storey frames, respectively. However, they were especially close for negative direction, which were 196.0 kN and 192.5 kN, respectively for one-storey and two-storey frames. For forward loading, first storey drift ratio values at the maximum load were 0.0120 and 0.0037, respectively for one-storey and two-storey frames. These ratios were 0.0038 and 0.0069 for backward loading. During testing of two-storey CI specimen, the entire test unit behaved nearly as a monolithic cantilever where failure took place at the base level in terms of yielding of the steel in the tension side column and concrete crushing and buckling of longitudinal steel in the compression side column. However, at the end of one-storey frame test, it was observed that some damage occurred in the infill; however, eventual exhaustion came with the failure of columns.

For both frames, the proposed technique led to a significant increase in the capacity and thus to a significantly better seismic performance meaning an effective behavior of plate strengthened hollow brick infill. In addition, one storey frame had more ductility as can be observed from the comparison of envelope curves given in Fig. 8. The difference in ductility is significant in the forward direction, but it does not seem to be much different in the backward direction. One-storey test frame have an envelope curve which is more wider, possibly caused by the pinching effect resulting from the large cracks developed on the infills. The more wider loops of one-storey specimen can easily be seen in the lateral load-top displacement graph given in Fig. 8. Photographs of both first storey infills of both specimens are given in Fig. 9, where the upper one is of two-storey frame and the lower is one-storey.

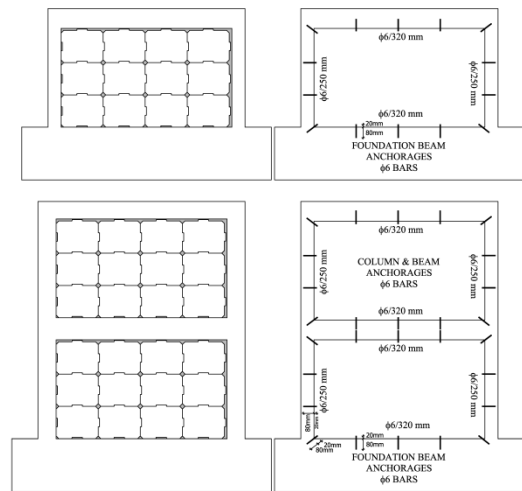


Fig. 7. Plate Arrangement for both CI Specimens

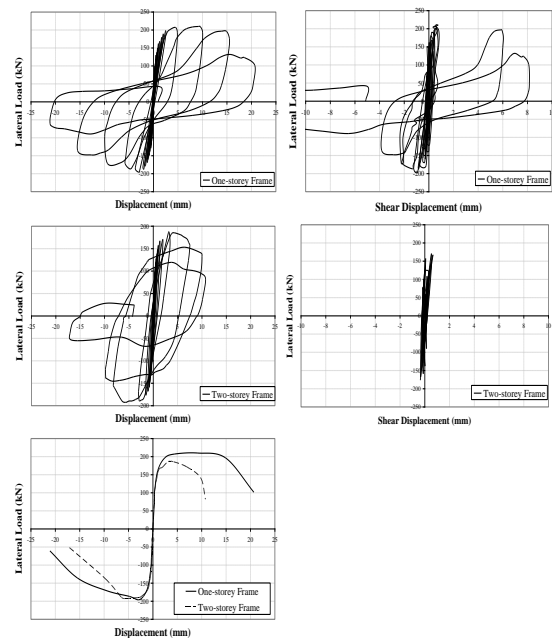


Fig. 8. Comparison of Lateral Load vs. First Storey Displacements of both CI Specimens

#### 4.1.3. Frames Strengthened by Using Type II Plates, CII

One or two storey frames strengthened with Type II plates were denoted as CII. The plate arrangement for both CII specimens is shown in Fig. 10. When the values in Table 2 are observed, it can clearly be seen that both types of frames showed significantly similar behavior for both loading directions in the perspective of lateral load capacity and response envelopes. One-storey and two-storey CII specimens reached lateral load capacities of 197.0 kN and 201.3 kN, respectively for forward loading and 187.4 kN and 198.2 kN, respectively for backward loading. Corresponding first storey drift ratio values were 0.0056 and 0.0089, respectively for one-storey and two-storey test frames for forward loading and 0.0066 and 0.0070, respectively for backward loading. The response

envelopes seem to be almost coinciding with each other. There is some difference between the curve shapes in the load-deformation plots of two frame types. As in the cases of both CI specimen tests, the entire two-storey specimen CII behaved nearly as a monolithic cantilever whereas it was observed that some damage occurred in the infill of the one-storey specimen CII. As compared to one-storey CI Specimen, this specimen has less narrow cracks and hence, less pinching effect most possibly stemming from this phenomenon. Lateral load-top displacement graphs for both specimens are given in Fig. 11.



Fig.9. Photographs of first storey infills (CI Specimens)

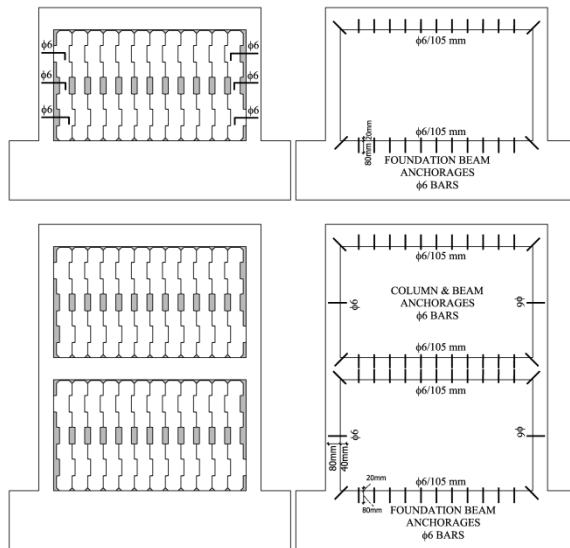


Fig. 10. Plate Arrangement for both CII Specimens

For both frames, cracking started at column bases at the same load level. Then, infill separation cracks were formed, a little later at the two-storey frame. Beam-column joint cracks appeared earlier and were more significant at the one-storey frame. At the two-storey frame, column flexural cracks were observed before joint

cracking. At the one-storey frame, plate cracking started at later cycles, and the infill was separated from the frame. The two tests ended similarly by damages in the column bases, but the one-storey frame had much greater damage at the joint region whereas two-storey frame had greater damage at the base level. Test results for both frame types are given in Table 2. Photographs of both first story infills of both specimens are given in Fig. 12, where the upper one is of two-storey frame and the lower is one-storey.

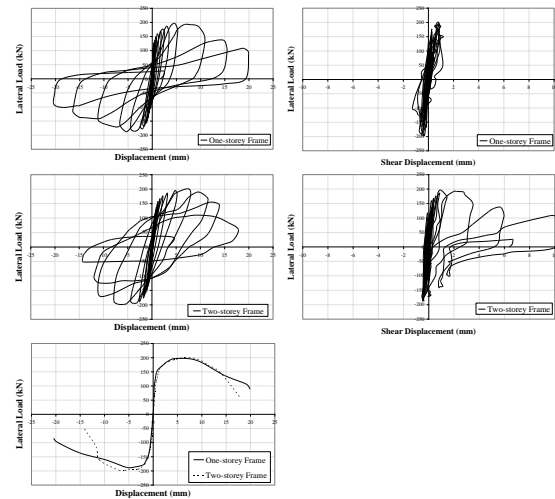


Fig. 11. Comparison of Lateral Load vs. First Storey Displacements of both CII Specimens

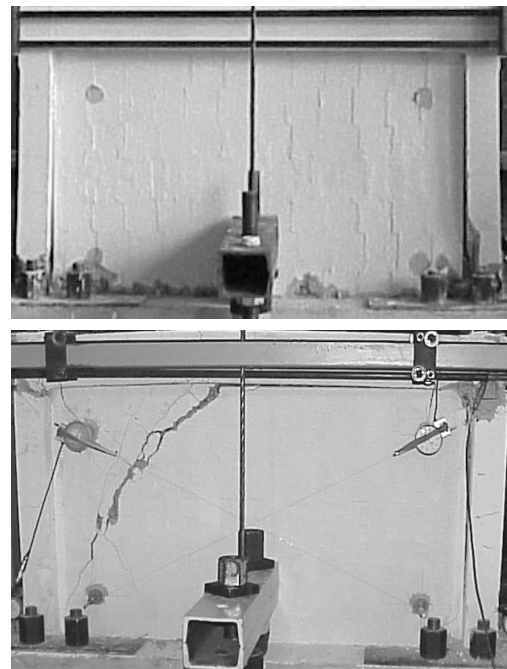


Fig.12. Photographs of first storey infills (CII Specimens)

#### 4.1.4. Frames Strengthened by Using Type III Plates, CIII

CIII specimens were Type III plate strengthened

frames with anchorage to all frame members in the first storey. The plate arrangement for both CIII specimens is shown in Fig. 13. Two frame types showed similar response as can be observed from the values given in Table 2 and response envelopes given in Fig. 14. For forward loading, one storey and two-storey test frames reached a lateral load capacity of 213.5 kN and 212.9 kN when the first storey drift ratio values were 0.0103 and 0.0055, respectively. For backward loading, they reached maximum load values of 204.0 kN and 218.5 kN at drift ratios of 0.0071 and 0.0062, respectively. One-storey specimen has higher ductility than the two-storey specimen, especially in the positive direction. In the negative direction, maximum lateral displacement of two specimen types seems to be similar. It can be noted here that, one-storey specimen has a little wider response envelope than the equivalent two-storey specimen which can possibly be attributed to the pinching effect stemming from the cracks occurred on the infill of the one-storey specimen.

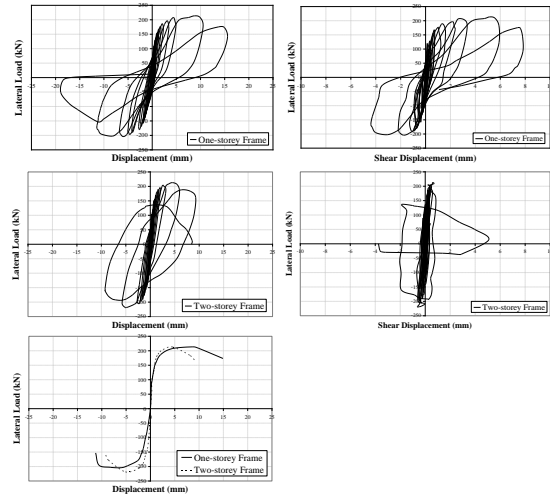


Fig. 14. Comparison of Lateral Load vs. First Storey Displacements of both CIII Specimens

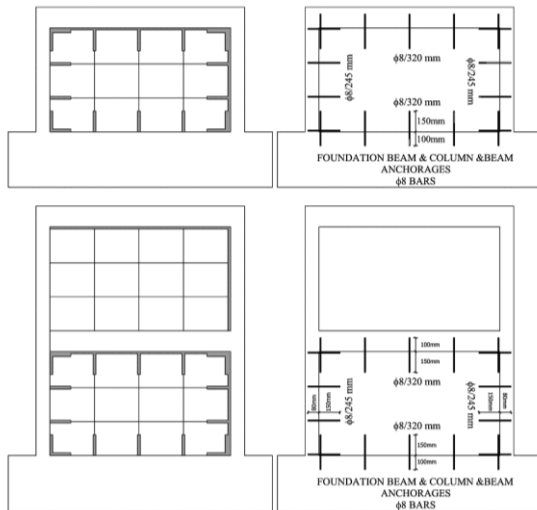


Fig. 13 . Plate Arrangement for both CIII Specimens

Separation of the infill from the columns and cracking at the column bases started in early cycles of both tests. Also, diagonal cracking on the plates started at the same load level for both cases. However, beam-column joints cracked at the one-storey frame before plate cracking, but at the two-storey frame, beam-column joint cracks occurred after plates started cracking. In the last cycles of both tests, column bases started to crush and the cover concrete dispersed. The two-storey frame failed from the column base crushing. On the other hand, the one-storey frame, also having significant damage at the column bases, failed by crushing at the beam-column joint suddenly. One-storey frame had much more wider cracks on the plates. Test results for both frame types are given in Table 2. Photographs of both first story infills of both specimens are given in Fig. 15, where the upper one is of two-storey frame and the lower is one-storey.

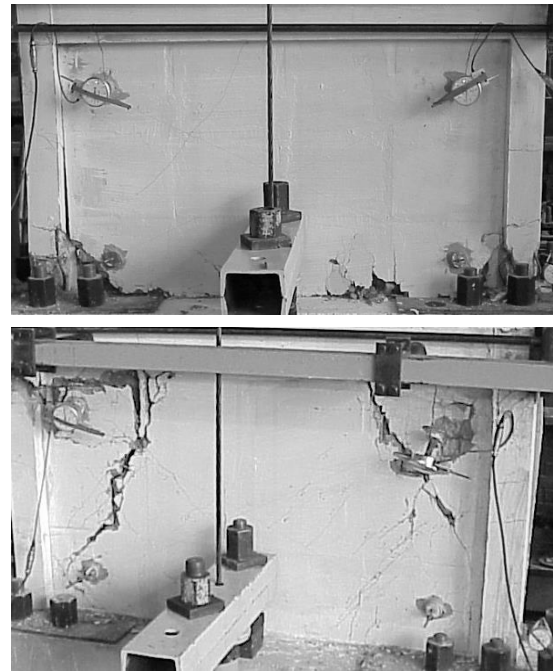


Fig. 15. Photographs of first storey infills (CIII Specimens)

#### 4.2. Initial Stiffness Values of Test Frames

The initial stiffness of a specimen was calculated by using the slope of the linear part of the first forward load excursion. It was used as a relative indicator in improvement of the rigidities of test frames. As it can be seen in Table 3, all one-storey specimens have higher initial stiffness values than the equivalent two-storey specimen. This situation can be owing to the fact that more compressive and shear stress occurring in the infill of the one-storey test frame leading to more stiffer infill. Instead, more tensile stress occurs at the tension side column of two-storey frames resulting from the more

overturning effect of the greater moment arm leading to less rigid specimen in early cycles.

Table 2. Test Results of all Specimens (Ratio of the value of one-storey test frame to that of two-storey test frame)

Sp.		One-St.	Two-St.	Ratio
CR	$f_{ik}$ (MPa)	15.6	16.6	-
	Max.(+)Load	86.6	76.8	1.13
	$(\delta_l/h_l)$	0.0037	0.0042	0.88
	Max.(-)Load	79.1	78.8	1.00
	$(\delta_l/h_l)$	0.0033	0.0030	1.10
CI	$f_{ik}$ (MPa)	18.7	18.2	-
	Max.(+)Load	209.6	186.2	1.13
	$(\delta_l/h_l)$	0.0120	0.0038	3.16
	Max.(-)Load	196.0	192.5	1.02
	$(\delta_l/h_l)$	0.0037	0.0069	0.54
CII	$f_{ik}$ (MPa)	12.2	13.0	-
	Max.(+)Load	197.0	201.3	0.98
	$(\delta_l/h_l)$	0.0056	0.0089	0.63
	Max.(-)Load	187.4	198.2	0.95
	$(\delta_l/h_l)$	0.0066	0.0070	0.94
CIII	$f_{ik}$ (MPa)	14.2	19.4	-
	Max.(+)Load	213.5	212.9	1.00
	$(\delta_l/h_l)$	0.0103	0.0055	1.87
	Max.(-)Load	204.0	218.5	0.93
	$(\delta_l/h_l)$	0.0071	0.0062	1.15

Table 3. Initial Stiffness Values of all Specimens (Ratio of the value of one-storey test frame to that of two-storey test frame)

Sp.	Initial Stiffness (kN/mm)		
	One-St.	Two-St.	Ratio
CR	95.8	64.7	1.48
CI	312.4	275.9	1.13
CII	308.0	197.6	1.56
CIII	294.0	196.1	1.50

#### 4.3. Shear Deformations in the First Storey Infill Walls of Test Specimens

Lateral load-first storey shear displacement curves of all specimens are presented in Fig. 6, Fig. 9, Fig. 12 and Fig. 15. As seen in these figures, there was a visible shear deformation on the first storey of Reference Specimens CR. After introducing PC plates, the shear deformation due to base shear reduced in first storey plates. PC plates behaved rigidly so that they prevented excessive shear deformations. In the case of comparing the equivalent

strengthened specimen pairs, shear displacement in the infills of two-storey specimens are less with the respect to that of one-storey specimens, as expected. This is more visible especially in the case of Specimens CI and Specimens CIII. In the case of Specimens CII, less crack formation on the first storey infill of one storey specimen may lead to the less shear deformation difference between this equivalent pair.

#### 4.4. Energy Dissipation Capacities of Test Specimens

When a structure deforms, the work done is stored as strain energy. Part of this energy is released in the unloading process, whereas the remaining energy is dissipated through different mechanisms.

Energy dissipation capacity is an important indicator of the structure's ability to withstand severe earthquakes. It is also an important indicator of the improved seismic behavior. For both type of test frames, the amount of dissipated energy was determined by adding the areas under the lateral load vs. load application level displacement curves for each cycle. It is important to note here that the energy dissipation characteristics of the test frames depend on the loading history.

Total amount of dissipated energy of each specimen is tabulated in Table 4. As it can be seen in this table, all one-storey test frames dissipated less energies with respect to their equivalent pairs except from Specimens CI, for which the dissipated energies by these specimens can be accepted as equal. More pinching effect observed in one-storey test frames seems to be one of the causes for this less energy dissipation.

All strengthened two-storey test frames behaved as a monolithic cantilever, meaning that heavy damage due to reversed cyclic lateral loads concentrated through the column bases together with the infill base. In addition, damage concentrated on the infill and beam-column joints for one-storey specimens, meaning that one-storey strengthened test frames exhibited frame behavior rather than monolithic cantilever.

Table 4. Energy Dissipation Capacities of all Specimens (Ratio of the value of one-storey test frame to that of two-storey test frame)

Sp.	Energy Dissipation (Joule)		
	One-St.	Two-St.	Ratio
CR	5.7	6.4	1.12
CI	15.5	15.3	0.99
CII	15.1	21.8	1.44
CIII	9.2	13.4	1.46

## 5. SUMMARY OF THE EXPERIMENTAL RESULTS

### 5.1. Effectiveness of the Proposed Strengthening Technique

Lateral load vs. displacement curves given in

previous section indicate a significant increase in the load carrying capacity and a delayed strength degradation, leading to a better ductile behavior when precast concrete plates are bonded on to the plastered infill wall. An overall interpretation of the test results are summarized in Table 5 in terms of load carrying capacity, lateral rigidity, ductility and energy dissipation capacity points of view. Table 5 shows the effectiveness of the proposed strengthening technique.

Table 5. Performance improvement by the proposed technique (for both frame types)

	Relative to reference frame
Lateral load capacity	~2.5 times
Lateral stiffness	~3 times
Ductility	~2 times
Energy dissipation	~3 times

## 5.2. Comparison of Infill Behavior

During the tests, the behavior of the one-storey frame is very similar to the first storey of the two-storey frame, while the upper storey of the two-storey frame remains with minor damage. Cracking at the frame members and the infill starts and progresses similarly in all cases. After some cracks occur on frame members, diagonal cracks start on the infill. Then, heavy damage concentrates at the column bases and beam-column joints, and following the failure or damage of the infill, the frame members fail at these regions. The main difference of observed damage between the one-storey and the two-storey frames is that the first storey beam-column joint region of the one-storey frame receives much more significant damage than the same place of the two-storey frame.

One-storey and two-storey frames of same application showed very similar behavior. Lateral load capacities of two frame types are very close. One of the main differences is the application level of loading. In two-storey frames, the lateral load was applied at a greater height and therefore moment arm is greater. Greater moment arm of lateral load results in more overturning effect. So, more tensile stress occurs at the tension side column of two-storey frames. Compressive and shear stresses are more dominant in one-storey frames. This is the most possible reason for higher initial stiffness of one-storey frames. Ductility of the two frame types are not largely different, but generally one-storey frames showed higher ductility which can be a result of more efficient behavior of the infill, which can be positively influenced by the confining effect of compressive forces.

When the lateral load-first storey displacement curve for one and two storey frames are compared, it is observed that there is a significant difference at the shape of the loops. Load-displacement curves for one-storey frames have a much more pinched shape than the curves for two-storey frames. This difference is small for the reference specimens. Pinching is the result of higher shear stresses causing larger crack widths, because when the

loading is reversed, no stiffness can be observed while the cracks are closing. Therefore, the main reason for more pinching in one-storey frames is the higher level of shear action.

## 6. CONCLUSIONS

The conclusions presented below are based on the limited data obtained from eight tests conducted;

- The seismic rehabilitation technique reported in the present study significantly increased the lateral load capacity and rigidity as well as improving the seismic behavior of the test frames.
- The effectiveness of the rehabilitation technique can easily be observed from the tests of both one and two-storey frames showing that plate bonded hollow brick infill walls behave efficient and effective under compressive and shear stresses as well as tensile stresses.
- One-storey and two-storey frames of same application showed very similar behavior, especially lateral load capacities of two frame types are very close, indicating that they are equally acceptable as test units and one-storey frames may be preferred in the cases where there exists space, time and testing facility limitations.
- In the tests of one-storey specimens, failure occurred with significant damage in the beam-column joints which indicates that the effectiveness of the proposed technique depends not only on the strengthening plate properties but also on the properties of the existing frame. To have a satisfactory strengthening performance, strengthening of the frame members prior to the introduction of plates will obviously be needed.

## ACKNOWLEDGEMENTS

The financial support given by the Scientific and Technical Research Council of Turkey (TÜBİTAK-İÇTAG I 575) and North Atlantic Treaty Organization (NATO-SFP 977231) are gratefully acknowledged.

## REFERENCES

- Baran, M. (2005). Precast concrete panel reinforced infill walls for seismic strengthening of reinforced concrete framed structures. PhD Thesis, Middle East Technical University, Ankara, Turkey.
- Baran, M., Canbay, E. and Tankut, T. (2010). "Seismic strengthening with precast concrete panels-theoretical approach." *UCTEA, Turkish Chamber of Civil Engineers, Technical Journal.*, Vol. 21, No. 1, pp. 4959 – 4978.
- Baran, M., Duvarcı, M., Tankut, T., Ersoy, U. and Özcebe, G. (2003). "Occupant friendly seismic retrofit (ofr) of rc framed buildings." *Seismic Assessment and Rehabilitation of Existing Buildings*, Nato Science Series, IV. Earth and Environmental Series, Vol. 29, pp. 433-456.
- Baran, M., Okuyucu, D., Susoy, M. and Tankut, T. (2011).

“Seismic strengthening of R/C frames by precast concrete panels.” *Magazine of Concrete Research*, Vol. 63, No. 5, pp. 321-332.

Baran, M., Susoy, M. and Tankut, T. (2011). “Strengthening of deficient RC frames with high strength concrete panels : an experimental study.” *Structural Engineering and Mechanics*, Vol. 37, No. 2, pp. 177-196.

Baran, M. and Tankut, T. (2011). “Experimental study on seismic strengthening of RC frames by precast concrete panels” *ACI Structural Journal*, Vol. 108, No. 2, pp. 227-237.

Frosch, R.J., (1996). Seismic rehabilitation using precast infill walls. PhD Thesis, The University of Texas at Austin, USA.

Frosch, R.J., (1999). “Panel Connections for Precast Concrete Infill Walls.” *ACI Structural Journal*, Vol. 96, No. 4, pp. 467-474.

Frosch, R.J., Li, W., Jirsa, J.O. and Kreger, M.E. (1996). “Retrofit of non-ductile moment-resisting frames using precast infill wall panels.” *Earthquake Spectra*, Vol. 12, No. 4, pp. 741-760.

Frosch, R.J., Li, W., Kreger, M.E. and Jirsa, J.O. (1996). “Seismic strengthening of a nonductile rc frame using precast infill panels.” *Eleventh World Conference on Earthquake Engineering*, Acapulco, Mexico.

Han, T. S., Feenstra, P. H. and Billington, S. L. (2003). “Simulation of highly ductile fiber-reinforced cement-based composite components under cyclic loading.” *ACI Structural Journal*, Vol. 100, No. 6, pp. 749-757.

Hanson, R.D. (1980). “Repair and strengthening of buildings.” *Proceedings of the 7th WCEE*, İstanbul, Turkey, Vol. 9, pp.71-74.

Isao, M., Hiroshi, T. and Ryoji, H.A. (1999). “A Seismic Strengthening Method for Existing R/C Buildings by Shear Walls Installed Precast Concrete Panel.” *Japan Science and Technology Agency, Concrete Journal*, Vol. 37, No. 11, pp. 20-26.

Kahn, L.F., Hanson, R.D. (1979). “infilled walls for earthquake strengthening.” *Proc. of the ASCE*, Vol. 105 (ST2), pp. 283-296.

Kaldjian, M.J. and Yuzugullu, O. (1983). “Efficiency of bolt connected shear panels to strengthen building structures.” *The First International Conference on Concrete Technology for Developing Countries*, Yarmouk University, 16-19 Oct., Irbid, Jordan.

Kanda, T., Watanabe, W., Li, V. C. (1998). “Application of pseudo strain hardening cementitious composites to shear resistant structural elements.” *Fracture Mechanics of Concrete Structures. Proceedings of FRAMCOS-3*, Freiburg, Germany, pp. 1477-1490.

Kesner, K., E. (2003). Development of seismic strengthening and retrofit strategies for critical facilities using engineered cementitious composite materials. PhD

Dissertation, Cornell University, Ithaca, NY.

Kesner, K. E., Billington, S. L. and Douglas, K., S. (2003). “Cyclic response of highly ductile fiber-reinforced cement-based composites.” *ACI Materials Journal*, Vol. 100, No. 5, pp. 381-390.

Kesner, K. and Billington, S.L. (2005). “Investigation of infill panels made from engineered cementitious composites for seismic strengthening and retrofit.” *ASCE Journal of Structural Engineering*, Vol. 131, No. 11, pp. 712-1720.

Kesner, K. E. and Billington, S. L. (2001). “Investigation of ductile cementbased composites for seismic strengthening and retrofit.” *Fracture Mechanics of Concrete Structures*, de Borst et al (eds), Swats & Zaltlinger, Lisse, pp. 65-72.

Li, W. (1997). Experimental evaluation and computer simulation of post tensioned precast infill wall system. PhD Thesis, The University of Texas at Austin, USA.

Matsumoto, T. (1998). “Structural Performance of SRC Multi-storey Shear Walls with Infilled Precast Concrete Panels.” *Japan Concrete Institute*, Tokyo.

Nakashima, M., (1995). “Strain hardening behavior of shear panels made of low-yield steel, I: test.” *Journal of Structural Engineering*, Vol. 121, No. 12, pp. 1742-1749.

Phan, T.L., Cheok, S.G. and Todd, R.D. (1995). “Strengthening methodology for lightly reinforced concrete specimens.” *Recommended Guidelines for Strengthening With Infill Walls*. Building and Fire Research Laboratory, National Institute of Standards and Technology (NIST), Gaithersburg.

Roberts, T. M. (1995). “Seismic resistance of steel plate shear walls.” *Engineering Structures*, Vol. 17, No. 5, pp. 344-351.

Sevil, T., Baran, M. and Canbay, E. (2010). “Tuğla dolgu duvarların B/A çerçevesi yapıların davranışına etkilerinin incelenmesi; deneysel ve kuramsal çalışmalar.” *International Journal of Research and Development (IJERAD)*, Vol. 2, No.2 pp. 35-42.

Susoy, M. (2004). Seismic strengthening of masonry infilled R/C frames with precast concrete panel infills. MSc. Thesis, Middle East Technical University, Ankara, Turkey.

Tankut, T., Ersoy, U., Özcebe, G., Baran, M. and Okuyucu, D. (2005). “In service seismic strengthening of RC framed structures.” *Seismic Assessment and Rehabilitation of Existing Buildings*. International Closing Workshop, NATO Project SIF 977231, İstanbul, Turkey.

Yuzugullu, O. (1979). “Strengthening of Reinforced Concrete Frames Damaged by Earthquake Using Precast Panel Elements.” *Turkish Scientific and Technical Council, Project No. MAG-494 (in Turkish)*, Ankara, Turkey.

# Turkish Journal of Engineering



*Turkish Journal of Engineering (TUJE)*  
*Vol. 3, Issue 4, pp. 189-196, October 2019*  
*ISSN 2587-1366, Turkey*  
*DOI: 10.31127/tuje.537871*  
*Research Article*

## **LOGIC THRESHOLD FOR MICRORING RESONATOR-BASED BDD CIRCUITS: PHYSICAL AND OPERATIONAL ANALYSES**

Ozan Yakar <sup>\*1</sup> and İlke Ercan <sup>2</sup>

<sup>1</sup> Boğaziçi University, Engineering Faculty, Electrical & Electronics Engineering Department, İstanbul, Turkey  
ORCID ID 0000-0003-1357-8920  
(ozan.yakar@boun.edu.tr)

<sup>2</sup> Boğaziçi University, Engineering Faculty, Electrical & Electronics Engineering Department, İstanbul, Turkey  
ORCID ID 0000-0003-1339-9703  
(ilke.ercan@boun.edu.tr)

---

\* Corresponding Author

Received: 10/03/2019 Accepted: 18/06/2019

---

### **ABSTRACT**

Moore's Law has been the fuel of expansive innovation in computing. The chip industry kept the Moore's law extant for almost four decades. However, the halt of the rapid progress of the silicon technology is incipient by reason of the physical limitations. Emerging computing proposals suggest several alternatives to current computing paradigms and technology-bases. The photonic circuitry is one of the most promising candidates with its high operation speed, energy efficient passive components, low crosstalk and appropriateness for parallel computation. Among various approaches to photonic logic, microring resonator-based Binary-Decision Diagram (BDD) architectures have a special place due to their small circuit footprint. However, the physical limitations imposed on their logic implementation has not been studied in depth to enable design of efficient circuits. In this paper, we study the physical structure and operational details of a microring resonator-based Half-Adder (HA) circuit and outline the conditions under which the performance and accuracy of information processing is compromised due to its physical characteristics. Our analyses significantly contribute to determining key physical features and operations concerning logic implementation of microring resonator based BDD HA, which informs the future design and operational optimization of the microring resonator-based BDD logic circuits.

**Keywords:** *Binary Decision Diagrams, Ring Resonators, Optical Processing, Photonic Logic*

## 1. INTRODUCTION

The performance of electronic technologies has improved exponentially with the shrinking of device sizes. Transistor-based circuits are limited by the bandwidth limitations caused by the silicon electronics and the printed metallic tracks. In addition, the increased heat generation caused by the denser designs leads to the inefficient operation of the transistors. Hence, the trend in the reduction of the size has come to an immediate halt in the recent years as the computer industry proposed multicore architectures with optical interconnects to create a parallelism of systems (Hardesty, 2009; Miller, 2010a).

The desire to continue the scaling of computing systems at thousand-fold pace in every 10 years without an increasing cost has driven a strong demand in the search of new technologies. Alternative proposals for the transistor technology have been made using carbon nanotubes (Bachtold *et al.*, 2001; Tans *et al.*, 1998; Aly *et al.*, 2015), graphene like 2D materials (Chhowalla *et al.*, 2016; Sordan *et al.*, 2009), spintronic materials (Pesin and Mac Donald, 2012; Gardelis *et al.*, 1999), novel technologies using quantum computing (Ladd *et al.*, 2010), neuromorphic computing (Shastri *et al.*, 2018; Woods and Naughton, 2012) and photonics (Rios *et al.*, 2015; Rios *et al.*, 2018; Stegmaier *et al.*, 2017; Cheng *et al.*, 2018; Lin *et al.*, 2012; Chattopadhyay, 2013; Fushimi and Tanabe, 2014). In the last decades, optics proved itself to be the best way of delivering data due to its high energy efficiency, rapid information transmission, low crosstalk and parallelism. However, optics can offer beyond communication with its energy efficient, low heat generative components and the intrinsic nature of optics allows fast and low energy computation compared to electronics (Caulfield and Dolev, 2010). Thence, photonics is one of the strongest candidates to replace the transistor technology. All-optical switching allows bypassing the optics to electronics conversions and vice versa. In addition, many pre- and post- processors have been proposed recently (Larger *et al.*, 2012; Paquot *et al.*, 2012) such as vector matrix multiplier, which reduced the computation time from  $O(N^2)$  to  $O(N)$  (Woods and Naughton, 2012).

In order to make a universal logic gate, a device needs to offer fan-out and bistability therefore logic level restoration, infinite cascibility and input-output isolation (Miller, 2010b). In the BDD architecture, the use of Y-splitters can allow the architecture to have a fan-out property. Similarly, mergers allow the electromagnetic field to be superposed, therefore they provide a fan-in property, which do not exist in electronics (Caulfield and Dolev, 2010). Without the using the fan-in property, microring resonator logic circuits can allow us to make reversible operations, in which one can reconstruct the inputs from the outputs. Although most of the photonic devices do not offer bistability, there are some promising examples of demonstration of bistability using chalcogenide phase-change materials in refs. (Rios *et al.*, 2015; Rios *et al.*, 2018; Stegmaier *et al.*, 2017; Cheng *et al.*, 2018). The BDD half-adder structure in ref. (Lin *et al.*, 2012) does not offer complete bistability, the resonant condition being not completely volatile allows the microring resonator to bypass this problem in video processing applications. Another constraint in the design of the logic circuits is the device footprint. Most photonic

devices having large footprint compared to electronics can be overcome by the design of 3D structures.

In the design of optical logic circuits, there are other candidates that offer switching, i.e. Mach Zehnder interferometers and photonic crystals. Although the Mach Zehnder interferometer offers switching capability, it is not preferable in the design of logic circuits because of its large footprint, reduced switching and true volatility of the state. Moreover, however, the photonic crystals are able to offer bistable switching and small footprint (Notomi *et al.*, 2005), their high scattering losses make them energy inefficient for logic applications.

A variety of materials have been used in the design of microring resonators (Wu *et al.*, 2016; Tazawa *et al.*, 2006; Guarino *et al.*, 2007). Because of the high index difference between the silicon and silicon-oxide (or air) light is confined well in the resonators, therefore the silicon microring resonators can have small footprints. In addition, the production techniques for silicon electronics are well developed. Hence, we use silicon wafer in order to be compatible with the current CMOS technology and small footprint (Bogaerts *et al.*, 2005; Green *et al.*, 2007; Fedeli, *et al.*, 2010; Gunn, 2006a; Gunn, 2006b; Bogaerts *et al.*, 2012).

The silicon-based photonic technologies are high in demand as they are constructed using widely known structures in well-established facilities. However, alternative architectures are introduced to perform logic operations using silicon-based photonic devices. This emerging trend raises questions around the physical constraints and performance limitations of these optical systems. To this day, although the physics of a single microring resonator is studied in refs. (Hammer *et al.*, 2004; Bogaerts *et al.*, 2006; Heebner *et al.*, 2004), very few attempts have been made to study the physical and operational details of photonic logic circuits. In this paper, we address this issue by using circuit designed in ref. (Lin *et al.*, 2012) as an illustrative example laying out the physical design relation between the resonators and the constraints it enforces to perform a logic operation.

BDD architecture allows the systems to be designed in a more scalable way compared to the conventional CMOS architectures, which are growing exponentially. For example, CMOS half-adder has 5 NAND gates, BDD NAND gate has 2 switching nodes and half-adder has 3 switching nodes.

This paper is organized as follows; we first introduce the fundamental principle of the BDD architecture and explain its microring resonator-based realization. In the next section, we perform extensive physical analyses on the BDD HA, discussing the transmission properties of the system and explain the interference phenomenon and the asymmetries it introduces. Later, we comment on the logic threshold, revealing the conditions under which accurate computation can be performed. Finally, we conclude by closing remarks and comments on our future work.

## 2. MICRORING RESONATOR IMPLEMENTATION OF BDD ARCHITECTURE

In this section, we explain the physical characteristics and operation dynamics of Binary Decision Diagram (BDD) based logic circuits. The BDD logic is an

alternative approach for performing Boolean logic operations that provide a compact representation allowing higher capacity for scaling with the increasing complexity of operations. The BDD architecture first has been proposed by Akers (1978), and refined by Bryant (1986). It is an alternative computation technique to the traditional computation techniques using Karnaugh Maps and algebraic manipulations (Akers, 1978; Bryant, 1986; Lin *et al.*, 2012). There are various physical realizations of this abstract computational model including Single Electron Tunneling (SET) Transistor Technology (Asahi *et al.*, 1997), quantum computing (Yoshikawa *et al.*, 2002), mirrors (Chattopadhyay, 2013), and optical microring resonators (Lin *et al.*, 2012). In this paper, we focus on physical realization of BDD architecture using microring resonator logic circuits.

The microring resonators have been introduced in ref. (Marcatili, 1969) and its theory has been developed by (Hammer *et al.*, 2004; Bogaerts *et al.*, 2006; Heebner *et al.*, 2004; Little *et al.*, 1997). Here, in this paper, we analyze the physical responses of multi-microring resonator devices both analytically and numerically.

Assume we have a Boolean function of  $n$  variables from  $x_1, \dots, x_n$  making the inputs of the function. In the binary decision mechanism, the signal is processed through serial switching nodes. In Fig. 1, a single BDD node is shown (left). At the node we test the variable  $x_i$  and depending on  $x_i = 0$  or  $x_i = 1$ , the control signal coming from the incident (root) is sent to one of the two leaves. And the signal is sent to the roots testing the variable  $x_{i+1}$ . This serial switching mechanism enforces one to control each and every layer of computation with a different parameter. In order to process the information, these parameters should be independent. Fig. 1 (right) depicts the microring resonator realization of a BDD node. The microring resonator is an optical traveling wave resonator made of one or two straight waveguides called bus waveguides and a circular or a racetrack shaped waveguide.

There is a control signal is sent through the incident port and the light propagating in the ring interferes with itself, therefore creates discrete constructive resonance conditions and if the second bus waveguide exists, some portion of the light is transmitted to the drop port in the certain wavelengths. The selection of the wavelengths is done in the directional couplers. Directional couplers allow the resonator to have two fundamental modes, i.e., symmetric and asymmetric modes that can be seen in Fig. 1 (right). All the modes are the superposition of these modes. Changing the optical pathlength of the ring by changing the index of the ring externally allows us to do the switching.

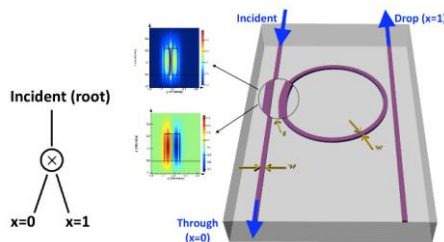


Fig. 1. Symbol of the BDD switching node (left), schematic diagram of a switch using ring resonator on SOI wafer (right) (Yakar *et al.* 2019).

### 3. PHYSICAL ANALYSIS OF MICRORING RESONATOR-BASED BDD HALF-ADDER

The BDD based microring resonator circuits are proposed as energy efficient alternatives in photonic logic. In this section we develop a thorough physical analysis of this emerging computing approach using the microring resonator based BDD Half Adder circuit proposed in ref. (Lin *et al.*, 2012). To the best of our knowledge, Wada's proposal is the first application of microring resonator based realization of BDD, and the analyses presented in this paper lead the way for developing efficient strategies to build new BDD circuits using microring resonators.

The BDD half adder circuit is depicted in Fig. 2 (left). The control signal is sent through the port I and tested in the resonator controlled by the variable  $a_0$  and two resonators controlled by the variable  $b_0$ . Variables  $a_0$  and  $b_0$  can be temperature, voltage or light intensity. The variables are able to change the effective indices of the rings, therefore changing the transfer functions of the field amplitudes  $T_1, T_2, K_1$  and  $K_2$ . In resonators the light splits into two waveguides with different proportions determined by the variables  $a_0$  and  $b_0$ . In the  $S_0$  port there are two possible paths, i.e., light going to the drop port of the resonator one, taking  $1b$  waveguide and going to the through port of the upper resonator then taking  $10$  waveguide and light going to the through port of the resonator controlled by parameter  $a_0$ , taking  $0b$  waveguide and going to the drop port of the upper resonator then taking  $01$  waveguide. The fields are superposed in the merger before  $S_0$  port. The optical pathlength difference in the two different optical paths changes the transmission spectrum hence the optical pathlength difference is an important parameter in the analysis of the system. The truth table of the half-adder is shown in Fig. 2 (right). The inputs  $\{a_0 b_0\} = \{01, 01\}$  are mapping to the same output, hence the effect of the 01 and 10 inputs should be symmetric to conduct a logic operations.

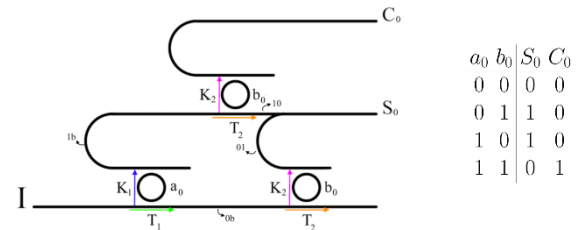


Fig. 2. Schematic diagram of BDD half-adder is shown (left). The transfer functions of the amplitudes have been shown with  $T_1, T_2, K_1$  and  $K_2$ . The waveguide names are denoted as  $0b, 1b, 01$  and  $10$ .  $S_0$ -port denotes the sum bit and  $C_0$ -port denotes the carry bit.  $I$  denotes the port where the signal in incident is sent. The truth table of half-adder is shown (right).  $a_0, b_0$  are the inputs and  $S_0$  denotes the sum bit and  $C_0$  denotes the carry bit.

In this section, we first calculate the transmission characteristics of the  $S_0$  port analytically, and discuss the critical conditions where these characteristics have implications for logic operations. We provide the effect of the temperature change and the optical pathlength differences and demonstrate the optimized cases for symmetric physical operations.

In the BDD half-adder in Fig. 2, the field that is resonant to the ring  $a_0$  goes to the upper guide and its phase evolves as it goes through the waveguide. Then, it goes through the second ring and its phase evolves again. The field that is not resonant to the ring  $a_0$  goes through a similar process. And these two fields are superposed before arriving to the port  $S_0$ . These two fields can be represented as  $B^{10}$  and  $D^{01}$  respectively.  $B^{10}$  and  $D^{01}$  can be represented as

$$D^{01} = e^{-i\Phi_{01}} K_2 e^{-i\Phi_{0b}} T_1 = e^{-i(\Phi_{01} + \Phi_{0b})} e^{ip_{01}} |D^{01}| \quad (1)$$

$$B^{10} = e^{-i\Phi_{10}} T_2 e^{-i\Phi_{1b}} K_1 = e^{-i(\Phi_{10} + \Phi_{1b})} e^{ip_{10}} |B^{10}| \quad (2)$$

where  $\Phi_{01}$ ,  $\Phi_{0b}$ ,  $\Phi_{10}$  and  $\Phi_{1b}$  are the phase changes in the waveguides are depicted in Fig. 2. The total phase delays represented by  $p_{01}$  and  $p_{10}$ , introduced at the rings and the couplers at the top of Fig. 2.

The fields are superposed before arriving the  $S_0$  port. Assuming the recombiner is symmetric, the theoretical total field becomes

$$S_0 = \frac{D^{01} + B^{10}}{\sqrt{2}} \quad (3)$$

The single recombiner is simulated using Lumerical varFDTD shown in Fig. 3. The transmission response of two beams confirms our assumption for  $1.55 \mu m$ , so we can claim the fields are superposed with equal weight up to this point. The simulations performed here are two-dimensional FDTD with effective-index method which may yield higher energy losses. In order to increase the accuracy of energy calculations three-dimensional simulations can be performed.

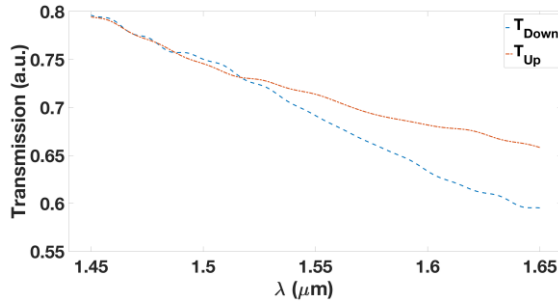


Fig. 3. Transmission spectra of recombiner is simulated in Lumerical MODE solutions. The simulation is run for two different beams sent from two different arms separately.  $T_{Up}$  (orange, dashed-dotted) line represents the case for the beam sent from the top arm and  $T_{Down}$  (blue, dashed) line represents the beam sent from the bottom arm.

Plugging the above Eq. (1) and (2) into Eq. (3) and factoring out the phases of  $D^{01}$  reduces the equation into

$$S_0 = \frac{e^{-i(\Phi_{01} + \Phi_{0b})} e^{ip_{01}} (|D^{01}| + |B^{10}| e^{i\Delta\Phi} e^{i\Delta p})}{\sqrt{2}} \quad (4)$$

So the transmission intensity becomes,

$$Tr = S_0^* S_0 = \frac{1}{2} (|D^{01}|^2 + |B^{10}|^2 + 2|D^{01}||B^{10}|\cos(\Delta\Phi + \Delta p)) \quad (5)$$

If we swap the input signals, i.e.  $a_0 b_0 \rightarrow b_0 a_0$ , it will lead  $\Delta p \rightarrow \Delta p$  because the effect of the resonators in Eq. (1) and (2) are symmetric. In order the transmission spectrum to be symmetric,  $\cos(\Delta\Phi + \Delta p)$  must be constant when input signals are swapped. So,  $\Delta\Phi = 2\pi m$ , where  $m \in \mathbb{Z}$ . That is why optical path length difference should be zero (or  $2\pi m$ ) in order to have a constant spectrum when we interchange the input signals. In order to tune the rings and the couplers there are various effects used such as electro-optic effect and thermo-optic effect. However, if these effects are not local, the optical path length difference will depend on the light intensity or temperature profiles. Light intensity or temperature profiles must be known in order to minimize the optical path difference.

Although the circuit in Fig. 2 is asymmetric by means of inputs, the physical responses can be made symmetric as seen in Figs. 4 and 5. However, the switching energies from logic-0 to logic-1 and logic-1 to logic-0 are not going to be identical to each other. This phenomenon is also seen in electronics, i.e., in transistor based electronic circuits, energetic cost of transitioning from logic-0 to logic-1 and logic-1 to logic-0 is not identical due to physical effects such as charge sharing and parasitics.

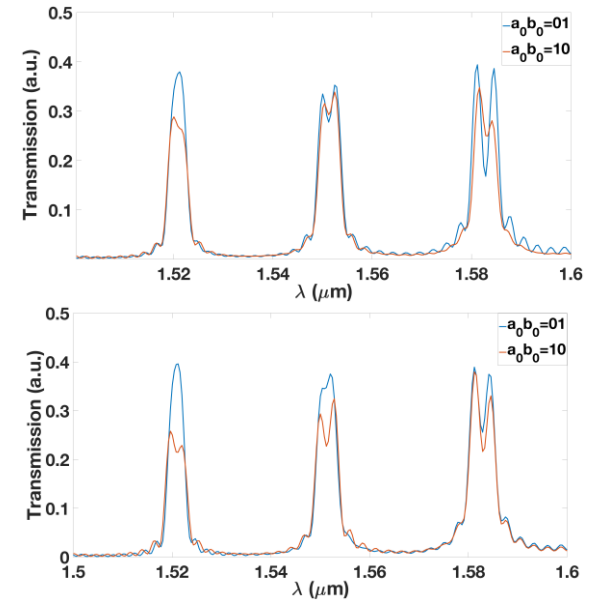


Fig. 4. Transmission spectrum of  $S_0$  port at  $1 \mu m$  (top) and  $1.05 \mu m$  (bottom) difference in the waveguides for 01 and 10 signals with at  $r = 2.7 \mu m$ ,  $g = 0.8 \mu m$  at one ring at 300 K and the other at 315 K.

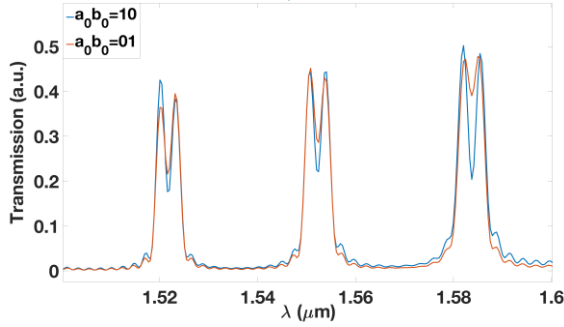


Fig. 5. Transmission spectrum of  $S_0$  port at  $r = 2.7 \mu\text{m}$ ,  $g = 0.8 \mu\text{m}$  at one ring at 300 K and the other at 340 K.

#### 4. THRESHOLD FOR LOGIC OPERATION

In the previous section, we have discussed the role of the physical effects in performing logic operations. The analyses we have developed provide a clear picture on physical conditions that are required to obtain accurate outcome of computation. The physical states that are used to represent logic-0 and -1 states have to be distinguishable for information processing to happen with precision. In this section, we define the threshold for logic operations to take place accurately.

The crosstalk in the computation is not completely avoidable. Even if, a completely symmetric structure is designed, there may be some variations while the circuits are manufactured. Ring resonators are very sensitive to these variations. Thus, the response of the circuits may change significantly for a small change in the dimensions of the components. Although we cannot overcome these variations in production and tuning in without consuming too much energy, we may still continue to do the logic operation with a carefully chosen threshold.

Logic mapping makes one to be able to envisage the possible outputs and their corresponding inputs. While the device is operated the physical response of the designated inputs must give well-defined outputs and the output sets must be disjoint. When these conditions are satisfied, it is appropriate to define regions, i.e. envelope curves, to quantize the outputs. Therefore, one can define a threshold for the decision-making.

In the half-adder structure, we need to group the inputs  $(a_0b_0)$  as  $\{00, 11\}$  and  $\{10, 01\}$  while inspecting the  $S_0$  bit in the Fig. 2 (right). We need to design the physical system so that the two groups of outputs, i.e. 0 and 1 state, are well defined and disjoint. When the two physical outputs have an intersection, the logic state will be indeterminate. If the envelope curves of two outputs are intersecting, there is a probability that the actual transmission curves of the manufactured system are intersecting because there can be some fluctuations because of the environment, production or tuning mechanism. In order to have a stable system, we need to separate the regions that are bounded by the envelope curves.

In Fig. 6 (top), physical response of inputs  $a_0b_0 = 11$  intersects the region bounded by  $S_0$  Low and  $S_0$  High. Hence, there is no threshold for logic for some optical pathlength. Due to some external effects or manufacturing, the device may not be able to conduct the logic operation. In the Fig. 6 (bottom),  $1.793\delta\lambda$  shift of the resonances will create a threshold for logic operation

at  $1.55 \mu\text{m}$ . Here, the coefficient 1.793 is set based on the numerical calculation of the input-output mapping. It can be precisely formulated for based on the physics and operation of any given optical logic circuit.

So, if the shift of two peaks is more than  $1.793\delta\lambda$ , the outputs are well defined and disjoint. As we increase the shift of two resonant peaks more and more, the transmission responses of two logic outputs will be more and more away from each other. This is illustrated in Figs. 7 (top) and 7 (bottom). As can be seen in Figs. 6 (bottom), 7 (top) and 7 (bottom) the  $S_0$  (Low) and  $S_0$  (High) come closer to each other with the increasing shift between the resonances of two layers of switching nodes since transmission responses have a less effect on each other with the increasing shift of the resonant wavelengths. Hence, if we increase the switching energy, the importance of the phase modulation will decrease inasmuch as the crosstalk is lower. That means the phase sensitivity decreases.

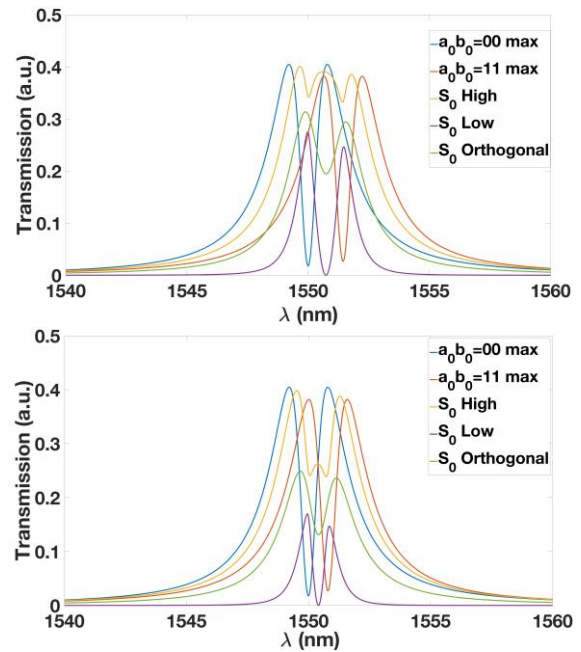
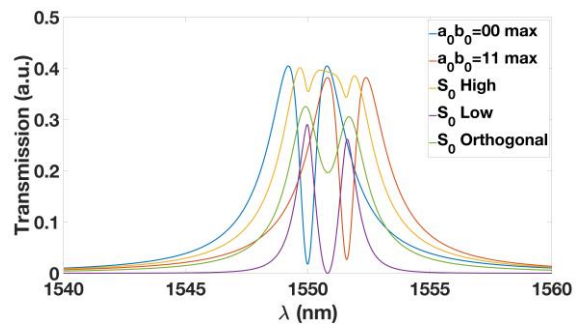


Fig. 6. The theoretical transmission response of the Half-Adder Structure with  $|K_1| = 0.8$ ,  $|K_2| = 0.75$ , efficiency 0.85 and the distance between two resonances as  $\delta\lambda$  (top) and  $1.793\delta\lambda$  (bottom). Vertical axis denotes the transmission in the linear scale and the horizontal axis denotes the wavelength in nm.



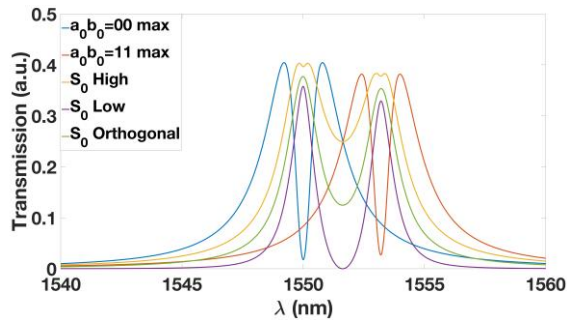


Fig. 7. The theoretical transmission response of the Half-Adder Structure with  $|K_1| = 0.8$ ,  $|K_2| = 0.75$ , efficiency 0.85 and the distance between two resonances as  $2\delta\lambda$  (top) and  $4\delta\lambda$  (bottom). Vertical axis denotes the transmission in the linear scale and the horizontal axis denotes the wavelength in nm.

## 5. CONCLUSIONS

In this paper, we perform a physical analysis of the BDD half-adder with microring resonator switching nodes. The physical analyses we perform show that, the switching parameter (temperature, voltage etc.) and optical pathlength are crucial factors in the design of microring resonator logic circuits because of the interference phenomenon. The transmission response of the device is made symmetric by tuning the tuning parameter, waveguide lengths or a mixture of these. Because of the high sensitivity of the silicon microring resonators, a threshold for logic operation is set. When the waveguide lengths are not optimized the minimum distance of the two resonant at the  $S_0$  port peaks should be  $1.793\delta\lambda$ , where  $\delta\lambda$  is the half-width half-maximum in the transmission vs. wavelength graph.

Physical realizations of BDD architecture are presented using Single Electron Tunneling (SET) transistors (Asahi *et al.*, 1997), quantum computing (Yoshikawa *et al.*, 2002), mirrors (Chattopadhyay, 2013), and microring resonators (Lin *et al.*, 2012). Although the physical analyses of single microring resonators are done in refs. (Hammer *et al.*, 2004; Bogaerts *et al.*, 2006; Heebner *et al.*, 2004), analysis of BDD logic circuits are done and the physical limitations of the microring resonator based BDD half adder are found for the first time in this work. These analyses will shine light on the future designs and energy optimizations of other microring resonator based BDD circuits.

The theoretical analyses we perform here present guidelines in designing the optimum physical circuit structure as well as information dynamics that leads to minimum energy dissipation in microring resonator-based logic circuits. As a part of our future work, we aim to design and analyse other microring resonator-based BDD logic circuits with varying complexity to illustrate how the performance scale with size and how the energy dissipation varies based on structure and operation.

## ACKNOWLEDGEMENTS

The authors would like to thank Ms. Blanca Ameiro Mateos for extensive support with technical drawing of the BDD circuit schematic and Mr. Gökberk Elmas for comments on the manuscript. This paper presents

preliminary findings from PI's MISTI: MIT-Boğaziçi University Seed Fund project.

## REFERENCES

- Akers, S. B. (1978). "Binary decision diagrams." IEEE Transactions on computers, Vol. 1, No. 6, pp. 509-16.
- Aly, M. M., Gao, M., Hills, G., Lee, C. S., Pitner, G., Shulaker, M.M., Wu, T.F., Asheghi, M., Bokor, J., Franchetti, F. and Goodson, K.E. (2015). "Energy-efficient abundant-data computing: The N3XT 1,000 x." Computer, Vol. 48, No. 12, pp. 24-33.
- Asahi, N., Akazawa, M. and Amemiya, Y. (1997). "Single-electron logic device based on the binary decision diagram." IEEE Transactions on Electron Devices, Vol. 44, No. 7, pp. 1109-16.
- Bachtold, A., Hadley, P., Nakanishi, T. and Dekker, C. (2001). "Logic circuits with carbon nanotube transistors." Science, Vol. 294, No. 5545, pp. 1317-20.
- Bogaerts, W., Baets, R., Dumon, P., Wiaux, V., Beckx, S., Taillaert, D., Luyssaert, B., Van Campenhout, J., Bienstman, P. and Van Thourhout, D. (2005) J. Lightwave Technol. Vol. 23, No. 1, pp. 401-412.
- Bogaerts, W., De Heyn, P., Van Vaerenbergh, T., De Vos, K., Kumar Selvaraja, S., Claes, T., Dumon, P., Bienstman, P., Van Thourhout, D. and Baets, R. (2012). "Silicon microring resonators." Laser & Photonics Reviews, Vol. 6, No. 1, pp. 47-73.
- Bogaerts, W., Dumon, P., Van Thourhout, D., Taillaert, D., Jaenen, P., Wouters, J., Beckx, S., Wiaux, V. and Baets, R. G. (2006). "Compact wavelength-selective functions in silicon-on-insulator photonic wires." IEEE Journal of Selected Topics in Quantum Electronics, Vol. 12, No. 6, pp. 1394-401.
- Bryant, R. E. (1986). "Graph-based algorithms for boolean function manipulation." IEEE Transactions on computers, Vol. 100, No. 8, pp. 677-91.
- Caulfield, H.J. and Dolev, S. (2010). "Why future supercomputing requires optics." Nature Photonics, Vol. 4, No.5, pp. 261.
- Chattopadhyay, T. (2013). "Optical logic gates using binary decision diagram with mirrors." Optics & Laser Technology, Vol. 54, pp. 159-69.
- Cheng, Z., Rios, C., Youngblood, N., Wright, C. D., Pernice, W. H. and Bhaskaran, H. (2018). "Device-Level Photonic Memories and Logic Applications Using Phase-Change Materials." Advanced Materials, Vol. 30, No. 32, pp. 1802435.
- Chhowalla, M., Jena, D. and Zhang, H. (2016). "Two-dimensional semiconductors for transistors." Nat. Rev. Mater., Vol. 1, No. 11, pp. 16052.
- Fedeli, J., Augendre, E., Hartmann, J., Vivien, L., Grosse, P., Mazzocchi, V., Bogaerts, W., Van Thourhout, D. and Schrank, F. (2010). "Photonics and electronics

- integration in the helios project." Proc., Proceedings of the 7th IEEE International Conference on Group IV Photonics (GFP), Beijing, China, pp. 356–358.
- Fushimi, A. and Tanabe, T. (2014). "All-optical logic gate operating with single wavelength." *Optics express*, Vol. 22, No. 4, pp. 4466-79.
- Gardelis, S., Smith, C. G., Barnes, C. H., Linfield, E. H. and Ritchie, D. A. (1999). "Spin-valve effects in a semiconductor field-effect transistor: A spintronic device." *Physical Review B*, Vol. 60, No. 11, pp. 7764.
- Green, W. M., Rooks, M. J., Sekaric, L. and Vlasov, Y. A. (2007). "Ultra-compact, low RF power, 10 Gb/s silicon Mach-Zehnder modulator." *Optics express*, Vol. 15, No. 25, pp. 17106-17113.
- Guarino, A., Poberaj, G., Rezzonico, D., Degl'Innocenti, R. and Gunter, P. (2007). "Electro-optically tunable microring resonators in lithium niobate." *Nature photonics*, Vol. 1, No. 7, pp. 407.
- Gunn, C. (2006). "CMOS photonics for high-speed interconnects." *IEEE micro*, Vol. 26, No. 2, pp. 58-66.
- Gunn, C. (2006). "Silicon Photonics: Poised to Invade Local Area Networks." *Photonics Spectra*, Vol. 40, No. 3, pp. 62-69.
- Hammer, M., Hiremath, K. R. and Stoffer, R. (2004). "Analytical approaches to the description of optical microresonator devices." Proc., AIP conference proceedings, AIP, Melville, NY, USA, Vol. 709, No. 1, pp. 48-71.
- Hardesty L. MIT News. 2009., <http://news.mit.edu/2009/optical-computing> [Accessed 23 Oct 2018].
- Heebner, J. E., Wong, V., Schweinsberg, A., Boyd, R. W. and Jackson, D. J. (2004). "Optical transmission characteristics of fiber ring resonators." *IEEE journal of quantum electronics*, Vol. 40, No. 6, pp. 726-30.
- Ladd, T. D., Jelezko, F., Laflamme, R., Nakamura, Y., Monroe, C. and O'Brien, J. L. (2010). "Quantum computers." *Nature*, Vol. 464, No. 7285, pp. 45.
- Larger, L., Soriano, M. C., Brunner, D., Appeltant, L., Gutierrez, J. M., Pesquera, L., Mirasso, C. R. and Fischer, I. (2012). "Photonic information processing beyond Turing: an optoelectronic implementation of reservoir computing." *Optics express*, Vol. 20, No. 3, pp. 3241-9.
- Lin, S., Ishikawa, Y. and Wada, K. (2012). "Demonstration of optical computing logics based on binary decision diagram." *Optics Express*, Vol. 20, No. 2, pp. 1378-84.
- Little, B. E., Chu, S. T., Haus, H. A., Foresi, J. and Laine, J. P. (1997). "Microring resonator channel dropping filters." *Journal of lightwave technology*, Vol. 15, No. 6, pp. 998-1005.
- Marcatili, E. A. (1969). "Bends in optical dielectric guides." *Bell System Technical Journal*, Vol. 48, No. 7, pp. 2103-32.
- Miller, D., (2010). "Device requirements for optical interconnects to CMOS silicon chips." Proc., Integrated Photonics Research, Silicon and Nanophotonics, Monterey, California, USA, pp. PMB3.
- Miller, D.A. (2010). "Are optical transistors the logical next step?" *Nature Photonics*, Vol. 4, No.1, pp. 3.
- Notomi, M., Shinya, A., Mitsugi, S., Kira, G., Kuramochi, E. and Tanabe, T. (2005). "Optical bistable switching action of Si high-Q photonic-crystal nanocavities." *Optics Express*, Vol. 13, No. 7, pp. 2678-87.
- Paquot, Y., Duport, F., Smerieri, A., Dambre, J., Schrauwen, B., Haelterman, M. and Massar, S. (2012). "Optoelectronic reservoir computing." *Scientific reports*, Vol. 2, pp. 287.
- Pesin, D. and MacDonald, A. H. (2012). "Spintronics and pseudospintronics in graphene and topological insulators." *Nat. Mater.*, Vol. 11, No. 5, pp. 409.
- Rios, C., Stegmaier, M., Cheng, Z., Youngblood, N., Wright, C. D., Pernice, W. H. and Bhaskaran, H. (2018). "Controlled switching of phase-change materials by evanescent-field coupling in integrated photonics." *Optical Materials Express*, Vol. 8, No. 9, pp. 2455-70.
- Rios, C., Stegmaier, M., Hosseini, P., Wang, D., Scherer, T., Wright, C. D., Bhaskaran, H. and Pernice, W. H. (2015). "Integrated all-photonic non-volatile multi-level memory." *Nature Photonics*, Vol. 9, No. 11, pp. 725.
- Shastri, B. J., Tait, A. N., Ferreira de Lima, T., Nahmias, M. A., Peng, H. T. and Prucnal, P. R. (2018). Principles of neuromorphic photonics. *Unconventional Computing: A Volume in the Encyclopedia of Complexity and Systems Science*, Second Edition, Springer Berlin, Heidelberg, Germany, pp. 83-118.
- Sordan, R., Traversi, F. and Russo, V. (2009). "Logic gates with a single graphene transistor." *Applied Physics Letters*, Vol. 94, No. 7, pp. 51.
- Stegmaier, M., Rios, C., Bhaskaran, H., Wright, C. D. and Pernice, W. H. (2017). "Nonvolatile All-Optical 1× 2 Switch for Chipscale Photonic Networks." *Advanced Optical Materials*, Vol. 5, No. 1, pp. 1600346.
- Tans S. J., Verschueren, A.R. and Dekker C. (1998). "Room-temperature transistor based on a single carbon nanotube." *Nature*, Vol. 393, No. 6680, pp. 49.
- Tazawa, H., Kuo, Y. H., Dunayevskiy, I., Luo, J., Jen, A. K., Fetterman, H. R. and Steier, W. H. (2006) "Ring resonator-based electrooptic polymer traveling-wave modulator." *Journal of lightwave technology*, Vol. 24, No. 9, pp. 3514.

Woods, D. and Naughton, T. J. (2012). "Optical computing: Photonic neural networks." *Nature Physics*, Vol. 8, No.4, pp. 257.

Wu, Z., Chen, Y., Xu, P., Shao, Z., Zhang, T., Zhang, Y., Liu, L., Yang, C., Zhou, L., Chen, H. and Yu, S. (2016). "Graphene-on-silicon nitride microring resonators with high modulation depth." *Proc., Asia Communications and Photonics Conference, Optical Society of America, Wuhan, China*, pp. AF2A-10.

Yakar, O., Nie, Y. Wada, K., Agarwal, A., and Ercan, İ., (2019). "Energy Efficiency of Microring Resonator (MRR)-Based Binary Decision Diagram (BDD) Circuits." Submitted.

Yoshikawa, N., Matsuzaki, F., Nakajima, N. and Yoda, K. (2002). "Design and component test of a 1-bit RSFQ microprocessor." *Physica C: Superconductivity*, Vol. 378, pp. 1454-60.

# Turkish Journal of Engineering



*Turkish Journal of Engineering (TUJE)*  
*Vol. 3, Issue 4, pp. 197-200, October 2019*  
*ISSN 2587-1366, Turkey*  
*DOI: 10.31127/tuje.563939*  
*Research Article*

## **EXPERIMENTAL INVESTIGATION OF A NOVEL FRICTION MODIFIER IN COMPOSITE MATERIALS**

İlker Sugözü <sup>\*1</sup> and Mücahit Güdük <sup>2</sup>

<sup>1</sup> Mersin University, Faculty of Engineering, Department of Mechanical Engineering, Mersin, Turkey  
ORCID ID 0000-0001-8340-8121  
ilkersugozu@mersin.edu.tr

<sup>2</sup> Mersin University, Institute of Natural and Applied Sciences, Department of Manufacturing Engineering, Mersin, Turkey  
ORCID ID 0000-0003-0745-856X  
mucahitguduk@gmail.com

---

\* Corresponding Author

Received: 13/05/2019      Accepted: 24/06/2019

---

### **ABSTRACT**

In this study, waste banana tree powder was turned into powder and its use in automotive brake lining was investigated. For this purpose, 3 different samples were produced by using powder metallurgy production techniques. Waste banana tree powder (WBTP) was added in different rates (3%, 6% and 9% by weight), keeping the determined content constant. Firstly, homogenous mixtures of the ingredients are provided and then final shapes are given by hot pressing method. The friction, wear, hardness and density analysis of the brake lining samples and the effects of the use of WBTP on the brake lining were evaluated.

**Keywords:** *Composite Materials, Brake Lining, Friction, Wear*

## 1. INTRODUCTION

Brake linings are the most important part of the brake system for slowing or stopping of vehicles. Brake linings are made of powdery materials with different content without asbestos. A brake lining is a composite of many different ingredients. Components are classified as fibers, binders, solid lubricants, fillers, abrasives, metallic fillers and friction modifiers (Bijwe *et al.*, 2012; Sugoza, Mutlu, and Sugoza 2018). In generally phenolic or their modified versions are used as binder materials for friction composites. After the prohibition of the use of asbestos in the brake linings, researchers began to create different balata contents (Li *et al.*, 2018; Ikpambese *et al.*, 2016; Kukutschová *et al.*, 2009). The brake linings must be stable and have high coefficient of friction at high temperatures and must be resistant to wear. The brake linings must be noiseless and without vibration during braking.

Today, most of the researchers have focused on the use of industrial and agricultural waste in vehicle brake linings (Sugözü and Kahya, 2018; Ibadode and Dagwa, 2008; Idris and Aigbodion, 2015). Alternative studies have been made such as hazelnut shell, coconut shell, palm kernel shell for asbestos-free brake linings (Yawas *et al.*, 2016; Akıncioğlu *et al.*, 2018; Ghazali *et al.*, 2011). The use of waste products on brake linings positively affects economic and environmental impacts.

The aim of this study is to develop a new organic brake lining without asbestos using agricultural waste. The banana tree has a fibrous structure, it is a cheap and easily available waste product. WBTPs were added in different rates (3%, 6% and 9% by weight) and were produced by the powder metallurgy method. The density of specimens was determined and the hardness was determined using the Rockwell hardness tester device (HRL). For friction performance tests, a full-scale brake lining device with grey cast iron disk was used. The specific wear rate was calculated according to the TSE 555 standard (TSE 555, 1992).

## 2. MATERIALS AND METHODS

In this study, a new automotive brake friction material was obtained by using WBTP. The waste banana tree parts were dried, then it was turned into small particles in the mill. It was powdered using mixer. WBTP was sieved and size analysis was conducted. WBTP in different ratios such as 3%, 6% and 9% was added to the brake lining. Other additive materials were kept constant. Table 1 shows the content of brake lining.

Table 1. The amount of ingredients used for brake lining (weight %)

Type of material	M0	M3	M6	M9
Phenolic resin	20	20	20	20
Steel wool	5	5	5	5
Alumina	8	8	8	8
Brass shavings	5	5	5	5
Graphite	5	5	5	5
Cu particle	8	8	8	8
Cashew	8	8	8	8
WBTP	0	3	6	9
Barite	41	38	35	32

Powder materials forming the contents of the brake lining were mixed in the mixer for 10 minutes then pressed at 80 bar pressure for 2 minutes at ambient temperature. The obtained brake lining samples were left hot pressing at 100 bar pressure for 10 minutes. Detailed conditions for each manufacturing step can be found in the literature (Sugözü *et al.*, 2016). Four different brake lining were produced in an inch diameter. Three experiments were made from a brake lining and the mean of the experiments were taken. Figure 1 shows the brake lining tester used in this study. Detailed information about the test device is described in other studies of the author (Sugözü *et al.*, 2016).



Fig. 1. Brake lining test device used in this study

The wear values of the brake linings are calculated with the equation specified in the TS 555 Turkish standards. Detailed information about the specific wear equation (1) is described in the author's other works (Sugözü *et al.*, 2016).

$$V = \frac{m_1 - m_2}{2 \cdot \pi \cdot R_d \cdot n \cdot f_m \cdot \rho} \quad (1)$$

The density of the brake linings was determined according to the principle of Archimedes. The hardness of the brake linings was determined by using Rockwell hardness tester. During the hardness measurement of the brake linings, 10 kgf preload and 60 kgf full load were applied with a 6.35 mm diameter steel ball. Hardness measurements were taken from the wear surfaces of the brake linings. Performance tests of the brake linings were carried out at 0,5 MPa pressure and 6 m/s speed for 10 minutes.

## 3. RESULTS

Coefficient of friction and wear are very important when evaluating the performance of the brake linings. The coefficient of friction of the brake linings is high; the wear rate is expected to be low. Figure 2-5 shows the coefficient of friction and temperature performance of the brake lining with WBTP. The coefficient of friction of the brake linings is expected to remain stable depending on the temperature (Kim *et al.*, 2008).

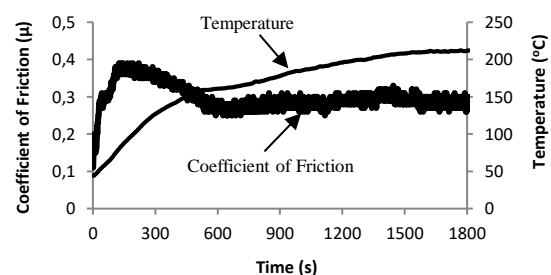


Figure 2. The coefficient of friction-temperature graphs

of the brake lining containing 0% WBTP

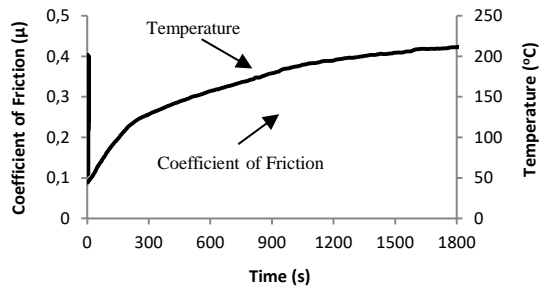


Figure 3. The coefficient of friction-temperature graphs of the brake lining containing 3% WBTP

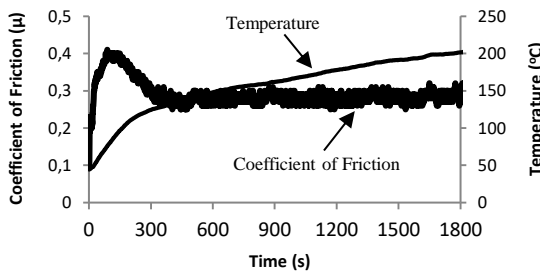


Figure 4. The coefficient of friction-temperature graphs of the brake lining containing 6% WBTP

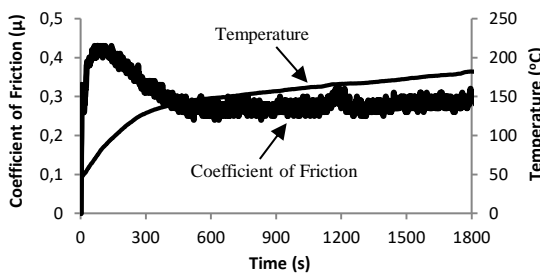


Figure 5. The coefficient of friction-temperature graphs of the brake lining containing 9% WBTP

The mean coefficient of friction of the linings was found at very close values. The mean coefficient of friction of the WBTP unused brake lining sample was 0.297. The coefficient of friction of the brake lining sample, which used 9% WBTP was 0.290. As the ratio of WBTP increased, the friction stability was low. When the shapes are examined, the friction performance were formed after 300 seconds. The highest stable coefficient of friction was 3% WBTP containing the lining sample. Temperature has decreased with increasing WBTP. The highest temperature was found in the brake sample with 3% WBTP content.

When the figures are examined, it is seen that the brake lining tests have become more stable after 300 seconds. The friction stability is known to be an important feature for commercial brake lining. To ensure good friction stability, the components of the brake lining should be selected carefully. The coefficient of friction is in the range of 0.3 industrial standard for the brake lining system (Leonardi *et al.*, 2018). In the literature, it is stated that the coefficient of friction ( $\mu$ ) generally varies between 0.1 and 0.7 depending on the friction force and the temperature of the disc coating interface (Ravikiran

and Jahanmir, 2001). The reduction in coefficient of friction at high temperatures seen in the figures results from the thermal decomposition of the phenolic resin used as a binder in the liner, which weakens the adhesion effect between the matrix and the components (Shin *et al.*, 2010).

Zero wear is not expected on brake linings. If very high-resistant materials are used to prevent wear in the lining, this will cause wear on the surface. Therefore, the choice of abrasives is one of the most important aspects of a liner formulation to improve wear resistance (Kahraman and Sugözü, 2019; Sugoçu *et al.*, 2018). Table 2 and Table 3 show the specific wear, average coefficient of friction, density, hardness and friction stability of lining samples containing 3% (M3), 6% (M6) and 9% (M9) WBTP and WBTP-free 0% (M0). As the amount of WBTP increased, the amount of wear increased proportionally.

Table 2. Tribological properties of brake lining specimens

Specimen Code	Specific wear rate ( $\text{cm}^3/\text{Nm}$ )	The average coefficient of friction
M0	$1.630 \times 10^{-6}$	0.297
M3	$2.030 \times 10^{-6}$	0.295
M6	$2.190 \times 10^{-6}$	0.293
M9	$2.230 \times 10^{-6}$	0.290

Table 3. Physical properties of brake lining specimens

Specimen Code	Rockwell hardness (HRL)	Density ( $\text{g}/\text{cm}^3$ )
M0	96	2.35
M3	91	2.15
M6	90	2.14
M9	77	2.06

Table 3 shows that the hardness and density of the specimens are decreased by increasing the amount of WBTP in the composite.

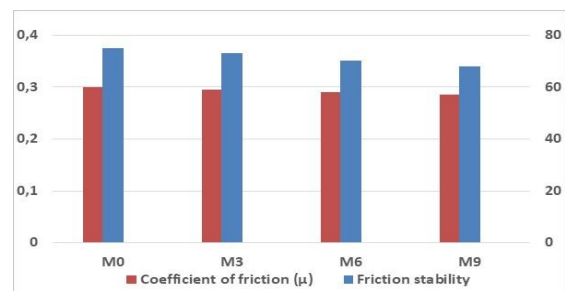


Fig. 6. The coefficient of friction and friction stability graphs of brake lining specimens

Figure 6 shows the friction stability and coefficient of friction of the brake lining samples. Improvements in friction stability were observed as the WBTP ratio decreased. High frictional stability is a sign of high friction performance of the brake lining.

#### 4. CONCLUSION

Composite brake linings with different proportions of WBTP were developed and their mechanical and tribological performances were evaluated according to

industrial standards. Based on the experimental results, the following conclusions were drawn:

- The coefficient of friction remained stable as the amount of WBTP increased.
- The coefficient of friction is in the range of 0.3 industrial standard for the brake lining system.
- Depending on the amount of WBTP increased, the density and hardness of the linings decreased.
- The wear resistance of the linings decreased with the increase in the amount of WBTP.
- The lining with 3% WBTP showed a more stable coefficient of friction performance.
- As a result of this experimental study, 3% WBTP could be used as an alternative material in automotive brake lining.

#### ACKNOWLEDGEMENTS

This study was supported by the Research Fund of Mersin University in Turkey with Project Number 2016-1-TP2-1396

#### REFERENCES

- Akincioglu, G., Öktem, H., Uygur, I., Akincioglu, S. (2018). "Determination of Friction-Wear Performance and Properties of Eco-Friendly Brake Pads Reinforced with Hazelnut Shell and Boron Dusts." *Arabian Journal for Science and Engineering* 43: 4727–37. <https://doi.org/10.1007/s13369-018-3067-8>.
- Bijwe, J., Aranganathan, N., Sharma, S., Dureja, N., Kumar, R. (2012). "Nano-Abrasives in Friction Materials-Influence on Tribological Properties." *Wear* 296: 693–701. <https://doi.org/10.1016/j.wear.2012.07.023>.
- Ghazali, C. M. R., Kamarudin, H., Jamaludin, S. B., Abdullah, M. M. A. (2011). "Comparative Study on Thermal, Compressive, and Wear Properties of Palm Slag Brake Pad Composite with Other Fillers." *Advanced Materials Research* 328–330: 1636–41.
- Ibhadode, A. O. A., Dagwa, I. M. (2008). "Development of Asbestos-Free Friction Lining Material from Palm Kernel Shell." *Journal of the Brazilian Society of Mechanical Sciences and Engineering* 30 (2): 166–73.
- Idris, U. D., Aigbodion, V. S. (2015). "Eco-Friendly Asbestos Free Brake-Pad : Using Banana Peels." *Journal of King Saud University - Engineering Sciences* 27 (2): 185–92. <https://doi.org/10.1016/j.jksues.2013.06.006>.
- Ikpambese, K. K., Gundu, D. T., Tuleun, L. T., (2016). "Evaluation of Palm Kernel Fibers (PKFs) for Production of Asbestos-Free Automotive Brake Pads." *Journal of King Saud University - Engineering Sciences* 28 (1): 110–18. <https://doi.org/10.1016/j.jksues.2014.02.001>.
- Kahraman, F., Sugözü B. 2019. "An Integrated Approach Based on the Taguchi Method and Response Surface Methodology to Optimize Parameter Design of Asbestos-Free Brake Pad Material." *Turkish Journal of Engineering* 3 (3): 127–32.
- Kim, Y. C., Cho, M. H., Kim, S. J., Jang, H. (2008). "The Effect of Phenolic Resin, Potassium Titanate, and CNSL on the Tribological Properties of Brake Friction Materials." *Wear* 264 (3–4): 204–10. <https://doi.org/10.1016/J.WEAR.2007.03.004>.
- Kukutschová, J., Roubíček, V., Malachová, K., Pavlíčková, Z., Holuša, R. Kubačková, J. Mička, V. MacCrimmon, D., Filip, P. (2009). "Wear Mechanism in Automotive Brake Materials, Wear Debris and Its Potential Environmental Impact." *Wear* 267 (5–8): 807–17. <https://doi.org/10.1016/J.WEAR.2009.01.034>.
- Leonardi, M., Menapace, C., Matějka, V., Gialanella, S., Straffelini, G. (2018). "Pin-on-Disc Investigation on Copper-Free Friction Materials Dry Sliding against Cast Iron." *Tribology International* 119 (March): 73–81. <https://doi.org/10.1016/J.TRIBOINT.2017.10.037>.
- Li, Z., He, M., Dong, H., Shu, Z., Wang, X. (2018). "Friction Performance Assessment of Non-Asbestos Organic (Nao) Composite-To-Steel Interface and Polytetrafluoroethylene (PTFE) Composite-To-Steel Interface: Experimental Evaluation And Application In Seismic Resistant Structures." *Construction and Building Materials* 174: 272–83.
- Ravikiran, A., Jahanmir, S. (2001). "Effect of Contact Pressure and Load on Wear of Alumina." *Wear* 251 (1–12): 980–84. [https://doi.org/10.1016/S0043-1648\(01\)00739-6](https://doi.org/10.1016/S0043-1648(01)00739-6).
- Shin, M. W., Cho, K. H., Lee, W. K., Jang, H. (2010). "Tribological Characteristics of Binder Resins for Brake Friction Materials at Elevated Temperatures." *Tribology Letters* 38 (2): 161–68.
- Sugözü, İ., Kahya, K. (2018). "Investigation of the Effect on Tribological Properties of the Use of Pinus Brutia Cone as a Binder in Brake Pads." *European Mechanical Science* 2 (4): 115–18. <https://doi.org/10.26701/ems.471131>.
- Sugozu, I., Mutlu, I., Sugozu, B. (2018). "The Effect of Ulexite to the Tribological Properties of Brake Lining Materials." *Polymer Composites* 39 (1): 55–62. <https://doi.org/10.1002/pc.23901>.
- Sugözü, İ., Mutlu, İ., Sugözü, B. (2016). "The Effect of Colemanite on the Friction Performance of Automotive Brake Friction Materials." *Industrial Lubrication and Tribology* 68 (1): 92–98. <https://doi.org/10.1108/ILT-04-2015-0044>.
- TSE 555. 1992. *Highway Vehicles-Brake System-Brake Pads for Friction Brake*. Ankara, Turkey.
- Yawas, D S, Aku, S. Y., Amaren., S. G. (2016). "Morphology and Properties of Periwinkle Shell Asbestos-Free Brake Pad." *Journal of King Saud University - Engineering Sciences* 28 (1): 103–9. <https://doi.org/10.1016/j.jksues.2013.11.002>.

# Turkish Journal of Engineering



*Turkish Journal of Engineering (TUJE)*  
*Vol. 3, Issue 4, pp. 201-205, October 2019*  
*ISSN 2587-1366, Turkey*  
*DOI: 10.31127/tuje.556349*  
*Research Article*

## REMOVAL OF COLOUR POLLUTIONS IN DYE BATHS WITH MORDANTS

Aslıhan Koruyucu \*<sup>1</sup>

<sup>1</sup> Namık Kemal University, Çorlu Faculty of Engineering, Department of Textile Engineering, Tekirdağ, Türkiye  
ORCID ID 0000-0002-8443-5188  
adelituna@nku.edu.tr

---

\* Corresponding Author

Received: 20/04/2019

Accepted: 05/07/2019

---

### ABSTRACT

In the current study, the colour vitality, wash, rubbing and diaphoresis fastness were evaluated for cotton substrates with and without anionic (tannin) mordanting. It was found that pre-mordanting with tannic acid affect both the colour characteristics and fastness properties of the cationic dye. Overall, mordanting with tannic acid gave the best results in terms of both colour vitality and fastness properties.

**Keywords:** *Mordant, Tannic Acid, Cationic Dyes, Fastness Properties, Cotton*

## 1. INTRODUCTION

Cotton is the best plentiful of all instinctively resulting organic materials and is extensively consumed. It is used either alone or in conjunction with other synthetic fibers in differing ranges of clothing. This material specifically presents superior tangible and synthetically properties in terms of water absorbency, dyeability and stability (Preston, 1986; Shore, 1995).

During several classes of dye can be favorably applied to the cotton fibers, containing direct, azoic, vat and reactive dyes. The use of cationic dyes has not acquired widespread success. In this study, for applying cationic dye to the cotton fibers the anionic agent (tannic acid) containing glucose esters of gallic acid was consumed and its effect was determined.

Tannins are delimited as naturally resulting water-soluble polyphenols of varying molecular weight (Bhat *et al.*, 1998). Tannins are found to be resulting in vascular plant tissues of leaves, seeds, and flowers (Mingshu *et al.*, 2006). Tannins are considered nutritionally unacceptable because they restrict digestive enzymes and affect the exercise of vitamins and minerals. Swallow of large quantities of tannins may result in unfavorable health effects. However, the consumption of a small amount of the right kind of tannins may be advantageous to human health (Gu *et al.*, 2003). They are detached into two classes: soluble and shortened (not soluble) (Haslam, 1966). Soluble tannins are toxic to animals and matter poisoning if devoured by them in large aggregate (Garg *et al.*, 1992). Tannins restrict the growth of a number of microorganisms, oppose microbial attack, and are recalcitrant to biodegradation (Field and Lettinga, 1992).

Despite the antimicrobial properties of tannins, many fungi, bacteria, and yeasts are quite resistant to tannins and can grow and develop on them (Bhat *et al.*, 1998). The importance of tannin biodegradation in accordance to industrial and agricultural uses has been published earlier (Archambault *et al.*, 1996). By considering these facts, an effort has been made to isolate and recognize cold-adapted tannic acid debasing bacteria by optimizing various parameters of deterioration.

Treatment cotton fabrics with tannins propose supplementary hydroxyl groups on the fiber matrix. A textile fibre pretreatment with a mordant, in order to achieve dyeings of improved fastness and depth of shade, has been practiced since time immemorial. The tannins play an important role in cotton dyeing to absorb colouring matter forever (Gulrajani, 1999). With these reasons, tannin was chosen to improve dye fixation and to remove dye pollutions in dye bath.

## 2. EXPERIMENTAL METHOD

### 2.1. Materials

#### 2.1.1. Fabric

100% Cotton woven fabric was consumed through out this work.

#### 2.1.2. Cationic Dye

Cationic dyes under commerce name of Maxilon produced by Setap Specialty Chemicals Co. were used

through out this study: Setacryl Red P-4B(C.I. Basic Red 46)

#### 2.1.3. Chemicals

Tannic acid ( $C_{34}H_{25}O_{23}$ ), acetic acid, sodium sulphate, sodium carbonate were laboratory class chemicals. Non-ionic detergent was consumed in this work. Tannic acid powder (No.0.0773.1000-1kg),(Merck) pattern was consumed as supplied.

## 2.2. Methods

### 2.2.1. Scouring of Cotton Fabrics

Fabrics were washed in bath contain 1g/L of non-ionic detergent and 2 g/L  $Na_2CO_3$  for 20 minutes at 60 °C. After washing the fabrics were rinsed and dried.

### 2.2.2. Treatment with Tannic Acid

The cotton fabrics were treated with tannic acid as a surface modifier to deliberate an anionic character to cotton fabric to improve its dyeability towards cationic dye. As shown in Fig. 1, the fabrics were treated with four diverse concentrations of tannic acid (zero, 5 %, 10 %, 15 %) before the dyeing process.

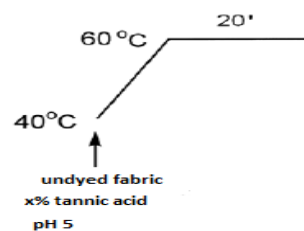


Fig. 1. Pre-mordanted fabrics with tannic acid

The treatments were carried out 20 minutes, 60 °C at 1:20 liquor to ratio; after which samples were stained with cationic dye.

### 2.2.3. Dyeing Process

The treated and untreated fabrics were dyed with % 4 cationic dye and 6g/L sodium sulfate  $Na_2SO_4$  to ensure good and uniform allocation of the dye within the dyebath. The pH of the dye bath was adjusted at 4-6 by adding acetic acid.

The temperature of dye bath was evenly raised to (80-100 °C). The dyeing process was accomplished 60 minutes at 80 and 100 °C. The dyed fabrics rinsed well in cold water and then washed in bath containing 1g/L non-ionic detergent at liquor to ratio 1:50 for 20 minutes at 70 °C. The dyeing process is illustrated in Fig. 2.

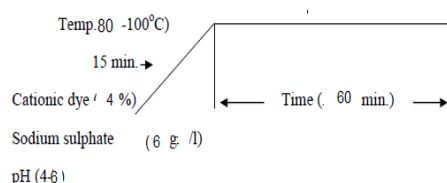


Fig. 2. Dyeing Process

#### 2.2.4. Testing

The results of the dyeing experiments were obtained according to the color measurements of the samples with a X-rite CFS 57 CA reflectance spectrophotometer under D65/10° illuminant between 320-750 nm. The colour intensity, expressed as the K/S value, calculated by the Kubelka-Munk equation (1):

$$K/S = \frac{(1 - R)^2}{2R} \quad (1)$$

where K is a constant about the light absorption of the dyed fabric; S, a constant about the light scattering of the dyed fabric and R, the reflectance of the dyed sample. The higher the K/S value, the greater is the color intensity and, hence the better is the dye uptake.

#### 2.2.5. Colour Fastness

Colour fastness to light was according to AATCC test method 16A-1971. Colour fastness to rubbing was accomplished in accordance with Colour fastness to rubbing dry & wet C8 consuming Crock-meter. Colour fastness to diaphoresis was carried out in accordance with AATCC test method 15-1973.

### 3. RESULTS AND DISCUSSION

#### 3.1. Effect of Tannic Acid Treatment

The synthetical formula for commercial tannic acid  $C_{34}H_{25}O_{23}$  is given in Fig. 3.

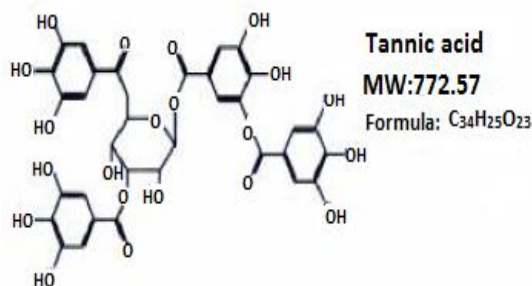


Fig. 3. Tannic acid formula

Its structure is based mainly on glucose esters of gallic acid. It is a yellow to light brown amorphous powder which is highly soluble in water. Treatment cotton fabrics with tannins introduce additionally hydroxyl and carboxyl groups on the fiber matrix. Tannic acid is an average mordant consumed in the dyeing process.

Increasing tannic acid concentration, dyeing pH value and dyeing temperature cause the cationic dye exhaustion to the cotton fibers to increase. With the time of dyeing, the colour vitality increases. For this reason, this process is accomplished 80-100 °C 60 minutes.

Fig. 4 shows the effects of tannic acid pretreated and untreated samples under changing dyeing pH on K/S values. It can be noticed that the colour vitality for all treated cotton fabrics showed higher colour vitality than untreated ones. The colour strength of dyed cotton fabrics

increases as the concentration of tannic acid enhance till reach 10% which is followed by some decrease in K/S.

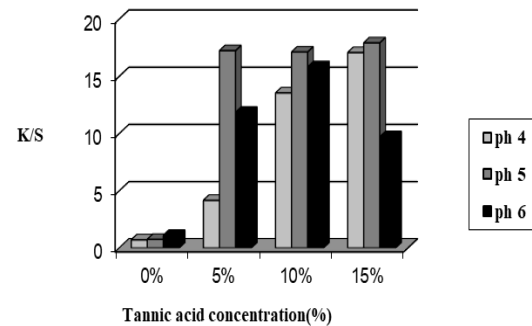


Fig. 4. K/S values of tannic acid-treated and untreated samples under different dyeing pH values.

In different circumstances, hydrogen bonding may also be produced between tannin and the hydroxyl groups of cotton cellulose as follows:

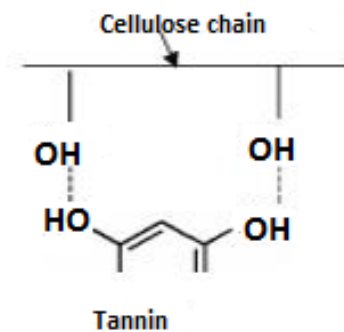


Fig. 5. Tannin compound

In these cases, the number of anionic sites on fibers i.e. cotton, will be enhanced as a result of pretreatment with tannic resulting in enhancing the responsiveness and approachability of cotton fibers to cationic dyes. At higher concentration of tannic acid, it would be expected that problems essential to aggregation would be much distinct, leading to decrease the substantivity of tannic acid to cotton fabrics and equilibrate its concentration in water and on fiber (Mahangad *et al.*, 2009). The effect of pH on the dyeing process with cationic dye, dyeing was carried out at different concentrations of treatment with tannic acid and under constant dyeing pH values. The colour vitality of the dyed samples were measured and the results are plotted in Fig. 6.

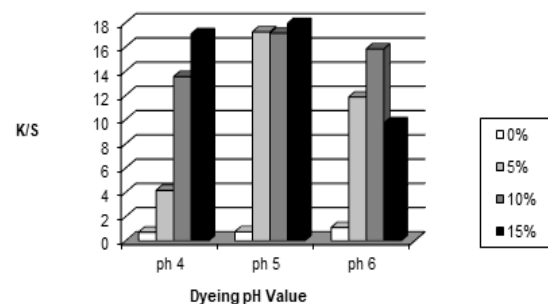


Fig. 6. K/S values of dyeing pH values under different tannic acid concentrations.

From Fig. 7, it can be seen that the colour vitality increases as the temperature increase till 100 °C. No substantial change in colour vitality is observed above 100 °C. It may be achieved from the results that 100 °C and pH 5 are found to be the most suitable dyeing conditions for giving maximum colour vitality with cotton fabrics.

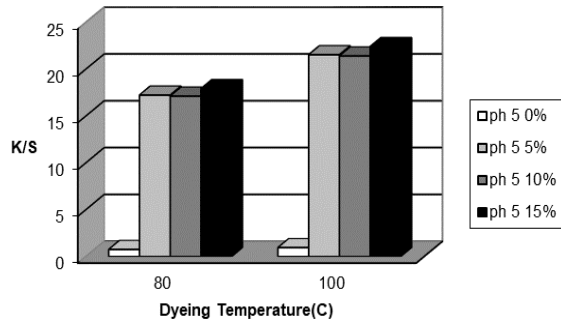


Fig. 7. K/S values of dyeing temperature under different tannic acid concentrations at dyeing pH 5.

### 3.2. Fastness Properties of Dyed Cotton Fabrics

The fastness properties (washing, rubbing, diaphoresis and light) of dyed cotton fabrics with cationic dye at the optimum condition after the treatment with tannic acid were cited in Table 1. It is clearly observed from Table 1 that the wash fastness, wet and dry rubbing fastness gave grades between 2 and 4-5 while fastness to acidic and alkaline diaphoresis showed good results as well as the fastness to light.

Table 1. Fastness properties of dyed cotton fabrics

Name of Cationic Die	Washing Fastness	Washing Fastness	Rubbing Fastness	Rubbing Fastness	Perspiration Fastness	Perspiration Fastness	Alkaline Medium		
	Color Change	Staining Cotton	Dry	Wet	Acid Medium Cotton	Color Change	Cotton	Color Change	Light Fastness
Setacril Red P-4B	1	3	4-5	2-3	3	4-5	3	4	1-2

Projected Mechanism For Composition of Tannic Acid–Cellulose Composite

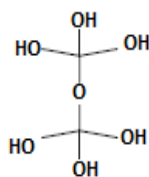


Fig. 8. Schematic representation of tannic acid

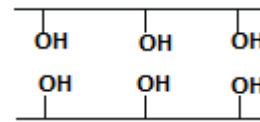


Fig. 9. Schematic representation of cellulose

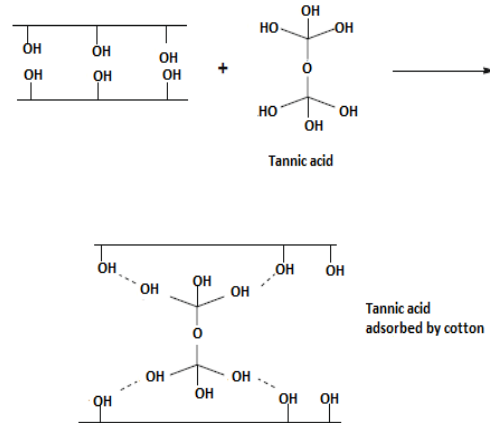


Fig 10. Composition of tannic acid-cellulosic composite.

Fig. 10 describes the composition of tannic acid-cellulose composite Cotton fabric tannic acid from its liquid solution. In this case, the interplay between tannic acid and cellulose is mainly hydrogen bonding and minor Van-der-Walls interplay. The good washing fastness properties of cotton fabric treated with tannic acid is ascribed to two reasons:

(i) The strong bond coordination formed between dyestuff ions, tannic acid and hydroxyl group of cellulose particles.

(ii) The composition of large insoluble composite particles impeded in cellulose particles. These two factors contribute to more or less same amount of augmentation in the washing fastness of cotton fabric treated with tannic acid-dyestuff composition.

### 4. CONCLUSIONS

Cotton fabrics were dyed with 4% cationic dye and after the treatment with different tannic acid concentrations under different dyeing pH values. It was found that the treatment with 10% of tannic acid gave higher colour strength. The optimum condition of dyeing cotton fabric with cationic dye was 4% cationic dye, 6g/L Na<sub>2</sub>SO<sub>4</sub>, pH 5 at 100 °C for 60 minutes.

### REFERENCES

- Archambault J, Lacki K, Duvnjak Z ,(1996). “ Conversion of catechin and tannic acid by an enzyme preparation from *Trametes versicolor*” *Biotechnol Lett* 18: 771–774
- Bhat T, Singh B, Sharma O (1998). “Microbial degradation of tannins —a current perspective”. *Biodegradation* 9: 343–357
- Field J, Lettinga G (1992). “ Biodegradation of tannins. In: Sigel H (ed) *Metal ions in biological systems* volume 28. Degradation of environmental pollutants by

microorganisms and their metalloenzymes. Marcel Dekker, New York, pp 61–97.

Garg S, Makkar H, Nagal K, Sharma S, Wadhwa D, Singh B (1992). “ Toxicological investigations into oak (*Quercus incana*) leaf poisoning in cattle”. *Vet Hum Toxicol* 34: 161–164.

Gu L, Kelm M, Hammerstone J, Beecher G, Holden J, Haytowitz D, Prior R (2003). “Screening of foods containing proanthocyanidins and their structural characterization using LC-MS/MS and thiolytic degradation”. *J Agric Food Chem* 51: 7513–7521.

M.L.Gulrajani,1999. “ Natural dye: part I-present status of natural dyes”; *Colourage*,7 (1999), pp.19-28.

Haslam E (1966). “The scope of vegetable tannin chemistry. Chemistry of vegetable tannins”. Academic, London, pp 1–13.

Mahangad ,P.R.; Varadarajan,P.V. , Verma, J.K. & Bosco H. ;"Indian Journal of Fibre and Textile Research", Vol.34, p.279-282 (2009).

Mingshu L, Kai Y, Qiang H, Dongying J, (2006) “Biodegradation of gallotannins and ellagitannins”. *J Basic Microbiol* 46: 68–84.

Preston C.;1986. “ The dyeing of cellulosic fibres.” West Yorkshire: Dyers’ Company Publications Trust.

Shore J.;1995. Cellulosics dyeing. West Yorkshire: Society of Dyers and Colourists

# Turkish Journal of Engineering



*Turkish Journal of Engineering (TUJE)*  
*Vol. 3, Issue 4, pp. 206-217, October 2019*  
*ISSN 2587-1366, Turkey*  
*DOI: 10.31127/tuje.554075*  
*Research Article*

## **FLEXURAL BEHAVIOR OF HYBRID FRP-CONCRETE BRIDGE DECKS**

İlker Fatih Kara <sup>1</sup>, Ashraf F. Ashour <sup>2</sup> and Cahit Bilim <sup>\*3</sup>

<sup>1</sup>Mersin University, Engineering Faculty, Civil Engineering Department, Mersin, Turkey  
ORCID ID 0000-0002-5663-1595  
ifkara@mersin.edu.tr

<sup>2</sup>University of Bradford, School of Engineering, Department of Structural Engineering, Bradford, UK  
ORCID ID 0000-0002-4800-6060  
A.F.Ashour@Bradford.ac.uk

<sup>3</sup>Mersin University, Engineering Faculty, Civil Engineering Department, Mersin, Turkey  
ORCID ID 0000-0002-0975-1391  
cbilim@mersin.edu.tr

---

\*Corresponding Author

Received: 15/04/2019      Accepted: 23/07/2019

---

### **ABSTRACT**

The main aim of this study is to investigate the behaviour of hybrid FRP-concrete decks. The hybrid FRP-concrete bridge systems consisting of different FRP cell units available on the market such as trapezoidal, triangular, honeycomb, rectangular with alternating diagonal, half-depth trapezoidal, hexagonal and arch cell units were computationally compared and examined using the finite element (FE) analysis to decide the most appropriate FRP composite deck for bridge systems. Design criteria such as the deflections were considered in selecting the most effective unit system. Different FRP bridge deck panels were analysed under static loading representing the standard European truck wheel. The finite element analysis of bridge deck systems was performed using a general purpose finite element analysis package ABAQUS, and the behaviour of these systems was then be compared in terms of stiffness and strength criteria. The results showed that Delta, Super and ASSET hybrid decks are stiffer than other deck systems. The results from FEA approach also indicated that the layer of concrete on the top surface of bridge deck reduces the vertical displacement of FRP bridge systems approximately 60%.

**Keywords:** *FRP Composites; Concrete; Bridge Decks; Hybrid Design; Finite element analysis*

## 1. INTRODUCTION

It is well known that bridges deteriorate with age. For example, reinforced concrete bridges slowly deteriorate during the first few decades of their design life (typically 50 years), followed by a rapid decline thereafter. In many North European countries, deterioration, caused by de-icing salts, is creating an increasing maintenance workload due to their corrosive effect on steel reinforcement of concrete bridges. A 2002 Federal Highway Administration and United States Department of Transportation (FHWA/USDOT) (2002) study estimates the direct cost of repairing corrosion on highway bridges to be \$8.3 billion annually, including \$3.8 billion over the next 10 years to replace structurally deficient bridges and \$2.0 billion for maintenance of concrete bridge decks. Longer design life structures, using the latest materials and design technologies, are needed to maintain a functional transportation network, provide longer service life, and improve the safety of the highway network. Among new construction materials, fiber reinforced polymers (FRP) composites are very attractive materials to structural engineers, due to their superior material properties such as high stiffness, high strength, high corrosion resistance, light weight, and durability.

Bridge decks have been considered as the most critical component in bridges that could significantly benefit from the appropriate use of FRP composite materials. FRP bridge decks have many advantages including light weight, corrosion resistance, quick installation, high strength and low life cycle maintenance cost (Hollaway, 2010; Bakis *et al.*, 2002; Keller, 2002). FRP bridge decks are approximately weigh 20% of the structurally equivalent reinforced concrete decks, that can produce massive savings throughout the bridge, in particular bridge foundations. The modular form of FRP bridge decks offers several benefits including minimum traffic disruption, safer and cheaper installation. In spite of all these advantages, large displacement can occur under concentrated point loads in FRP bridge decks. It has been reported that the local deformation under concentrated point loads resulting from vehicle wheels is large for all FRP composite bridge decks due to the relatively low stiffness of FRP composites. Therefore, a thin layer of concrete on top of the FRP bridge deck enhances the overall stiffness of the deck, reduces the local deformation of the deck top flange and improve the overall serviceability of the wearing surface. In addition, FRP deck can act as a permanent formwork to cast the concrete layer. Sebastian *et al.* (2013) showed that a 30mm thick layer of polymer concrete surfacing significantly improved the load carrying capacity of glass fiber reinforced polymer (GFRP) bridge deck by 261% in comparison to the un-surfaced GFRP deck. However, this increase was only 90% when the plan dimensions of the applied load were increased.

Davalos *et al.* (2001) presented a combined analytical and experimental characterization of FRP honeycomb deck panels. The authors concluded that the equivalent orthotropic properties developed in their

study could be used for the analysis and design of the FRP sandwich panels.

Keller and Gurtler (2006) tested Duraspan and Asset FRP decks. In-plane compression and in-plane shear tests were carried out on panels made of three adhesively bonded components with all bending test. The failure mode of ASSET deck was brittle and linear elastic up to failure, while Duraspan deck exhibited some ductility.

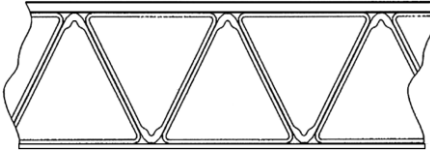
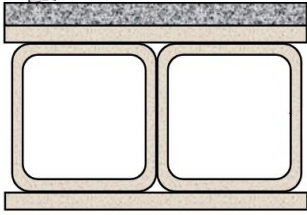
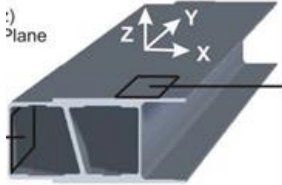
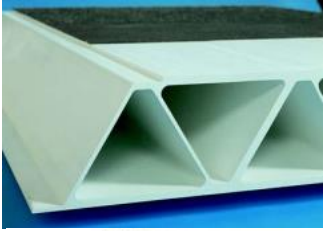
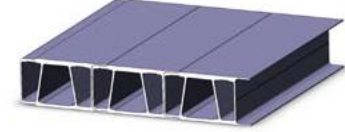
Saiidi *et al.* (1994) carried out an experimental and analytical study of hybrid beams that consist of graphite/epoxy (G/E) sections and reinforced concrete (RC) slabs. They concluded that the use of epoxy resin to bond concrete to G/E sections was found to be only partially effective. Kitane *et al.* (2004) developed a basic concept of a hybrid FRP-concrete bridge superstructure. The structural type was a trapezoidal box sections. A thin layer of concrete was placed in the compressive zone of the section, and was surrounded with GFRP. They concluded that concrete bridge superstructure is very promising, from structural engineering view point.

The main aim this study is to investigate the behaviour of hybrid FRP-concrete decks. The hybrid FRP-concrete bridge systems consisting of different FRP cell units available on the market such as trapezoidal, triangular, honeycomb, rectangular with alternating diagonal, half-depth trapezoidal, hexagonal and arch cell units were computationally compared and examined using the finite element (FE) analysis to decide the most appropriate FRP composite deck for bridge systems. Design criteria such as the deflections were considered in selecting the most effective unit system. Different FRP bridge deck panels were analysed under static loading representing the standard European truck wheel. The finite element analysis of bridge deck systems was performed using a general purpose finite element analysis package ABAQUS (Hibbit, Karlsson & Sorensen, Inc., 2006), and the behaviour of these systems was then be compared in terms of stiffness and strength criteria.

## 2. ANALYSIS OF FRP DECK SYSTEMS

There are many different types of FRP deck solutions available on the market, each one having different geometric and physical properties and suitable for different uses. Table 1 shows seven typical bridge decks types, each from a different manufacturer. These FRP bridge decks were considered and a thin layer of concrete was placed on the top surface of the FRP deck for the formation of the hybrid deck systems (see Fig. 1 (a-b)) for EZ span deck). The interface between the concrete and the FRP plate was assumed perfectly bonded. All the hybrid decks were analysed and compared using the finite element (FE) analysis to decide the most appropriate two FRP composite decks for bridge systems. Design criteria such as the global deflection was considered in selecting the most effective two system. Different FRP bridge deck panels were analysed under static loading representing the standard European truck wheel.

Table 1. FRP deck types and properties (Brown and Zureick (2001))

Deck System	Deck Thickness (mm)	Deck Weight (kN/m <sup>2</sup> )	Manufacturer	Illustration of the Deck
EZ Span Deck	216	0.96	Creative Pultrusion Inc. USA	
Superdeck	203	1,01	Creative Pultrusion Inc. USA	
Strongwell	170	1.08	Strongwell, USA	
DuraSpan	195	0.95	Martin Marietta Composites, USA	
Asset	225	0.93	Fiberline, Denmark	
Delta Deck	200	1.76	Korea	
Holes Deck	216	0.9	Spare Composites Corp. at Nanjing, China	

To evaluate these systems, a bridge superstructure was designed as a simply supported single span one-lane bridge with a length of 2.7 m as suggested by Keller and Schollmayer (2004) for serviceability states in designing process. As all decks have different geometry, the width of the bridge deck systems varies between 950 mm to 1200 mm. The concrete layers reduces the local deformation of the top surface of the bridge under concentrated loads that represent truck wheel loads

(Alnahhal *et al.* (2007)). The thickness of the concrete layer is a key design parameter to optimize the hybrid structural system. According to Kitane (2004), concrete can be used efficiently to increase the flexural rigidity until the concrete thickness equals about 10% of the bridge depth. Therefore, as the depth of the decks changes between 195 and 216 mm, the same concrete thickness of 2 cm was selected for all hybrid FRP deck systems.

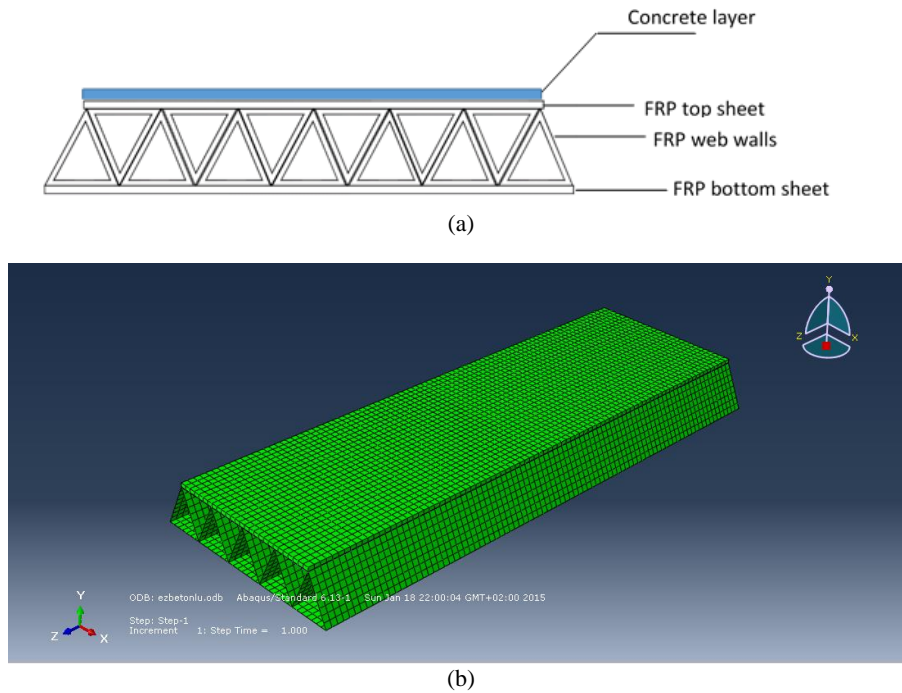


Fig. 1 (a-b) Section and finite element modelling of EZ Span hybrid bridge deck

Road traffic loads according to the European Code EC1(2002) were used. Figure 2 shows a patch load used in the structural analysis of the deck panel. The wheel load, as specified in, was uniformly distributed pressure load over a tyre-contacting area of 0.4 m x 0.4 m.

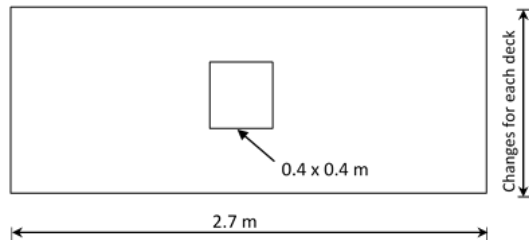


Fig. 2. Patch load used in the structural analysis of the hybrid deck panel

The finite element calculations of the bridge decks were carried out using ABAQUS (Hibbit, Karlsson& Sorensen, Inc., 2006). The FRP decking systems are modelled with 3D deformable shell elements (4 nodes). Orthotropic material properties are utilized with the mechanical characteristics as given in Table 2. 4 nodes shell elements are used due to the more detailed implicit hollow configuration. The steel loading plate is modelled using 3D deformable solid elements (8 nodes). For the steel members a Young's modulus of 220 GPa and a Poisson's ratio of 0.3 was utilized. The concrete compressive strength were assumed to be 40 MPa for all hybrid deck systems in this study. The behavior of hybrid bridge deck can be predicted by assuming the linear FEA if the strain induced in the materials is within the strain range where the elastic moduli of the materials were computed.

Table 2. Mechanical properties of deck specimens

Deck System	Top Sheet								
	$E_x$ (Mpa)	$E_y$ (Mpa)	$E_z$ (Mpa)	$G_x$ (Mpa)	$G_y$ (Mpa)	$G_z$ (Mpa)	$\rho_x$	$\rho_y$	$\rho_z$
Asset	23000	18000		2600	600	600	0.3	0.3	
DuraSpan	21240	11790	4140	5580	600	600	0.32	0.3	0.3
EZ Span Deck	31000	8300		4000			0.25		
Delta Deck	16600	13200							
Superdeck	24100			3400					
Strongwell	13790	9652							
Holes deck	31000	5000	5000	6000	6000	5000	0.2	0.2	0.3

	Web								
Deck System	E <sub>x</sub> (Mpa)	E <sub>y</sub> (Mpa)	E <sub>z</sub> (Mpa)	G <sub>x</sub> (Mpa)	G <sub>y</sub> (Mpa)	G <sub>z</sub> (Mpa)	ρ <sub>x</sub>	ρ <sub>y</sub>	ρ <sub>z</sub>
Asset	17300	22700		3150	600	600	0.3	0.3	
DuraSpan	17380	9650	4140	7170	600	600	0.3	0.3	0.3
EZ Span Deck	8300	31000			4000			0.3	
Delta Deck	28800	10100							
Superdeck		24100			3400				
Strongwell	11000	5516							
Holes deck	31000	5000	5000	6000	6000	5000	0.2	0.3	0.2
	Bottom Sheet								
Deck System	E <sub>x</sub> (Mpa)	E <sub>y</sub> (Mpa)	E <sub>z</sub> (Mpa)	G <sub>x</sub> (Mpa)	G <sub>y</sub> (Mpa)	G <sub>z</sub> (Mpa)	ρ <sub>x</sub>	ρ <sub>y</sub>	ρ <sub>z</sub>
Asset	16500	25600		2000	600	600	0.3	0.3	
DuraSpan	21240	11790	4140	5580	600	600	0.32	0.3	0.3
EZ Span Deck	31000	8300		4000			0.25		
Delta Deck	16600	13200							
Superdeck	24100			3400					
Strongwell	13790	9652							
Holes deck	31000	5000	5000	6000	6000	5000	0.2	0.2	0.3

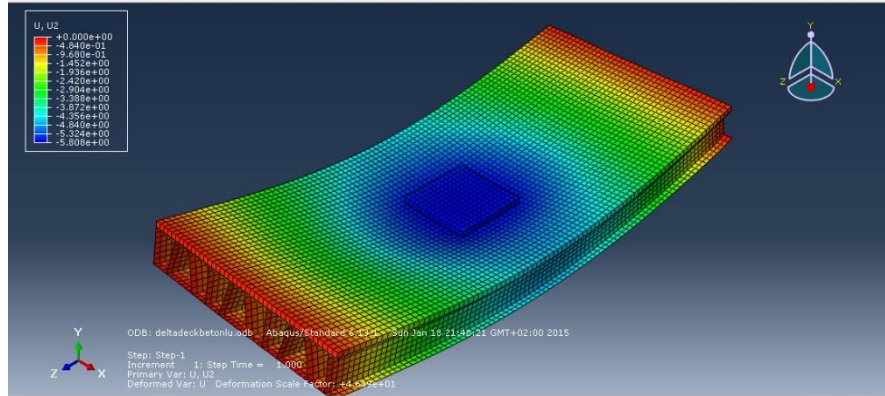
### 3. RESEARCH RESULTS

The load combination specified in the European Code EC1 (2002) for the serviceability and ultimate limit state was applied to all hybrid bridge systems. The maximum midspan vertical displacements for serviceability limit state (SLS) are presented in Table 3. The deflected shape and displacement result of finite element method for all concrete decks considered here are shown in Fig. 3. The variation of longitudinal deflections is also obtained for all deck systems. Fig. 4 presents the comparison of these deflections for hybrid deck systems. It can be seen from Fig. 4 and Table 3, the

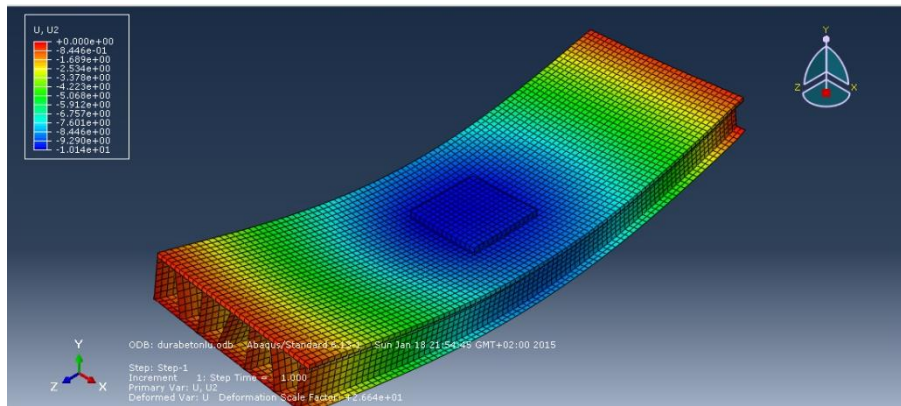
displacements in Delta, ASSET and Super hybrid FRP-concrete decks are smaller than the other deck systems. These three hybrid decks have also smaller deflection than the deflection limit of L/300 (9 mm) suggested by Keller and Schollmayer (2004). All the deck systems were also analyzed without placing of concrete on the top surface. The variation of midspan section displacement in longitudinal direction for hybrid and non-hybrid specimens are given in Figs. 5. As seen in Figs. and Table 3, the placement of thick layer concrete on the top surface reduces the maximum displacement of FRP bridge decks approximately 60%.

Table 3. Maximum vertical displacement in SLS

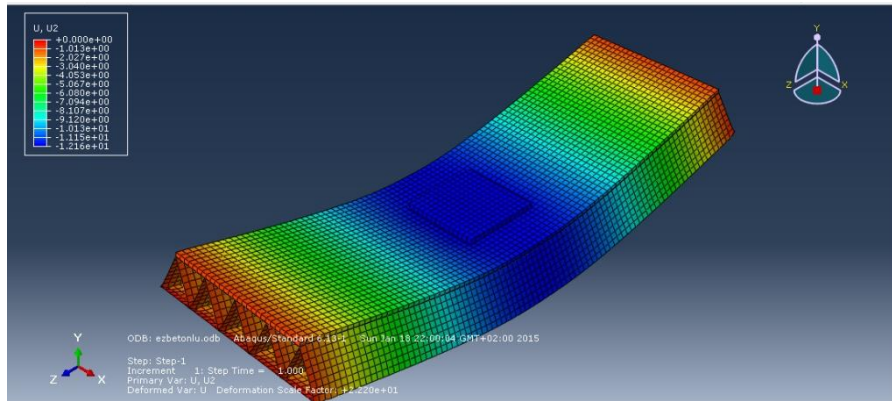
		Maximum Vertical Displacement (mm)	
		Hybrid FRP Concrete Deck	FRP Deck
FRP Deck Systems	DuraSpan	10.14	16.47
	Asset Deck	8.162	11.83
	Superdeck	8.58	13.05
	EZ Span Deck	12.16	16.39
	Strongwell	13.61	23.29
	Delta Deck	5.81	10.0
	Holes deck	9.76	18.18



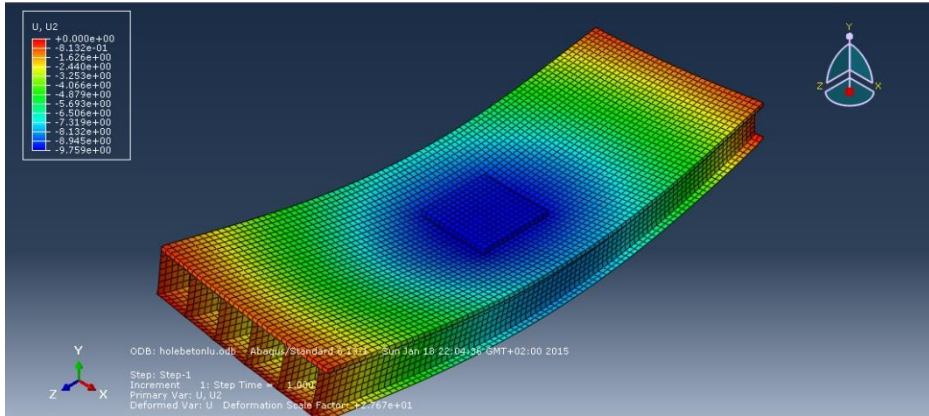
(a) Delta Hybrid FRP Concrete Deck



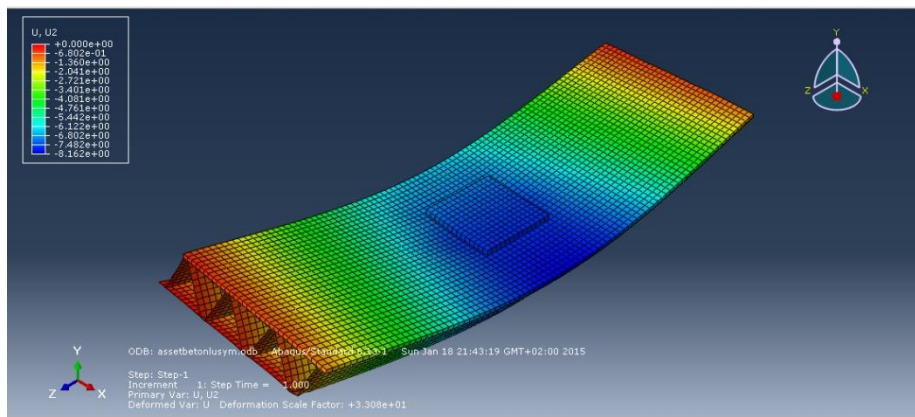
(b) Dura Span Hybrid FRP Concrete Deck



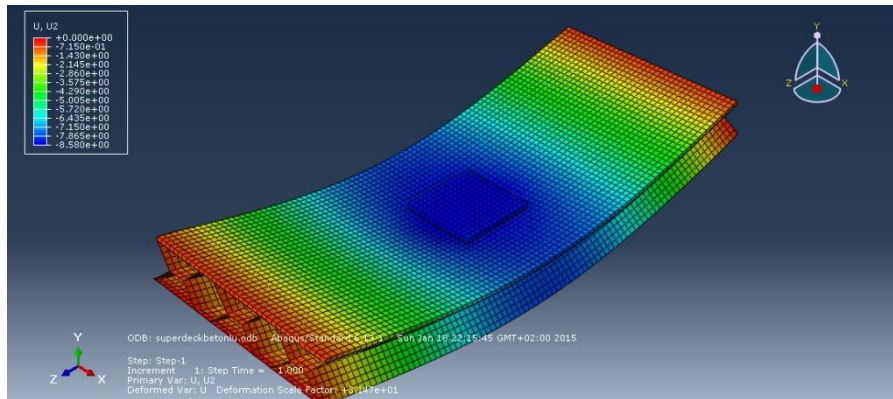
(c) EZ Span Hybrid FRP Concrete Deck



(d) Holes Hybrid FRP Concrete Deck



(e) Asset Hybrid FRP Concrete Deck



(f) Super Hybrid FRP Concrete Deck

Fig. 3 (a-f) Deflected shape and deflection results of hybrid FRP-concrete decks

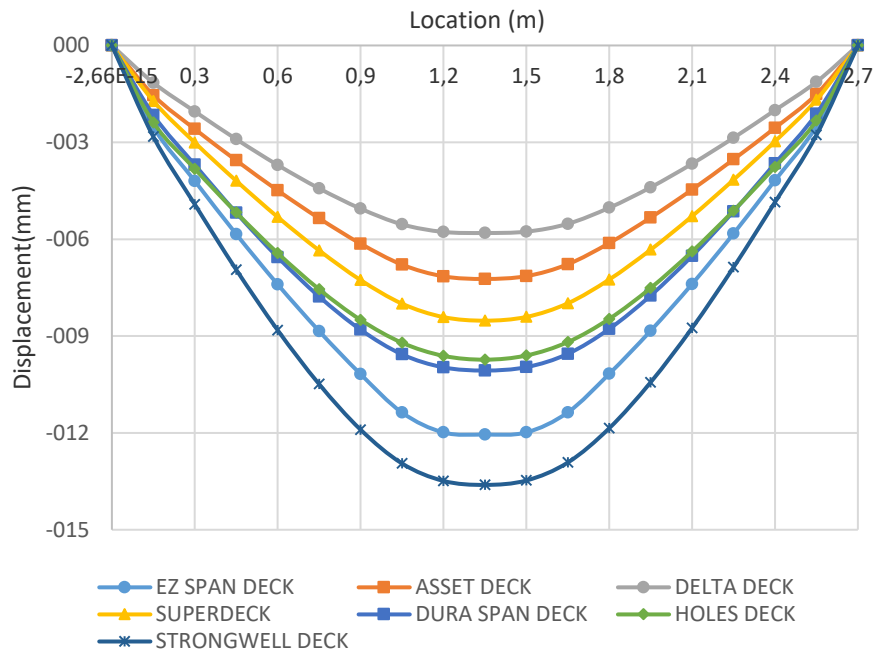
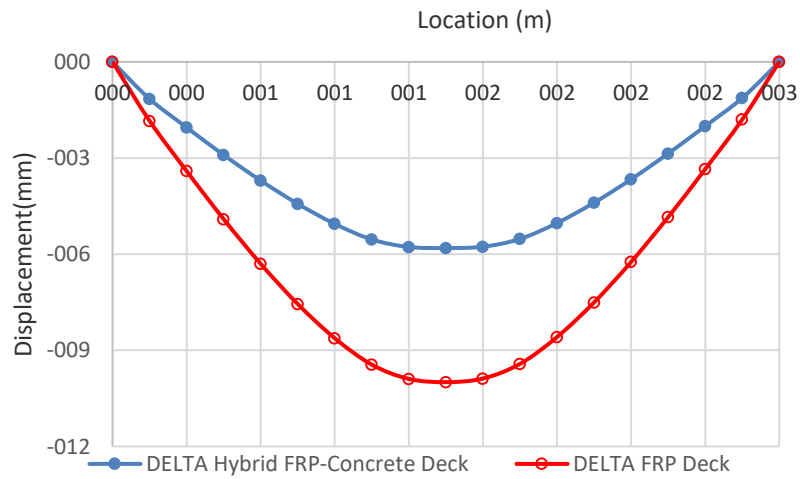
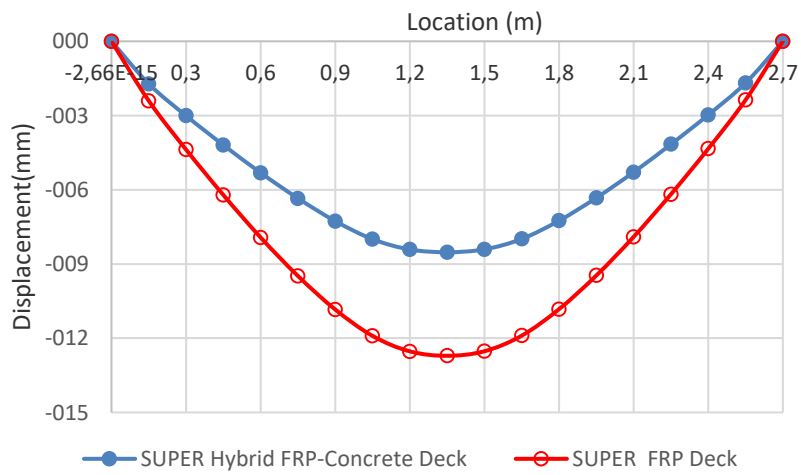


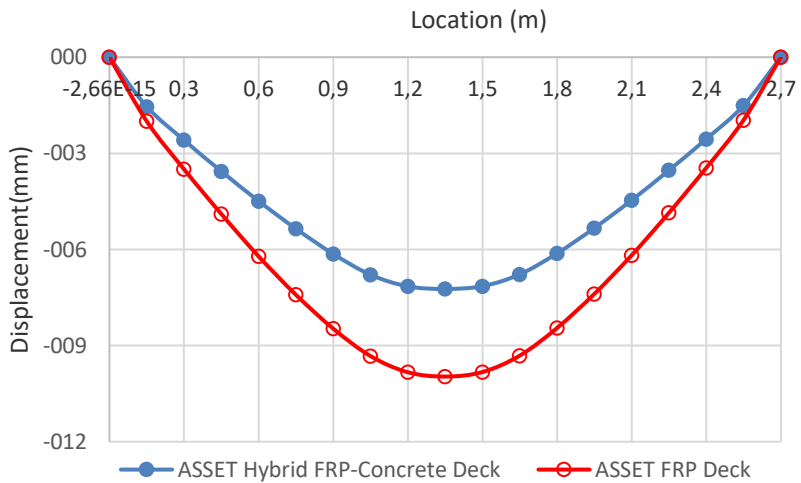
Fig. 4 Comparison of longitudinal maximum displacement of hybrid FRP-concrete decks



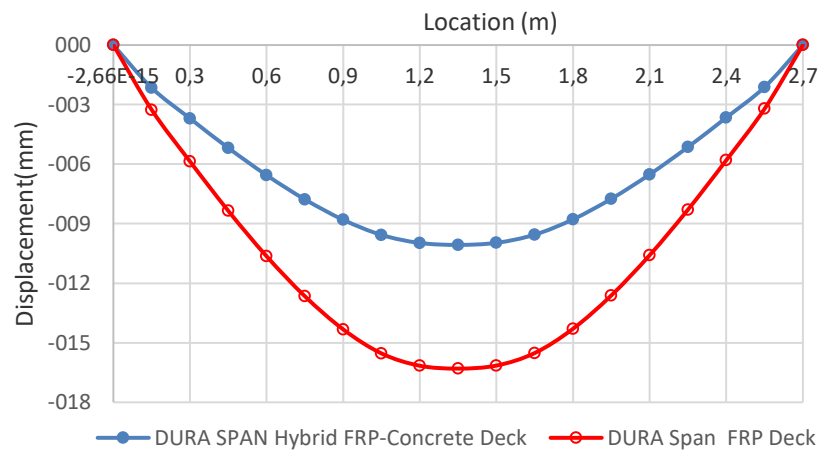
(a) Delta Deck



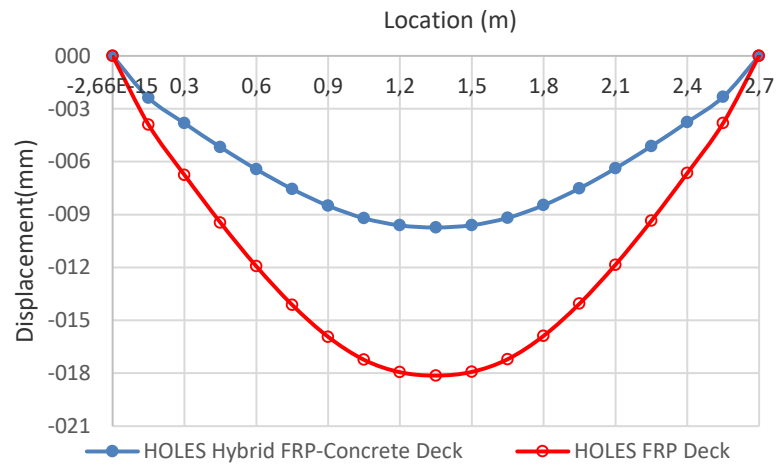
(b) Super Deck



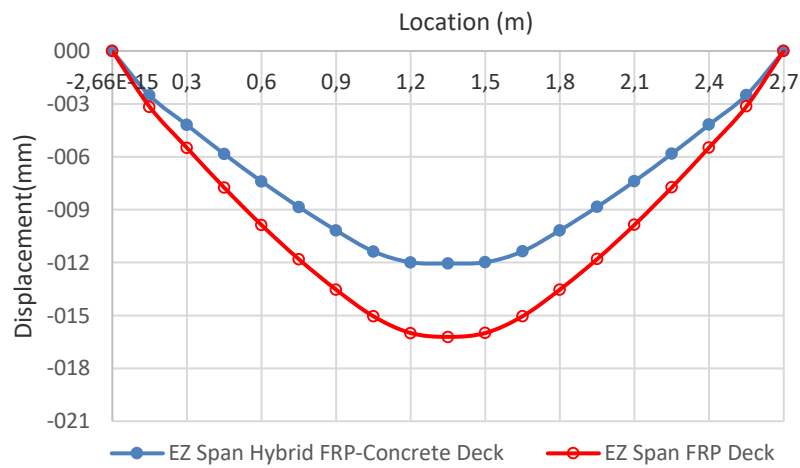
(c) Asset Deck



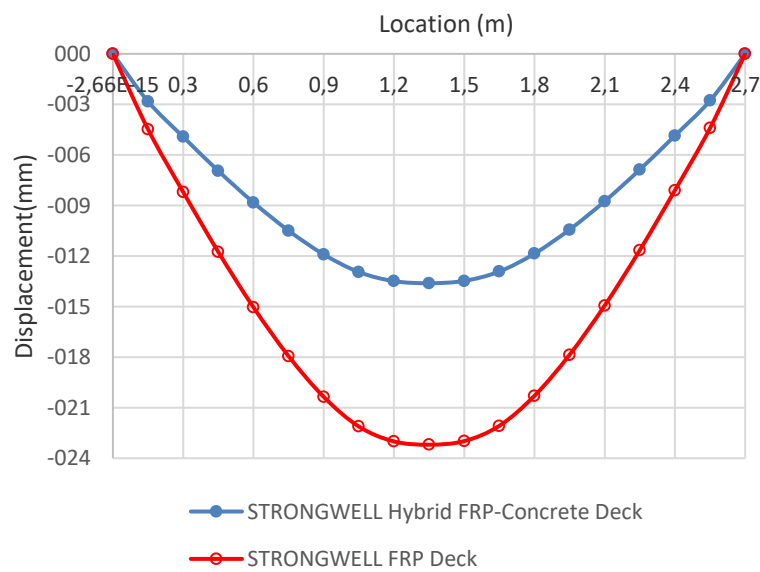
(d) Dura Span Deck



(e) Holes Deck



(f) EZ Span Deck



(g) Strongwell Deck

Fig. 5 (a-g) Comparison of longitudinal displacement of hybrid and non-hybrid FRP decks

Table 4 shows the maximum concrete compressive stress as well as tensile stresses in concrete element of hybrid deck systems. As seen in Table 4, the compressive stresses in concrete elements were all smaller than its compressive strength limit ( $0.85 \cdot f_c$ ) in all bridge systems, which is located at the top of the concrete under the load area. The maximum compressive stress in Delta, Asset and Super decks are smaller than the other hybrid deck systems. On the other hand the maximum tensile stresses ( $f_t$ ) exceeds the tensile strength of concrete for the decks systems except that EZ span hybrid deck. As expected the maximum tensile strength occurs at the bottom of the concrete layer in all bridge decks.

Table 4. Maximum concrete stress in SLS

		Maximum Concrete Stress	
		Compressive Stress (MPa)	Tensile Stress (MPa)
FRP Deck Systems	DuraSpan	22.22	7.26
	Asset Deck	20.94	5.20
	Superdeck	21.16	4.99
	EZ Span Deck	22.37	1.47
	Strongwell	27.17	10.28
	Delta Deck	13.07	4.94
	Holes deck	22.14	6.22

The load combination for the ultimate state was also applied to all the bridge systems. The results of the maximum vertical displacement is presented in Table 5. As seen in Table 5, the displacements in Delta, ASSET and Super hybrid FRP-concrete decks are smaller than the other deck systems as in the case of the SLS. The similar results for the variation of deflections, and also the maximum longitudinal stress in FRP decks were also obtained with that of SLS.

Table 5. Maximum vertical displacement for ultimate limit state (ULS)

		Maximum Vertical Displacement (mm)	
		Hybrid FRP Concrete Deck	FRP Deck
FRP Deck Systems	DuraSpan	13.68	22.24
	ASET Deck	11.02	15.98
	Superdeck	11.58	17.61
	EZ Span Deck	16.42	22.13
	Strongwell	18.38	31.44
	Delta Deck	7.841	13.51
	Holes deck	13.17	24.55

#### 4. CONCLUSION

Different hybrid FRP-concrete bridge decks were investigated numerically by using finite element (FE) analysis. A simplified FEM approach, which uses a single layer of thick shell elements to simulate a FRP deck, that has top and bottom face sheets and web, was proposed. The structural performance of the hybrid deck panels were compared with that of the non-hybrid deck

panels. The comparisons among these bridge systems were also carried out to select the most efficient two decks. The results showed that Delta, Super and ASSET hybrid decks are stiffer than other deck systems. The results from FEA approach also indicated that the layer of concrete on the top surface of bridge deck reduces the vertical displacement of FRP bridge systems approximately 60%. The FEA results also show that Delta, ASSET and Super hybrid decks were more efficient than other FRP decks considered here.

#### REFERENCES

Federal Highway Administration and United States Department of Transportation (FHWA/USDOT). (2002). "Corrosion costs and preventative strategies in the United States." A Supplement to Materials Performance (MP), NACE International, Houston.

Hollaway, L. C. (2010), "A review of the present and future utilisation of FRP composites in the civil infrastructure with reference to their important in-service properties", Construction and Building Materials, Vol. 24, pp. 2419–2445.

Bakis C.E., Bank L.C., Brown V.L., Cosenza E., Davalos J.F., Lesko J.J. (2002), "Fiber-reinforced polymer composites for construction-state-of-art review", J. Compos. Construct., ASCE;6(2):73–87.

Keller, T. (2002), "Overview of Fibre-Reinforced Polymers in Bridge Construction", In: Structural Engineering International, May, No. 2, p. 66–70.

Alnahhal W., Aref A., Alampalli S. (2007), "Composite behavior of hybrid FRP-concrete bridge deck on steel girders", Compos. Struct., 84, 29-43.

Kitane, Y. and Aref, A. (2004), "Static and fatigue testing of hybrid fiber-reinforced polymer-concrete bridge superstructure", J. Compos. for Const., 8(2),182-190.

Sebastian, W.M., Keller, T. and Ross, J. (2013) "Influences of polymer concrete surfacing and localised load distribution on behaviour up to failure of an orthotropic FRP bridge deck," Composites: Part B, Vol. 45, pp. 1234–1250.

Brown RT, Zureick AH. Lightweight composite truss section decking. Marine Struct 2001;14:115–32.

Davalos, J. F., Qiao, P., Xu, X. F., Robinson, J., and Barth, K. E. (2001). "Modeling and characterization of fiber-reinforced plastic honeycomb sandwich panels for highway bridge applications." Composite Structures, 52(3-4), 441-452.

Keller T. and Schollmayer M., Plate bending behavior of a pultruded GFRP bridge deck system, Composite Structures 64, 285–295, 2004.

Keller T, Gürtler H. 2006. In-plane compression and shear performance of FRP bridge decks acting as top chord of bridge girders. Compos. Struct. ;72(2):151–62.

Saiidi, M., Gordaninejad, F., and Wehbe, N. (1994), "Behavior of Graphite/Epoxy Concrete Composite Beams", *Journal of Structural Engineering*, Vol. 120, No. 10, pp. 2958-2976.

European Committee for Standardization (CEN): Eurocode 1— Actions on Structures, part 2: traffic loads on bridges. Pr EN 1991-2, 2002.

Hibbit, Karlsson& Sorensen, Inc. (2006), *ABAQUS/Standard User's Manual*, Version 6.6, Hibbit, Karlsson& Sorensen, Inc.



## CONTENTS

### CLOSED LOOP SUPPLY CHAIN MANAGEMENT PERFORMANCE EVALUATION CRITERIA

Emel Yontar and Süleyman Ersöz ..... 157

### AUTOMATIC DETECTION OF CYBERBULLYING IN FORMSPRING.ME, MYSPACE AND YOUTUBE SOCIAL NETWORKS

Çiğdem İnan Acı, Eren Çürük and Esra Saraç Eşsiz ..... 168

### BEHAVIOR OF R/C FRAMES WITH CONCRETE PLATE BONDED INFILLS

Mehmet Baran ..... 179

### LOGIC THRESHOLD FOR MICRORING RESONATOR-BASED BDD CIRCUITS: PHYSICAL AND OPERATIONAL ANALYSES

Ozan Yakar and İlke Ercan ..... 189

### EXPERIMENTAL INVESTIGATION OF A NOVEL FRICTION MODIFIER IN COMPOSITE MATERIALS

İlker Sugözü and Mücahit Güdük ..... 197

### REMOVAL OF COLOUR POLLUTIONS IN DYE BATHS WITH MORDANTS

Ashihan Koruyucu ..... 201

### FLEXURAL BEHAVIOR OF HYBRID FRP-CONCRETE BRIDGE DECKS

İlker Fatih Kara, Ashraf F. Ashour and Cahit Bilim ..... 206

ISSN 2587-1366

# TURKISH JOURNAL OF ENGINEERING